

**UNIVERSITY OF TURKISH AERONAUTICAL ASSOCIATION  
INSTITUTE OF SCIENCE AND TECHNOLOGY**

**DESIGNING OF A THREE-PHASE INVERTER WITH D-STATCOM  
CAPABILITY FOR MICROGRID**

**MASTER'S THESIS**

**Raad Salih JAWAD**

**A THESIS SUBMITTED IN PARTIAL FULFILLMENT OF THE  
REQUIREMENTS FOR THE  
DEGREE OF MASTER OF SCIENCE IN  
ELECTRICAL AND ELECTRONICS ENGINEERING**

**MARCH, 2017**

**UNIVERSITY OF TURKISH AERONAUTICAL ASSOCIATION  
INSTITUTE OF SCIENCE AND TECHNOLOGY**

**DESIGNING OF A THREE-PHASE INVERTER WITH D-STATCOM  
CAPABILITY FOR MICROGRID**

**MASTER'S THESIS**

**Raad Salih JAWAD**

**1403630040**

**A THESIS SUBMITTED IN PARTIAL FULFILLMENT OF THE  
REQUIREMENT FOR THE  
DEGREE OF MASTER OF SCIENCE IN  
ELECTRICAL AND ELECTRONICS ENGINEERING**

**Supervisor: Assist. Prof. Dr. Ibrahim Mahariq**

**MARCH, 2017**

Raad Salih JAWAD, having student number 1403630040 and enrolled in the Master Program at the Institute of Science and Technology at University of Turkish Aeronautical Association, after meeting all of the required conditions contained in the related regulations, has successfully accomplished, in front of the jury, the presentation of the thesis prepared with the title of: " DESIGNING OF A THREE-PHASE INVERTER WITH D-STATCOM CAPABILITY FOR MICROGRID ".

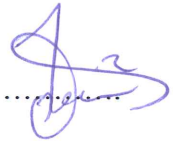
**Supervisor : Assist. Prof. Dr. Ibrahim MAHARIQ**  
**University of Turkish Aeronautical Association** .....



**Jury Members : Prof. Dr. Mehmet Timur AYDEMIR**  
**Gazi University**



**: Assist. Prof. Dr. Javad RAHEBI**  
**University of Turkish Aeronautical Association** .....



**: Assist. Prof. Dr. Ibrahim MAHARIQ**  
**University of Turkish Aeronautical Association** .....



**Thesis Defense Date: 24.03.2017**

**UNIVERSITY OF TURKISH AERONAUTICAL ASSOCIATION  
INSTITUTE OF SCIENCE AND TECHNOLOGY**

I hereby declare that all the information in this study I presented as my Master's Thesis, called: DESIGNING OF A THREE-PHASE INVERTER WITH D-STATCOM CAPABILITY FOR MICROGRID has been presented in accordance with the academic rules and ethical conduct. I also declare and certify with my honor that I have fully cited and referenced all the sources I made use of in this present study.



**24.03.2017**

**Raad Salih JAWAD**

## **ACKNOWLEDGEMENTS**

First of all, I am grateful to The Almighty God for helping me to complete this thesis.

I would like to acknowledge my thesis advisor Assist. Prof. Dr. Ibrahim Mahariq at University of Turkish Aeronautical Association for his guidance and encouragement through my research for this thesis.

Finally, I would present my full gratitude to Eng. Israa Ismael Hussein for all her efforts to help me in my thesis.

**MARCH, 2017**

**Raad Salih JAWAD**

## TABLE OF CONTENTS

ACKNOWLEDGEMENTS .....	i
TABLE OF CONTENTS .....	ii
LIST OF TABLES .....	vi
LIST OF FIGURES.....	vii
LIST OF ABBRIVIATIONS .....	xi
LIST OF PUPULICATIONS .....	xiii
ABSTRACT .....	xiv
ÖZET.....	xv
<b>CHAPTER ONE</b> .....	1
<b>1. INTRODUCTION</b> .....	1
1.1 Overview on DSTATCOM .....	1
1.2 Literature Survey .....	2
1.3 Objectives of the Thesis .....	10
1.4 Purpose of the Study.....	10
1.5 Significance of the Study.....	11
1.6 Material and Method .....	11
1.7 Organization of the Thesis.....	12
<b>CHAPTER TWO</b> .....	13
<b>2. POWER QUALITY PROBLEMS</b> .....	13
2.1 Power Quality .....	13
2.2 Problems of Power Quality .....	16
2.2.1 Voltage Dip .....	17

2.2.2 Voltage Swell .....	18
2.2.3 Interruption .....	19
2.2.3.1 Very Short Interruption .....	19
2.2.3.2 Long Interruptions.....	20
2.2.4 Transients .....	21
2.2.4.1 Impulsive Transients .....	21
2.2.4.2 Oscillatory Transients .....	21
2.2.5 Harmonic Distortion.....	22
2.2.6 Voltage Fluctuation .....	24
2.2.7 Noise.....	24
2.2.8 Voltage Unbalance .....	25
2.3 Causes of Power Quality Problems .....	26
2.4 Poor Quality Effects on Power System Devices .....	26
2.5 The Mitigation Techniques for Power Quality Problems.....	27
<b>CHAPTER THREE .....</b>	<b>31</b>
<b>3. D-STATCOM AND CONTROL METHODS .....</b>	<b>31</b>
3.1 D-STATCOM.....	31
3.2 Basic Elements of DSTATCOM .....	32
3.2.1 Voltage Source Converter .....	33
3.2.1.1 Distribution Static Synchronous Compensator (D-STATCOM) based on Six-Pulse VSI.....	34
3.2.1.1.1 Reactive Power Exchange .....	35
3.2.1.1.1.1 Analysis of the AC current signals .....	35
3.2.1.1.1.2 Conduction period transistors and diodes.....	40
3.2.1.1.1.3 Capacitor Current.....	42
3.2.1.1.1.4 DC Capacitor Voltage.....	43

3.2.1.1.2 Reactive and active power exchange.....	48
3.2.1.1.2.1 Capacitor current.....	51
3.2.1.2 Twelve Pulse Converter .....	54
3.2.1.2.1 AC Current Signals.....	60
3.2.1.2.1.1 Six-pulse AC current .....	65
3.2.1.2.2 Capacitor Current .....	69
3.2.1.2.3 DC Capacitor Voltage .....	72
3.2.2 L-C Passive Filter .....	73
3.2.3 Coupling Transformer .....	74
3.2.4 Control Block .....	74
3.2.4.1 Basic Hysteresis Controller.....	75
3.2.4.2 Design of Hysteresis Controller .....	75
3.2.5 Energy Storage Device .....	76
3.3 Main Features of DSTATCOM.....	76
3.4 Basic Principle of DSTATCOM .....	76
3.4.1 Reactive Power Exchange .....	77
3.4.2 Active Power Exchange .....	78
3.5 Control Algorithms.....	78
3.5.1 IRP Theory .....	78
3.5.2 SRF Method.....	82
3.5.3 Adaline-Based Control Algorithm .....	84
3.5.4 PI Controller for Maintaining Constant DC Bus Voltage of D-STATCOM.....	87
<b>CHAPTER FOUR.....</b>	<b>88</b>
<b>4. CALCULATIONS AND RESULTS.....</b>	<b>88</b>
4.1 Arrangement of Results.....	88



4. 2 DSTATCOMs Analysis and Design .....	88
4.2.1 Design of a Three-Phase Three Wire DSTATCOM .....	89
4.2.2 Three-Phase Three-Leg VSC Based DSTATCOM's Design .....	89
4.2.2.1 Selection of the DC Bus Voltage .....	89
4.2.2.2 Selection of a DC Bus Capacitor .....	90
4.2.2.3 AC Inductor Selection.....	90
4.2.2.5 Voltage and Current Ratings of the Solid-State Switches .....	91
4.3 Design of the 12-Pulse D-STATCOM .....	91
4.3.1 Inverter Design .....	94
4.3.2 Capacitor Sizing .....	94
4.3.3 Transformer Configuration.....	95
4.3.4 Controller Configuration .....	96
4.4 Simulation Results of 33 KV System.....	97
4.4.1 MATLAB/ SIMULINK model of 33 KV Distribution System .....	97
4.4.1.1 Voltage Dip of 33KV System without D-STATCOM.....	98
4.4.1.2 Voltage Swell of 33KV System without D-STATCOM.....	100
4.4.1.3 Voltage Dip of 33KV System with D-STATCOM.....	101
4.4.1.4 Voltage Swell of 33KV System with D-STATCOM.....	104
<b>CHAPTER FIVE.....</b>	<b>107</b>
<b>5. CONCLUSIONS AND FUTURE WORKS.....</b>	<b>107</b>
5.1 Conclusions .....	107
5.2 Future Works on D-STATCOM.....	108
<b>REFERENCES.....</b>	<b>109</b>
<b>CURRICULUM VITAE.....</b>	<b>114</b>

## LIST OF TABLES

<b>Table 2.1</b>	: Problems of power quality (causes and effects ) .....	29
<b>Table 4.1</b>	: Designing parameters .....	96

## LIST OF FIGURES

<b>Figure 2.1</b>	: Voltage sag.....	18
<b>Figure 2.2</b>	: Voltage swell.....	19
<b>Figure 2.3</b>	: Very short interruptions.....	20
<b>Figure 2.4</b>	: Long interruptions.....	20
<b>Figure 2.5</b>	: Impulsive transients.....	21
<b>Figure 2.6</b>	: Oscillatory transients.....	22
<b>Figure 2.7</b>	: Harmonic distortion.....	23
<b>Figure 2.8</b>	: Voltage fluctuation.....	24
<b>Figure 2.9</b>	: Noise.....	25
<b>Figure 2.10</b>	: Voltage unbalance.....	25
<b>Figure 3.1</b>	: D-STATCOM.....	31
<b>Figure 3.2</b>	: Components of D-STATCOM.....	33
<b>Figure 3.3</b>	: Six-pulse VSI D-STATCOM.....	34
<b>Figure 3.4</b>	: Phase relationship between the inductor voltage and the fundamental current.....	36
<b>Figure 3.5</b>	: Relationship between DC voltage; fundamental; and harmonics current.....	37
<b>Figure 3.6</b>	: AC system voltage and voltage compensator $V_{an}(t)$ .....	37
<b>Figure 3.7</b>	: AC current waveform.....	40

<b>Figure 3.8</b>	: Q1 and D1 conduction period.....	42
<b>Figure 3.9</b>	: Capacitor current; a) generating reactive power; b) absorbing reactive power.....	46
<b>Figure 3.10</b>	: DC capacitor voltage.....	46
<b>Figure 3.11</b>	: Voltage waveforms with a finite DC capacitor.....	47
<b>Figure 3.12</b>	: Capacitor current and DC capacitor voltage waveform.....	47
<b>Figure 3.13</b>	: AC system voltage and compensator voltage, $V_{an}(t)$ .....	48
<b>Figure 3.14</b>	: AC current waveform with $\phi=15^\circ$ .....	50
<b>Figure 3.15</b>	: Instantaneous capacitor current.....	51
<b>Figure 3.16</b>	: Test circuit.....	52
<b>Figure 3.17</b>	: Instantaneous capacitor voltage.....	53
<b>Figure 3.18</b>	: AC instantaneous current with: a) $\phi=0^\circ$ , b) $\phi=-0.5^\circ$ .....	54
<b>Figure 3.19</b>	: a) $V_{ab}(t)$ and $V_{abY}(t)$ ; b) 12-pulse voltage.....	57
<b>Figure 3.20</b>	: 12-pulse VSI D-STATCOM.....	58
<b>Figure 3.21</b>	: 12-pulse D-STATCOM line to neutral voltages.....	59
<b>Figure 3.22</b>	: $V_{ab}(t)_{12}$ voltage Fourier spectrum.....	59
<b>Figure 3.23</b>	: Phasorial diagram.....	61
<b>Figure 3.24</b>	: Relationship between the DC voltage, the fundamental and harmonics current.....	61
<b>Figure 3.25</b>	: AC system voltage and fundamental voltage compensator $V_{an}(t)$ .....	62
<b>Figure 3.26</b>	: AC current waveform.....	65

<b>Figure 3.27</b> : AC current of each six-pulse VSI.....	68
<b>Figure 3.28</b> : Q1 and D1 currents.....	68
<b>Figure 3.29</b> : First converter capacitor current; a) generating reactive power; b) absorbing reactive power.....	70
<b>Figure 3.30</b> : Second converter capacitor current; a) generating reactive power; b) absorbing reactive power.....	71
<b>Figure 3.31</b> : Capacitor current; a) generating; b) absorbing reactive power.....	72
<b>Figure 3.32</b> : DC capacitor voltage; a) generating; b) absorbing reactive power.....	73
<b>Figure 3.33</b> : Hysteresis controller.....	75
<b>Figure 3.34</b> : Block diagram of the reference current extraction using IRP theory.....	79
<b>Figure 3.35</b> : Basic circuit diagram of the D-STATCOM system.....	80
<b>Figure 3.36</b> : Block diagram of the reference current extraction using SRF theory.....	83
<b>Figure 3.37</b> : Block diagram of the reference current extraction using Adaline- based theory.....	85
<b>Figure 4.1</b> : 12-pulse D-STATCOM.....	92
<b>Figure 4.2</b> : MATLAB/Simulink model of transformers combination.....	93
<b>Figure 4.3</b> : MATLAB/Simulink model of the 12-pulse D-STATCOM.....	93
<b>Figure 4.4</b> : MATLAB/Simulink model of D-STSTCOM controller.....	96
<b>Figure 4.5</b> : MATLAB/Simulink model of the proposed system.....	98
<b>Figure 4.6</b> : 33 KV +/-MVAR D-STATCOM (Simulink model).....	98
<b>Figure 4.7</b> : Voltage at PCC (without D-STATCOM).....	99
<b>Figure 4.8</b> : P, Q (without D-STATCOM).....	99

<b>Figure 4.9</b>	: PQ_B3, V_B1, and V_B3 (without D-STATCOM).....	99
<b>Figure 4.10</b>	: Voltage at PCC (without D-STATCOM).....	100
<b>Figure 4.11</b>	: P, Q (without D-STATCOM).....	100
<b>Figure 4.12</b>	: PQ_B3, V_B1, and V_B3 (without D-STATCOM).....	101
<b>Figure 4.13</b>	: Voltage and current at PCC (with D-STATCOM).....	101
<b>Figure 4.14</b>	: D-STATCOM inverter voltage.....	102
<b>Figure 4.15</b>	: Iq, Iqref (pu).....	102
<b>Figure 4.16</b>	: P, Q (with D-STATCOM).....	102
<b>Figure 4.17</b>	: Vdc of D-STATCOM.....	102
<b>Figure 4.18</b>	: Modulation index of D-STATCOM.....	103
<b>Figure 4.19</b>	: PQ_B3 (with D-STATCOM).....	103
<b>Figure 4.20</b>	: V_B1 and V_B3 (with D-STATCOM).....	103
<b>Figure 4.21</b>	: Ia of D-STATCOM.....	103
<b>Figure 4.22</b>	: Voltage and current at PCC (with D-STATCOM).....	104
<b>Figure 4.23</b>	: D-STATCOM inverter voltage.....	104
<b>Figure 4.24</b>	: Iq, Iqref (pu).....	105
<b>Figure 4.25</b>	: P, Q (with D-STATCOM).....	105
<b>Figure 4.26</b>	: Vdc of D-STATCOM.....	105
<b>Figure 4.27</b>	: Modulation index of D-STATCOM.....	106
<b>Figure 4.28</b>	: PQ_B3 (with D-STATCOM).....	106
<b>Figure 4.29</b>	: V_B1 and V_B3 (with D-STATCOM).....	106
<b>Figure 4.30</b>	: Ia of D-STATCOM.....	106

## LIST OF ABBRIVIATIONS

<b>STATCOM</b>	: Static Synchronous Compensator
<b>DSTATCOM</b>	: Distribution Static Synchronous Compensator
<b>SVC</b>	: Static VAR Compensator
<b>VSC</b>	: Voltage Source Converter
<b>ASDs</b>	: Adjustable Speed Drives
<b>FACTS</b>	: Flexible Alternating Current Transmission Systems
<b>PWM</b>	: Pulse Width Modulation
<b>DC</b>	: Direct Current
<b>AC</b>	: Alternating Current
<b>SPWM</b>	: Sinusoidal Pulse Width Modulation
<b>IGBTs</b>	: Insulated Gate Bipolar Transistors
<b>GTO</b>	: Gate Turn-Off Thyristor
<b>MOSFET</b>	: Metal-Oxide Semi-conductor Field Effect Transistor
<b>Q</b>	: Reactive Power
<b>P</b>	: Active Power
<b>PQ</b>	: Power Quality
<b>R</b>	: Resistor
<b>L</b>	: Inductor
<b>C</b>	: Capacitor
<b>THD</b>	: Total Harmonic Distortion
<b>VSI</b>	: Voltage Source Inverters
<b>ASD</b>	: Adjustable Speed Drive
<b>BESS</b>	: Battery Energy Storage System
<b>CPD</b>	: Custom Power Device
<b>ESS</b>	: Energy Storage System
<b>EPQ</b>	: Electric Power Quality
<b>FFT</b>	: Fast Fourier Transform

<b>IEEE</b>	: Institute of Electrical and Electronics Engineers
<b>IRPT</b>	: Instantaneous Reactive Power Theory
<b>SRF</b>	: Synchronous Reference Frame
<b>PI</b>	: Proportional Integral
<b>PLC</b>	: Programmable Logic Controller
<b>PLL</b>	: Phase Locked Loop
<b>PQ</b>	: Power Quality
<b>PSCAD</b>	: Power System Computer Aided System
<b>SMESS</b>	: Super Magnetic Energy Storage System
<b>SSSC</b>	: Static Synchronous Series Compensator
<b>DIN</b>	: Distortion Index
<b>GTO</b>	: Gate Turn Off Thyristor
<b>MATLAB</b>	: Matrix Laboratory
<b>PCC</b>	: Point of Common Coupling



## LIST OF PUPULICATIONS

**Raad S. Jawad, Israa I. Hussein, I. Mahariq**, "FACTS Technology: Current Challenges and Future Trends", ICEEPIV, researchgate.net, pp. 45-50, 6-7 April 2016.

Online paper link:

[https://scholar.google.com.tr/scholar?q=FACTS+Technology%3A+Current+Challenges+And+Future+Trends&btnG=&hl=en&as\\_sdt=0%2C5&as\\_vis=1](https://scholar.google.com.tr/scholar?q=FACTS+Technology%3A+Current+Challenges+And+Future+Trends&btnG=&hl=en&as_sdt=0%2C5&as_vis=1)

**Raad S. Jawad, Israa I. Hussein, I. Mahariq** , "Design and Simulation of Three Phase and Single Phase Z-Source Inverters", ICEEPIV, researchgate.net, pp. 58-64, 6-7 April 2016.

Online paper link:

[https://scholar.google.com.tr/scholar?q=Design+And+Simulation+Of+Three+Phase+And+Single+Phase+ZSource+Inverters&hl=en&as\\_sdt=0&as\\_vis=1&oi=scholart&sa=](https://scholar.google.com.tr/scholar?q=Design+And+Simulation+Of+Three+Phase+And+Single+Phase+ZSource+Inverters&hl=en&as_sdt=0&as_vis=1&oi=scholart&sa=)

## **ABSTRACT**

### **DESIGNING OF A THREE-PHASE INVERTER WITH D-STATCOM CAPABILITY FOR MICROGRID**

Jawad, Raad

M.Sc., Department of Electrical and Electronics Engineering

Supervisor: Assist. Prof. Dr. Ibrahim Mahariq

March 2017, 114 pages

Day by day, FACTS technology have been getting increasingly important for their capability to solve the problems of power quality in electrical systems , these devices have proven their ability to improve the power quality of power systems, to provide better performance, surpassing many of the problems, which opposes the work of the electrical system. D-STATCOM, it is a miniature version of STATCOM device designed to operate in distribution systems (the low and medium voltage).

This thesis has been present and studying and designing a three phase inverter with D-STATCOM capability, in terms of the problems that can be addressed and in terms of its components and methods of control used to control it, as well as this thesis has provided a mathematical analysis to the heart of this device, which is a VSC. Two common types of VSC that used especially in medium voltage systems are analyzed and presented in this thesis and a MATLAB model for a twelve pulse D-STATCOM in 33 kV system has been presented to mitigate voltage dip (sag) and voltage swell that yields when connecting or disconnecting a heavy loads or due to faults occurrence, to study the behavior of the system before and after connecting the

D-STATCOM device.the results were discussed in terms of D-STATCOM ability to address these power quality problems.

**Keywords:** D-STATCOM, MATLAB, Power Quality, Voltage Dip, Voltage Swell.

## ÖZET

### MİKRO ŞEBEKELER İÇİN D-STATCOM KABİLİYETİNE SAHİP ÜÇ FAZLI İNVERTER TASARIMI

Jawad, Raad

Yüksek Lisans, Elektrik ve Elektronik Mühendisliği Bölümü

Danışman: Doç. Dr. İbrahim Mahariq

Mart 2017, 114 sayfa

Her geçen gün, elektrik sistemlerinde güç kalitesi sorunlarını çözme kabiliyeti sayesinde FACTS teknolojisi ve elektrik sistemlerinde çalışmayı engelleyen pek çok sorunu aşma ve elektrik şebekelerinin uygulanabilirliğini iyileştirme kabiliyetini ispatlayan cihazların önemi giderek artmaktadır. Dağıtım sistemlerinde (alçak ve orta gerilim) çalışmak üzere tasarlanan STATCOM cihazlarının minyatür bir versiyonu olan D-STATCOM, dağıtım sistemlerinde (alçak ve orta gerilim) çalışmak üzere tasarlanan STATCOM cihazlarının minyatür bir versiyonudur).

Bu tez, yanıt bulunabilecek sorunlar, bileşenleri ve kontrolü için kullanılan yöntemler özelinde D-STATCOM kabiliyetine sahip bir üç fazlı inverter incelenmesi ve tasarlanması amacıyla sunulmuş olup, tez aynı zamanda bir VSC olan bu cihazın özüne dair bir matematiksel analiz sunmaktadır. Özellikle orta gerilim sistemlerinde yaygın olarak kullanılan iki tip VSC bu tez kapsamında incelenmiş ve sunulmuş olup, sistemin D-STATCOM cihazı bağlanması öncesi ve sonrası davranışlarını incelemek adına da yüksek yük verilmesi ya da kesilmesi yahut hata oluşumu sonucu meydana gelen gerilim düşme ve gerilim yükselmelerini telafi etme amacıyla 33 Kv'lık bir sistemde on iki atışlı bir D-STATCOM'a yönelik bir MATLAB modeli sağlanmıştır. Sonuçlar, D-STATCOM'un bu güç kalitesi sorunlarına yanıt olma kabiliyeti özelinde irdelenmiştir.

**Anahtar Kelimeler:** D-STATCOM, MATLAB, Güç Kalitesi, Gerilim Düşüşü, Gerilim Yükselmesi.

## **CHAPTER ONE**

### **INTRODUCTION**

#### **1.1 Overview on DSTATCOM**

Electricity supplies play a significant role in the technological and economic progress around the world. Recently, with the growth of industry manufacturers and population, electric power quality becomes more and more important. The growth of a country's economics plays a key role in determining the quality and reliability of power supplies. However, there are still a lot of problems hinder the achievement of a quality and reliable power supply due to its disturbances such as sags, flickers, swells, harmonics, voltage imbalance etc.

Nowadays, most of consumers around the world ask for a high-quality power supply to meet their sensitive loads. Hence, load equipment in modern industries started using certain electronic controller that is sensitive to poor voltage quality and has the advantage of shutting down when there is depressed supply voltage and may also mal-operate when there is an excessive harmonic distortion of the supply voltage. Load perturbations and faults may occur in the distribution systems because of the weakness of isolated systems [1].

These systems do not receive any support from the grids, thus they are more susceptible to the faults and load variations. Accordingly, it becomes urgent to find compensators that meet the real and reactive power needs of the system whether in the steady state or transient circumstances.

As such, Custom Power Devices are employed in distribution systems in order to ease the problems of power quality. The number of configurations is growing in use worldwide. A custom power device can be series connected, shunt connected or both can be simultaneously connected across the system.

The device offers a compensation that relies on the design of voltage source converter (VSC) i.e. DC link capacitor, device rating of IGBT switches and interface inductors. Distribution Static Compensator (D-STATCOM), Dynamic Voltage Regulator (DVR), Unified Power Quality Conditioner (UPQC), BESS are among the devices of custom power that are employed at distribution level [2].

A distribution static compensator or D-STATCOM is a fast response, solid-state power controller that provides flexible voltage control at the point of coupling (PCC) and it is a voltage source converter (VSC) based power electronic device that is connected in a parallel way with the system to the utility distribution feeder for the sake of mitigating the problems of power quality. In case of coupling it with energy storage system (ESS), it has the property of exchanging both active and reactive power with the distribution system through the varying of amplitude and phase angle of the converter voltage in relation to the system voltage. A controlled current flow results by the interfacing inductance between D-STATCOM and the distribution system.

## **1.2 Literature Survey**

Lots of research is conducted in the custom power field. A review of literature for D-STATCOM is done below:

**D.G. Flinn, et al. [1]** tackled the problems of the power quality which may be found in the power system as well as discussing the appropriate methods that identify these problems. Actually there are an increased number of complaints of by customers about the electric utilities because of these types of problems. Thus, there is a need to have a systematic plan to identify the problems of power quality in the various facilities in industry, commerce or residence. This paper explains the on-site field measurements and routine checks on the system, which can be utilized to determine these problems. The data collected from these measurements help in the identification of the problems' nature as well as helping to correlate the events to these problems.

**A. El Mofly, et al. [2]** studied real-time industrial disturbances of power quality which usually occur due to load switching, non-linear loads, system faults, load variations, motor start, arc furnaces and intermittent loads. These reasons result in certain electrical disturbances such as voltage dip, voltage surge, harmonic distortions,

flickering and interruption. This study analyzed the real-time industrial electrical disturbances and power disturbance log. Further, some suggestions are introduced to decrease or stop problems triggered by disturbances of power.

**J. Sun, et al. [3]** illustrated the phenomenon of voltage flicker, which is known as disturbing light intensity fluctuation, caused by great rapid changes in the industrial load. This phenomenon has been a serious issue for both power companies and customers. Distribution Static Compensator (D-STATCOM) is characterized by rapid response which qualifies it to be a very good means to improve the quality of power in distribution systems. The phenomenon of voltage flicker in the system of distribution are modeled and simulated. Studies over the mitigation of voltage flickers with a current controlled PWM-based D-STATCOM are also discussed.

**Walmir Freitas, et al. [4]** studied the AC generators' effects (induction and synchronous machines) and distribution static synchronous compensator (D-STATCOM) devices conducted on the distribution networks' dynamic behavior. It analyzed D-STATCOM's performance as a power factor controller or voltage controller. The effects of these controllers on the distribution networks' stability and protection system with distributed generators are identified. Results of computer simulation indicated that a D-STATCOM voltage controller can achieve significant improvement in the stability performance of induction generators. On the other hand, a D-STATCOM power factor controller could cause an adverse effect on the synchronous generators' stability performance. Moreover, It is noted that a D-STATCOM exercises no effect on short-circuit currents supplied by AC generators during faults.

**Bhim Singh, et al. [5]** have discussed D-STATCOM (Distribution Static Compensator) for power factor correction, load balancing, neutral current elimination and voltage regulation in three-phase, four wire distribution system that feed domestic and commercial consumption. An employment of four leg voltage source inverter (VSI) configuration with a dc bus capacitor is done as DSTATCOM. In order to control D-STATCOM, a modified instantaneous reactive power theory (IRPT) is employed.

The dynamic modeling and the control design of a distribution static compensator (D-STATCOM) which is coupled with ultra-capacitor energy storage

(UCES) for improving the power quality of power systems is explained by **M. G. Molina, et al. [6]**. The operation modes include current/voltage harmonics mitigation, dynamic active power control and voltage control for voltage fluctuations ride-through.

**V. B. Virulkar, et al. [7]** talked about flicker mitigation due to electric arc welder via the use of D-STATCOM with Battery Energy Storage System (BESS). They showed that active power control along with reactive power control mitigates the problem of voltage flicker in an effective way. In addition, the software of PSCAD/EMTDC is used to analyze the mitigation of voltage flicker of Electric Arc Welder with D-STATCOM along with BESS.

**Cristian A. Sepúlveda, et al. [8]** explained that the disturbances of Power Quality have been met through Devices of Custom Power such as Distribution Static Compensator (D-STATCOM) and Static Series Compensator (SSC). Each one of these supplies certain part of the needed compensation capability. In order to give total functionality, either the two above-mentioned equipment can be operated or to employ a Unified Power Quality Conditioner (UPQC) which gets the two topologies integrated supplying total compensation capabilities as well as improving the characteristics of compensation.

**Sumate Naetiladdanon, et al. [9]** showed the voltage sag's compensation performance via the use of D-STATCOM. This study dealt with the voltage sag compensation's steady state performance via D-STATCOM along with series inductor and the storage of energy. A discussion is made on three current injection schemes for the voltage sag compensation with various purposes. The results of simulation confirmed that system of D-STATCOM with extra series inductor and energy storage could help in improving the compensation performance of voltage sag. Thus, D-STATCOM is proved to be a significant feature in power system in the mitigation of problems of power quality in the next generations.

**P. N. Boonchiaml, et al. [10]** have discussed using an energy storage device connected to a D-STATCOM in order to supply a flow of real power and reactive power. The study introduces the control, design, and analysis of a D-STATCOM enhanced with the device of energy storage when coupled with a wind farm comprising fixed speed induction generator. This proves that the D-STATCOM, controlled

through the technique of decoupled vector control, is a successful approach of reducing emissions of voltage flicker at the point of common coupling, eliminating the fluctuation of wind speed and improving the wind's transient stability.

**Sumate Naetiladdanon, et al. [11]** have said that D-STATCOM is able to compensate voltage sags through the injection of the reactive power into the distribution system. However, there is a chance for the occurrence of false compensation because of the interaction with the system. As such, an analysis was made to the design considerations of D-STATCOM for the compensation of voltage sag. Moreover, the compensation performance of voltage sag with various current injection schemes was explicated in brief, in addition to the description of the interaction. Later, D-STATCOM system design with controller for the compensation of voltage sag is suggested. The results of simulation stressed that D-STATCOM proper system design can fulfill a compensation performance of good voltage sag with no need for interacting with system.

**M. G. Molina, et al. [12]** illustrate the D-STATCOM's control design and Dynamic Modelling, coupled with ultra-capacitor energy storage (UCES) for the sake of power quality's reliability in power systems. The theory of instantaneous power is used as a control technique on the synchronous rotating dq reference frame. The rapid response device proves to have efficiency needed to enhance the quality of distribution power, and to mitigate disturbances like voltage swell, voltage/current harmonic distortion, and voltage sag among some other transients.

**M. G. Molina, et al. [13]** have discussed the dynamic performance of D-STATCOM, which is integrated with ESS (an energy storage system) to decrease transients and to get the power quality of distribution systems improved. This integrated D-STATCOM/ESS compensator is regarded as a voltage controller, an active power controller and a power factor controller. Studies on dynamic system simulation showed that the proposed multi-level control approaches are effective in the synchronous rotating dq reference frame. Through the results, it is shown that there is a good performance of the multilevel controller in addition to the interests of using it in the distribution level of power quality.

**Vasudeo Virulkar, et al. [14]** have discussed the DSTATCOM dynamic performance, coupled with BESS for the sake of mitigating the flicker resulting from



electric arc furnace. D-STATCOM modeling with BESS is managed by the acting of controller on the system of battery energy storage, the voltage at PCC and the dc-link voltage. Besides, the results obtained showed more accuracy in mitigating flicker with D-STATCOM and BESS than using D-STATCOM alone via the active and reactive power support at specific time which achieve improvement in the power quality in the systems of electric distribution. It is influential in making a compensation for reactive power and an improvement to the factor of power of the distribution system.

**Marcelo G. Molina, et al. [15]** have proposed using D-STATCOM along with SMES (superconducting magnetic energy storage) as an operational controller of tie-line power flow of microgrids incorporating wind generation. Fluctuations of tie-line power flow are caused by high penetration of wind generation which influences operations of power system significantly. Severe problems are created by this like system frequency oscillations, and/or lines capability violations. Rapid controllability of the D-STATCOM-SMES operating in the four-quadrant model is checked by multi-level control scheme, which helps in increasing the transient and the microgrid's dynamic stability.

**Suvire Gastón O., et al. [16]** explored the use of D-STATCOM with FESS (Flywheel Energy Storage System) in order to ease the power quality problems, which are presented in the electric system by wind generation. There is one control mode for active power in the current control technique in this system as well as two control modes are there for reactive power, namely voltage control and power factor correction. The obtained results showed that with the suggested device and control mode, there is an effective compensation for the fluctuations of power resulting from a WG. Also, it displays that the system of WGDSTATCOM/ FESS is able to create a constant active power for certain range of time of seconds or may be more, as per the storage capacity.

**G. V. R. Satyanarayana, et al [17]** proposed a kind of D-STATCOM cascaded multilevel inverter to create compensation for problems of power quality in utility voltages in system of power distribution. The results showed that with this kind of inverter, the requirement of dc voltage reduces as with low dc voltage and produces higher AC voltages. Additionally, a multilevel topology can be used to eliminate the

filter at the output of the inverter which then reduces the filter's cost and leads to satisfactory limits of the total harmonic distortion.

Again, **Marcelo G. Molina, et al. [18]** have proposed using the system of an ultra-capacitor energy storage (UCES) along with a D-STATCOM as an effectively distributed energy storage in order to stabilize and control the flow of tie-line power of microgrids incorporating wind generation. A proposition of a multilevel control algorithm which is based on a decoupled current control strategy in the synchronousrotating d-q reference frame is made. Such scheme helps rapid controllability of the D-STATCOM-UCES, which works on increasing the transient and the microgrid's dynamic stability.

**Alka Singh, et al. [19]** also conducted discussions over D-STATCOM's application to a small distribution System from 42.5kVA diesel generator. The isolated system did not have support from the grid, thus it was disposed to different faults and disturbances in the system. The performance of the installed D-STATCOM with this system has been demonstrated for linear loads and for disturbances of load side particularly various kinds of faults. The system of battery energy storage is designed and modeled to act as a source of leading or lagging source current. Though there is no support from the grid to the DG system, an influential controller design can provide load compensation and system support during faults. This paper helps boosting the research in certain small dispersed generation and compensator's application under faults and disturbances. The conclusion is that D-STATCOM can be employed to improve quality of power on the small isolated system.

Validating the D-STATCOM system's performance to improve the performance of distribution system under all kinds of faults is done in a study by **S. H. Hosseini, et al. [20]**. In this scheme the 12- pulse D-STATCOM configuration with IGBT was designed as well as developing the graphic based models of the D-STATCOM via the use of the program of PSCAD/EMTDC electromagnetic transient simulation. The results of simulation proved the control scheme's robustness and reliability in the system response to the voltage sags due to all kinds of faults such as Single Line to Ground (SLG), fault and three-phase fault, and fault and Double Phase to Ground (DPG).

**G.O. Suvire, et al. [21]** talk about the incorporation of (D-STATCOM) coupled with FESS (flywheel energy storage system) which is employed to ease the transient stability's problems presented by wind generation in the electrical system. Fuzzy logic and special filter are the basis for using the control technique. The result is that the complete system (D-STATCOM/FESS plus WG) generates a smoother power response than that of the system without the D-STATCOM/ FESS. This output power's smoothing effect grows with the number of flywheels. At the end, it comes to the conclusion that the control of active power suggested for the D-STATCOM/ FESS managed successfully the stored energy because of correcting the fluctuations of wind-power with the storage device neither discharged nor overloaded.

Power quality problems have been described by **Annapoorna Chidurala, et al. [22]**. These problems include overvoltage, dip/swells, harmonics and voltage unbalances. They propose a novel perception of operating PV inverter as a Solar-D-STATCOM with a new kind of control topology in order to enhance power quality. The results of simulation stressed that voltage rise, VU, voltage dips, swells and THD levels at different operating ways with the suggested Solar-D-STATCOM are well in the light of the suggested IEEE standards.

**C. H. Lin, et al. [23]** propose the use of D-STATCOM to create compensations for reactive power during peak solar irradiation for the sake of preventing voltage violation. Accordingly, an increase occurs in the PV penetration level of a distribution feeder in order to fully exploit solar energy. D-STATCOM's voltage control scheme is used to help mitigating system voltage violation resulting from excessive PV power generation during peak solar irradiation periods. As a result, solar energy can be fully exploited.

**Rajiv K. Varma, et al. [24]** introduces an original concept of making use of photovoltaic (PV) solar farm (SF) as a flexible AC transmission systems controller—static synchronous compensator, to have regulation for the point of common coupling voltage in the period of nighttime when there is no active power produced by the SF. This concept is used for the scenario of a distribution feeder, which has connection with both PV solar and wind farms. The suggested control will help in the increase of connections of renewable energy sources in the grid. In order to validate the suggested

concept, A MATLAB/Simulink-based simulation study is introduced under variable wind power generation and fault condition.

**Rajiv K. Varma, et al. [25]** presents a novel technology of utilizing Photovoltaic (PV) Solar Farms in the nighttime. New controls are developed for the solar farm inverters to operate as STATCOM – a Flexible AC Transmission System (FACTS) Controller, using the entire inverter capacity in the night for accomplishing various power system objectives, such as voltage regulation, improvement of power transfer capacity, load compensation, etc. During the daytime, the same objectives can be achieved to a substantial degree with the inverter capacity remaining after real power generation. This technology is termed PV-STATCOM.

**Vivek Nandan Lal, et al [26]** consider a high-power three-phase single-stage PV system. A distribution network is connected with this system, with a modified control strategy, which contains compensation for grid voltage dip and reactive power injection capability. In order to regulate the dc-link voltage, a modified voltage controller employing feedback linearization scheme with feed forward PV current signal is introduced. Stability/eigenvalue analysis of a grid-connected PV system with the complete linearized model is done to evaluate the controller's robustness and the decoupling character of the grid-connected PV system. An evaluation of the dynamic performance is performed on a real-time digital simulator.

**Rajiv K. Varma, et al [27]** presents a novel concept of utilizing PV solar farm inverter as STATCOM, termed PV-STATCOM, for improving stable power transfer limits of the interconnected transmission system. The entire inverter rating of PV solar farm which remains dormant in the nighttime is utilized with voltage and damping controls to enhance stable power transmission limits. During daytime, the inverter capacity left after real power production is used to accomplish the above objective. Transient stability studies are conducted on a realistic single machine infinite bus power system having a midpoint located PV-STATCOM using EMTDC/ PSCAD simulation software.

**Rajiv. K. Varma, et al [28]** presents a novel optimal utilization of photovoltaic solar system as STATCOM for voltage regulation and power factor correction during both nighttime and daytime. The PV solar system conventionally generates real power during the day but the entire asset remains idle at night. This novel PV solar system

operated as STATCOM is termed PV-STATCOM which utilizes the entire inverter capacity in the night and that remaining after real power generation during the day for accomplishing various STATCOM functionalities.

### **1.3 Objectives of the Thesis**

In this thesis work, design D-STATCOM model for voltage sag and swell for the 33KV system will be implemented by using MATLAB/Simulink software. The system will be investigated and studied under IEEE Standards.

A DSTATCOM is a voltage source converter (VSC) based power electronic device that is connected in a parallel way with the system. It is normally backed-up by energy storage device like a capacitor. In case of associating a D-STATCOM with certain load, it injects compensating current, therefore the overall demand meets the specifications for utility connections.

D-STATCOM works on generating capacitive and inductive reactive power in an internal way. It has the merit of fast control and is able to supply an adequate reactive compensation to the system.

D-STATCOM can be efficiently used to regulate voltage for an industrial load of heavy induction motors, which draw large starting currents (5-6 times) of full rated current and may disturb the operation of other sensitive loads, connected to the system.

### **1.4 Purpose of the Study**

Flexible alternating current transmission system (FACTS) devices have been proved as a good option to enhance the quality of power systems by enhancing voltage, extending the capacity of the transmission lines to the thermal limits, giving system flexibility, and improving stability in steady state as well as emerging state. Facts technology has got a large importance year by year due to their fast response to treat or overcome most of issues or problems that affect the power systems. One of FACTS applications is that the Distributed- STATCOM which is named D-STATCOM.

The main purpose of this study is that to design and simulate a D-STATCOM model in MATLAB /Simulink software for 33 KV power system to regulate voltage under the effect of voltage sag or (voltage dip) and voltage swell.

This study will give us an overview of the contributions of D-STATCOM to enhance the voltage profile and to overcome the main problem which facing power systems.

### **1.5 Significance of the Study**

Many studies which intend to study the D-STATCOM, present the advantages and disadvantages of the studied device. In our study, we will present a MATLAB/Simulink model for D-STATCOM in 33 kV system and study the capability of this device to overcome issues that limit the 33 kV system against the voltage sag or voltage swells.

- The main significant purpose of this thesis is that it presents a design for D-STATCOM with a controller modeled by simulation software to study 33 kV system suffering from voltage sag or voltage swell and give a spotlight on the importance of this custom devices and their ability to maintain voltages and keeping secure for medium voltage system. The other objects for this thesis is:
- To investigate the capability of D-STATCOM technique to mitigate voltage sag, swell
- To study and analyze the operation of D-STATCOM device in 33 kV voltage system.

### **1.6 Material and Method**

This thesis objected to building a MATLAB /Simulink model of D-STATCOM for 33Kv system .the operation of this device has been analyzed to show the capability of D-STATCOM to enhance the voltage of the system. All design equations that used to calculate the parameters of the system and determined the values of the element has been stated also. Principles of operation of system elements explained obviously to

understand the principles of reactive power compensation by D-SATCOM. All references will be cited according to their appearance among thesis chapters.

## **1.7 Organization of the Thesis**

The work performed in this thesis has been assembled in six chapters. Short descriptions are presented as below:

### **1. Chapter 1: Introduction**

This chapter presents an overview and scope of the work. It also contains the organization of this thesis. The thesis outline is also introduced here. And also, presents the background of the thesis objectives, purpose, and significance of the study, methodology and research structure.

Also this chapter presents a literature review for the important researches and papers that deal with this subject, some of the literature regarding the thesis topic is also included in this chapter.

### **Chapter 2: Power Quality Problems**

The chapter describes the power quality problems. Gives highlights on the most problems that facing the power systems.

### **Chapter3: D-STATCOM and control Methods of D-STATCOM**

This chapter includes the descriptions for control methods of D-STATCOM.

### **Chapter 4: Calculations and Results**

This chapter presents the proposed system of D-STATCOM for 33 KV, explain in details the controller and give the MATLAB / SIMULINK of this system. All the calculations required determining the parameters related to the proposed system of D-STATCOM have been done. The model has been implemented in MATLAB /SIMULINK software. All results have been obtained and organized and discussed.

### **Chapter 5: Conclusions and Future Works**

Finally, a conclusion on the obtained results is presented. This also includes the contribution of this thesis and suggestions for future works.

## **CHAPTER TWO**

### **POWER QUALITY PROBLEMS**

#### **2.1 Power Quality**

Electric power quality (PQ) as a term is utilized to assess the power's quality and to keep up it at the levels of generating, transmitting, distributing, and using AC electrical power. On account of the serious contamination at the using level of in the systems of electric power supply, it gets to be distinctly critical to study toward the end clients' terminals in the distribution systems.

A few causes prompt to the AC supply systems' contamination; some of them are natural causes like hardware disappointment, lightening, flashover, and issues (faults around 60%) and others are constrained reasons like notches and voltage distortions (around 40%). Besides of that, a portion of the equipment utilized by customers likewise causes contamination for the supply system caused by their draw of non-sinusoidal current and appear as a nonlinear loads.

Consequently, the quality of power is evaluated in relation to voltage, current, or frequency deviation of the supply system, which could be responsible for the failure or equipment's mal-operation. Normally, a few issues of power quality related with the voltage at the PCC are the existence of notches, swell, sag/dip, voltage harmonics, surge, fluctuations, unbalance, outrages, spikes, glitches, flickers,...etc. , where various types of loads are applied.

Such issues occur in the supply system as a result of a few disturbances in the system or as a result of the presence of various nonlinear loads like adjustable speed drives (ASDs), furnaces and uninterruptible power supplies (UPSs). In any case, there are a few issues of power quality related with the current gotted from the AC mains for example, poor power factor, reactive power burden, harmonic current, unbalanced



current and excessiveness of neutral current in polyphase systems that yield from harmonic currents and unbalanced produced from nonlinear loads.

These issues in the power quality are the reasons of failure in the capacitor banks, vibrations, noise, and rises the losses in the distributing networks and electrical machines, excessive current and over voltages related to resonance and negative sequence currents in electrical machines, for example, rotor heat, cables derating, dielectric breakdown, interference in communication systems, false metering, relay and breaker malfunctions, signal interference, obstructions to the computerized controllers and engine controllers, and so on.

Such issues exist in the supply system reported as critical problems when solid-state controllers are utilized, that caused troubles to distribution systems, according to the cost and reduction in size, and the simplicity of controllers, saving energy, and no wear or tear, also reduction in the requirements of maintenance in the modern electrical grids.

Tragically, the commercial loads and industrial loads even they are have high energy-efficient grades but they all controlled electronically, that controllers are sensitive to PQ problems. Addition to that, they cause power quality problems due to their using of solid-state controllers. These problems led to expand research fields to investigate and to find out an acceptable solutions to enhance the power quality in the electrical power facilities.

These industrial and commercial loads corresponded as a serious challenge to the electricity producers. They have to fulfil the demands of consumers by delivering a high grade of quality power to them to run their equipment, thus forced manufacturers to develop and improve their electric equipment and getting them protected against disturbances or at least to surpass them.

There are many techniques have presented to mitigate power quality problems that exist in the systems or equipment to decrease their effects and enhance quality of supplied power. This has encouraged engineers to develop a new era of research especially in fields of power electronics, control engineering and other branches of engineering to design devices and techniques to overcome PQ problems.

these developments researches has been changed the state of power electronics and as a result to increase numbers of equipment that depending on power converters at the front end which requires modifying to be meet the emerging requirements. That led to some of converters to be outdated thus increase the need to satisfy the demand by setting a better substitutes.

Some special applications demand need urgently to develop a new circuit configuration have front-end converters. For that a certain standards has been developed by some organizations like International Electro-technical Commission (IEC) and Institute of Electrical and Electronics Engineers (IEEE) they benchmarks and enforced them on the electricity producers , manufacturers, , and customers to put down or decrease the PQ problems .

The techniques used to improve PQ in the systems are divided in a different way from those techniques executed in the new advanced equipment.

These methods with their mitigating impact have been sub-partitioned for the electric loads and supply system as both have diverse sorts of issues of PQ. In current nonlinear loads, having these issues of excessiveness in neutral current, unbalanced currents, poor power factor, and harmonic current. A series of power filters of various types like passive, active, and hybrid in parallel, series, or a combination of both arrangements are working externally depends on the loads nature for example, current or voltage fed loads, and a mix of both loads to have such issues relieved.

Though, in specific cases, the PQ issues could be other than those issues of harmonics like that in the distribution systems, and some of custom devices like DVRs (dynamic voltage restorers), DSTATCOMs (distribution static compensators), and UPQCs (unified power quality conditioners) have been employed to mitigate current, voltage or both types of PQ problems.

The techniques of enhancing PQ working in new propelled systems depend on adjusting the entry stage of these systems with power factor corrected converters, as well, known as enhanced power quality AC–DC converters (IPQCs), AC–AC conversion or AC-DC matrix converter, multi-pulse AC–DC converters, as so on. Which employed to mitigate numbers of the PQ issues and issues in the supply system by means of getting clean power from the electric power suppliers.

This chapter investigates the issues of power quality, their roots and in addition to their adverse impacts so as to understand some solutions containing voltage sag (voltage dip) and voltage swell.

Power Quality, this term has a different meaning to different people. Power quality is "The delivery of voltages and system design so that the client of electric power can consume electric energy from the distribution system effectively without obstruction or interference".

Institute of Electrical and Electronic Engineers (IEEE) defines power quality as "the idea of driving and establishing delicate electronic hardware in a way reasonable for the equipment" [3].

A wide meaning of power quality limits on system reliability, dielectric selection on equipment and conductors, long-term outages, voltage unbalance in three-phase systems, power electronics and their interface with the electric power supply and numerous different areas.

Power quality has turned out to be one of the motivating areas for research in the electric systems because of its monetary effects for all of different layers of producers, clients and electricity companies. Power quality is characterized basically as an arrangement of electrical limits that enable certain equipment to function appropriately and as required with no considerable loss of execution or future [4]. This definition involves that we request two things from an equipment; namely performance and expectation of long working life.

## **2.2 Problems of Power Quality**

Problems related to Power Quality become a most important concern nowadays. The power supply voltage is perfect when it keeps up a steady magnitude and an uninterrupted sinusoidal wave form. Phenomenon producing an alteration in this perfect state would have its disturbing impact.

The huge number of power electronics based equipment has exercised a great influence on the quality of electric power supplies. The widespread electronic equipment's use as in information technology equipment, power electronic like ASD (Adjustable speed drives), PLC (programmable logic controllers), and energy-efficient

lighting cause harmonics in the network voltages [3]. Moreover, welding machines and large arc furnaces as conventional loads are the causes of fluctuation and imbalance in voltage, as well as the flicker.

These loads are the major causes as well as the major victims of the problems of power quality. In line with the progress in technology, the international economy has developed towards globalization and the decrease in profit margins of many activities becomes notable.

The majority of processes whether industrial, services and even residential are so sensitive to the problems of PQ, thus, the availability of electric power quality becomes a key factor for competitiveness in every sector. The most critical areas are the continuous process industry and the services of information technology. The occurrence of disturbance causes great financial losses due to the consequent loss of productivity and competitiveness.

Actually, serious efforts have been considered by utilities. Consumers for example require a higher level of Power Quality than the one supplied by modern electric networks. This entails the need to take some measures that help in achieving higher levels of PQ. Various types of disturbances have been defined to the normal power system voltage. The term of “Power Quality” is associated with different kinds of disturbances such as harmonics, transients, outages, faults, sags, swells, dips and flicker. Some of these disturbances are mentioned in the following:

### **2.2.1 Voltage Dip**

The definition of voltage dip or sag is “a decrease in the normal voltage level between 10 and 90% of the nominal RMS voltage at the power frequency, for durations of 0.5 cycle to 1 minute”. Figure 2.1 shows that because of the voltage sag, there is a decrease in the voltage magnitude. These voltage sags are commonly triggered by heavy loads connection, large motors start-up as well as faults in the installation of consumers. Large induction motors’ starting can be the cause for voltage dip because these motor’s current is drawn up to 10 times than the full load current when starting.

Voltage sag’s consequences are efficiency loss and disconnection in electric rotating machines, tripping of electromagnetic relays and also malfunction of

information technology equipment specifically systems of microprocessor-based control [1].

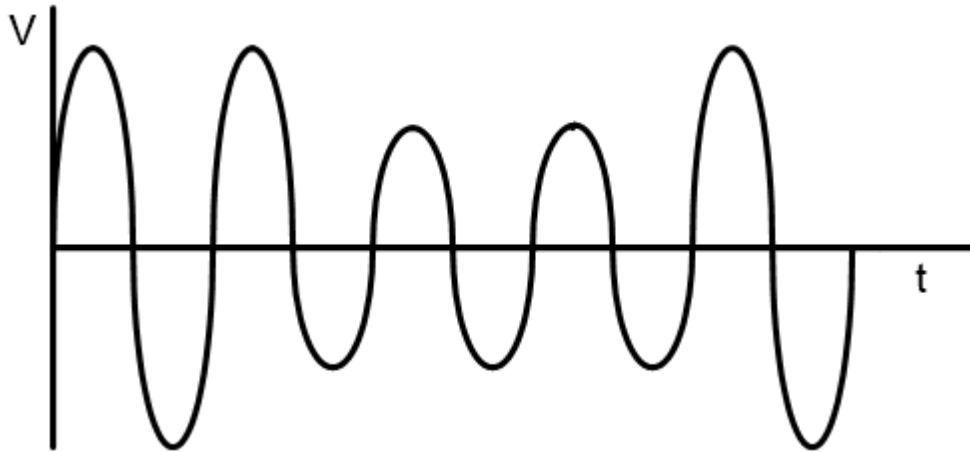


**Figure 2.1:** Voltage sag.

### **2.2.2 Voltage Swell**

Voltage swell can be defined as “a momentary increase of the voltage at the power frequency, outside the normal tolerances, with duration of more than one cycle and typically less than a few seconds” [3]. Figure 2.2 indicates that voltage swell causes an increase in voltage magnitude. Swelling in the voltage is caused by badly dimensioned power sources, line faults and incorrect tap settings in tap changers in substations.

A single line to ground (SLG) fault can cause a swelling in the voltage in the healthy phases. The energizing of large capacitor bank could be a cause for swell. The consequences of voltage swell are the flickers occur in screen and lighting, and loss of data and damage or stop of sensitive equipment.

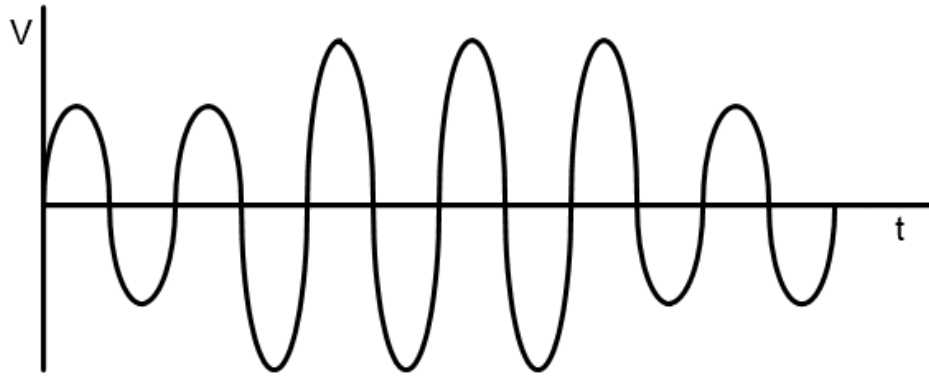


**Figure 2.2:** Voltage Swell.

### **2.2.3 Interruption**

It can be defined as a decrease in line voltage or current to less than 10 percent of the nominal value, not exceeding 60 seconds in length. It has two kinds mentioned below:

#### **2.2.3.1 Very Short Interruption**

The definition of 'Very short interruption' is an overall interruption of electrical supply for duration from few milliseconds to one or two seconds as in figure 2.3. It can be caused by lightning, insulation failure, faults in the system, failure of equipment and insulator flashover. Very short interruption results in the loss of information and malfunction of data processing equipment, tripping of protection devices and stoppage of sensitive equipment [2].

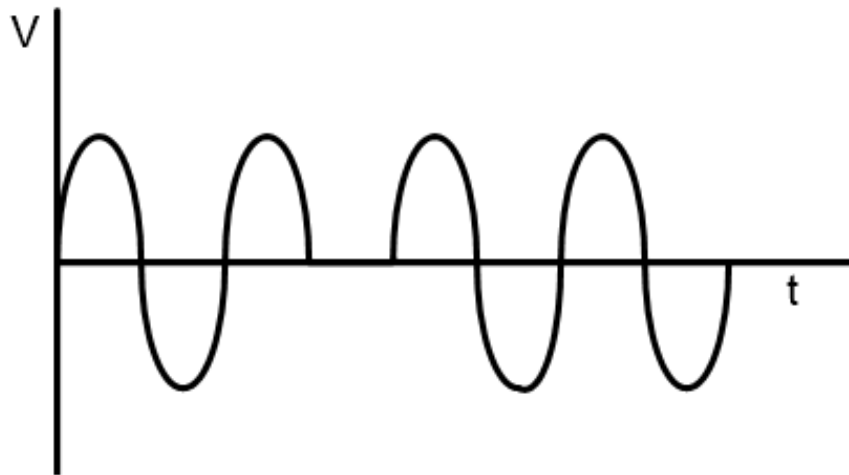


**Figure 2.3:** Very short interruptions.

### 2.2.3.2 Long Interruptions

Long interruptions can be defined as utility power loss which lasts more than 2 minutes as a result of major local area or regional electrical events which are seen in figure 2.4. Such interruptions are caused by failure of equipment in the power system network and objects striking lines or poles, storms, malfunctioning of control and faults in power system. Long interruptions' consequences are equipment stoppage.

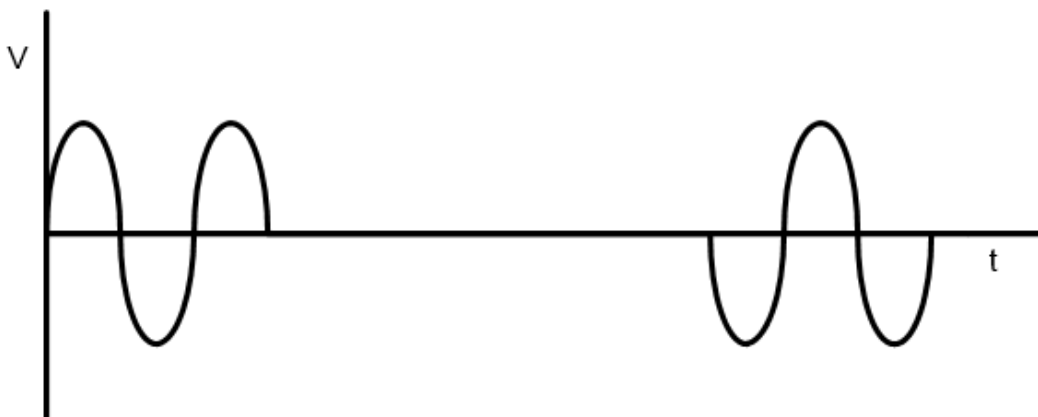


**Figure 2.4:** Long interruptions.

## 2.2.4 Transients

Transients are defined as the very fast variation occurs in the voltage values for durations from multi microseconds to few milliseconds. Such variations can reach thousands of volts, even in low level of voltage. Two kinds of transients are mentioned below:

### 2.2.4.1 Impulsive Transients

They can be defined as a brief, unidirectional variation in current, voltage, or both of them on a power line as explained in figure 2.5. They are caused by disconnection of heavy loads, lightning, and inductive loads switching. Their consequences are the failure of insulation materials, electronic components destruction, errors in data processing and electromagnetic interference [1].



**Figure 2.5:** Impulsive transients.

### 2.2.4.2 Oscillatory Transients

They are brief, bidirectional variations in current, voltage or both of them on a power line as seen in figure 2.6, which are caused as a result of inductive loads switching, power factor correction capacitors, and transformer Ferro-resonance. Such transients have the consequences of insulation materials failure, equipment and electromagnetic interference and cables overheating.





**Figure 2.6:** Oscillatory transients.

### **2.2.5 Harmonic Distortion**

The definition of Harmonics is a steady-state distortion of voltage and current waveforms as a result of power system's non-linear loads. Among the non-linear loads are arc furnaces, electronic power converters and adjustable-speed drives. The waveform corresponds to the sum of different sine waves with different phase and magnitude, which have multiple frequencies of power system frequency as seen in figure 2.7.

The causes of harmonics are the electrical machines that exceed the knee of the magnetization curve (magnetic saturation) in their work, welding machines, DC brush motors and non-linear loads (such as power electronics equipment including ASDs, arc furnaces, rectifiers, switched mode power supplies, high-efficiency lighting and equipment of data processing).

Their consequences are a growing probability in the occurrence of resonance, cables overheating and equipment, neutral overload in 3-phase systems, efficiency loss in electric machines as well as an electromagnetic interference with communication systems [3].

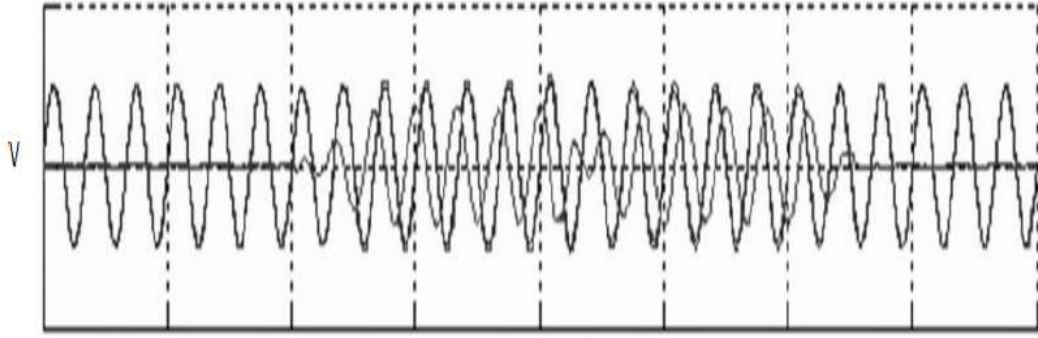


**Figure 2.7:** Harmonic distortion.

Levels of harmonic distortions can be identified via the calculation of THD (total harmonic distortion) which works on measuring the complete harmonic spectrum with magnitudes and phase angles of every individual harmonic component. The representation of THD is the square-root of sum of the squares of every individual harmonic component. Voltage THD is given by:

$$V_{THD} = \frac{\sqrt{\sum_{n=2}^{\infty} V_n^2}}{V_1} \quad (2.1)$$

Where  $V_1$  is the rms magnitude of the fundamental component and  $V_n$  is the rms magnitude of component  $n$ , where  $n=2, \dots, \infty$ .

This approach is problematic in the sense that if there is no fundamental component, THD become infinity. To end this obscurity, an alternate definition is used to represent the harmonic distortion. It is named the distortion index (DIN) which is:

$$DIN = \frac{\sqrt{\sum_{n=2}^{\infty} V_n^2}}{\sqrt{\sum_{n=1}^{\infty} V_n^2}} \quad (2.2)$$

THD and DIN are interrelated by the equations below:

$$DIN = \frac{THD}{\sqrt{1 + THD^2}} \quad (2.3)$$

$$THD = \frac{DIN}{\sqrt{1 - DIN^2}} \quad (2.4)$$

### 2.2.6 Voltage Fluctuation

Fluctuations of voltage are defined as systematic variations of voltage or a series of casual changes in voltage magnitude that lies in the range of 0.9 to 1.1p.u as illustrated in figure 2.8 [4]. These fluctuations result from frequent start or stop of electric motors, arc furnaces and oscillating loads. Their consequences include voltages and flickers of screens and lightings [2].

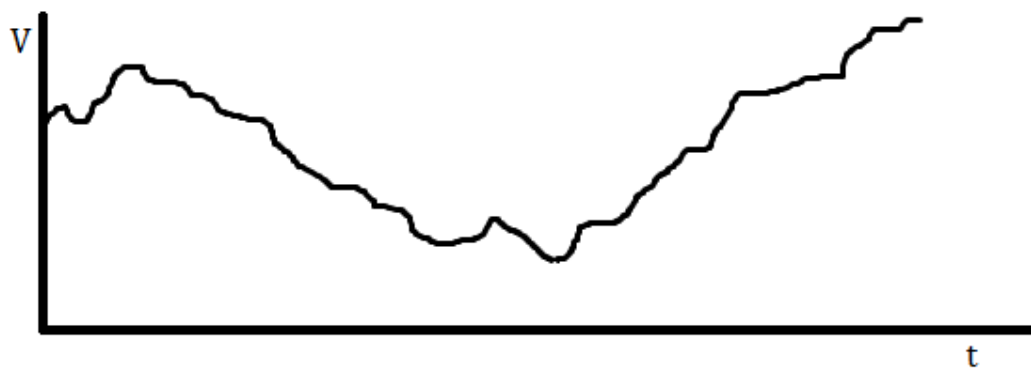


**Figure 2.8:** Voltage fluctuation.

### 2.2.7 Noise

Noise is defined as the superimposition of signals that have high-frequency on the waveform of the power-system frequency. The waveform caused by the noise is shown in figure 2.9. This noise results from television diffusion and radiation because of welding machines, electromagnetic interferences triggered by Hertzian waves like arc furnaces, microwaves, and electronic equipment and incorrect grounding. The noise's consequences include disturbances occur on sensitive electronic equipment and errors in data processing.



**Figure 2.9:** Noise.

### 2.2.8 Voltage Unbalance

Voltage unbalance can be defined as the variation of voltage in a three-phase system in which the three voltage magnitudes or the phase angle differences between them are not equal as illustrated in figure 2.10. This unbalance is triggered by large single-phase loads such as traction loads and induction furnaces and bad distribution of all single-phase loads by the system's three phases (fault could also be a possible reason).

Such unbalance leads to unbalanced systems that show the existence of a harmful negative sequence to all the three phase loads. Three-phase induction machines are the most affected loads.

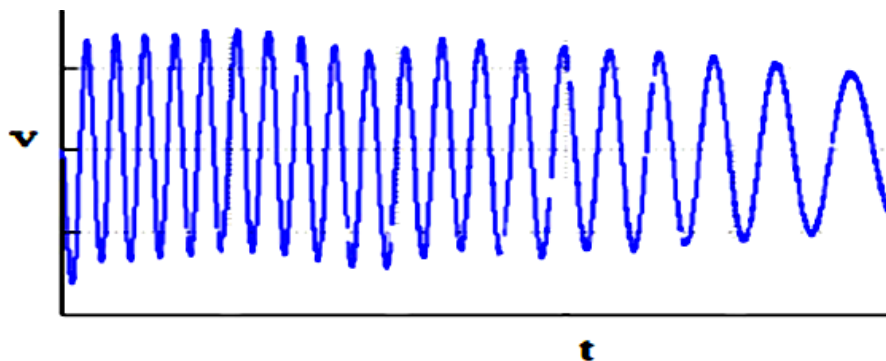


**Figure 2.10:** Voltage unbalance.

### **2.3 Causes of Power Quality Problems**

There are a few issues of power quality in the modern quick paced changing electrical systems. These issues of PQ can be brought on by real causes which are partitioned into natural and man-made causes in respect of voltage, current, frequency.... and so forth.

Poor power quality is s brought on by natural causes, for example, lightning, faults, and terrible states of climate like disappointment or hurricanes ... and so on. Then again, man-made causes are to a great extent connected to system operations or loads.

The man-made causes related with the loads contain nonlinear loads such as saturating transformers and electric equipment, or loads with solid-state controllers like systems of vapor lamp-based lighting, ASDs, computer power supplies, UPSs, TVs, and arc furnaces.

The reasons for such issues related with system operations are huge loads, feeders, transformers switching, and capacitors. The effects of natural reasons are PQ issues that have transient nature, such as voltage sag (dip), swell, distortion of voltage, and oscillatory and impulsive transients. Then again, the consequences of man-made causes are both steady state and transient kinds of issues in PQ [29].

Table 2.1 shows numerous issues of PQ and additionally their causes. One of the eminent issues of PQ is the presence of harmonics as a result of many loads that demonstrate in a nonlinearly behavior, changing between conventional ones like electrical machines, transformers, and furnaces to new ones like converters of power in vapor lamps, ASDs utilizing cyclo-converters, AC-DC converters, AC voltage controllers, SMPS (switched-mode power supplies), HVDC transmission, static VAR compensators, ... and so forth.

### **2.4 Poor Quality Effects on Power System Devices**

There are serious financial ramifications in the power quality for electricity utilities, clients, and industrialists of electrical equipment. The current drift is to

modernize and automate the industry through increasing and encouraging computers use, micro-processors, and power electronic systems like adaptable speed drives [4].

Then, the understanding of how such disturbances are caused and how do they influence the components are necessary to stop failures. Even if there is no failure, poor power quality and harmonics increase losses and reduce the lifetime of power components and end-use devices. Below are some of the major detrimental effects of poor power quality:

- 1) Heating, noise and reduced life on capacitors, fuses, surge suppressors, cables rotating machines, and customers' equipment.
- 2) Instability of Harmonics could be triggered by big and unpredicted harmonic sources like arc furnaces.
- 3) Extra loss of transmission lines, generators, cables, transformers, and AC motors could also be caused because of harmonics.
- 4) Unpredicted disturbances may cause failure of power system components and customer loads like magnifications of voltage and or current because of the Ferro-resonance and parallel resonance.
- 5) Protective devices and controllers malfunctioning may also occur like fuse and relays.
- 6) Utility companies concerned with distribution transformer might be in need to be de-rated in order to evade premature failure because of over-heat.
- 7) Inter-harmonics could happen perturbing ripple control signals and causing flicker at sub-harmonic levels.

## **2.5 The Mitigation Techniques for Power Quality Problems**

Due to the increase of issues resulting from power quality in terms of financial loss, raw material waste, loss of production... etc., various kinds of techniques emerged to improve the power quality in the past decades. They include passive components like reactors, capacitors, improved power quality AC–DC converters, a series of power filters, custom power devices, and matrix converters. Yet, the problems of PQ might not be caused due to harmonics in certain cases as in systems of

distribution where problems like poor voltage regulation, load unbalancing, excessive neutral current, low power factor...etc., exist. [29]

Problems of PQ like poor power factor due to reactive power demands could be mitigated via the use of lossless passive elements like reactors and capacitors. In addition, devices of custom power like DSTATCOMs, DVRs, and UPQCs are widely employed to mitigate the voltage, current or both kinds of PQ issues.

Due to the existence of harmonics and other issues of PQ, a series of power filters of different kinds like passive, active and hybrid in parallel, series, or a combining the two structures in single-phase two-wire, three-phase three-wire, and three-phase four-wire systems are employed externally as retrofit solutions to mitigate the problems of power quality via compensating nonlinear loads or voltage-based PQ problems in the AC mains.

Because of the great number of circuits of filters, the filter's more proper configuration is selected to depend upon the loads' nature like voltage-fed loads, current-fed loads, or a blend of both to get the problems mitigated.

The techniques of improving power quality utilized in the up-to-date equipment depend on the adjustment of the input stage of such systems with PFC converters, (also called as IPQCs), AC-AC conversion, multi-pulse AC-DC converters, matrix converters for AC-DC... etc., which works on mitigating the issues of power quality inherently and also in the supply system via clean power drawing from utilities.

There are several circuits of the converters of buck-boost, boost, buck, multilevel, and multi-pulse kinds for uni-directional and bi-directional power flow with and without isolation in three-phase and single-phase supply systems to be suitable for applications of special kind.

These are employed as front-end converters in the input stage as a part of the whole equipment. In some cases, they immune this equipment against the problems of power quality in the supply system.

**Table 2.1: Problems of power quality (causes and effects)**

Problems	Category	Categorization	Causes	Effects
Transients	Impulsive	Peak, rise time and duration	Lightning strikes, transformer energization, capacitor switching	Power system resonance
	Oscillatory	Peak magnitude and frequency components	Line, capacitor, or load switching	System resonance
Short-duration voltage variation	Sag	Magnitude, duration	Motor starting, single line to ground faults	Protection malfunction, loss of production
	Swell	Magnitude, duration	Capacitor switching, large load switching, faults	Protection malfunction, stress on computers and home appliances
	Interruption	Duration	Temporary faults	Loss of production, malfunction of fire alarms
Long-duration voltage variation	Sustained Interruption	Duration	Faults	Loss of production
	Under voltage	Magnitude, duration	Switching on loads, capacitor de-energization	Increased losses, heating
	Over voltage	Magnitude, duration	Switching off loads, capacitor energization	Damage to household appliances
Voltage imbalance		Symmetrical components	Single-phase load, single phasing	Heating of motors



**Table 2.1 (Continue): Problems of power quality (causes and effects)**

Problems	Category	Categorization	Causes	Effects
Waveform distortion	DC offset	Volts, amperes	Geomagnetic disturbance, rectification	Saturation in transformers
	Harmonics	THD, harmonic spectrum	ASDs, nonlinear loads	Increased losses, poor power factor
	Inter harmonics	THD, harmonic spectrum	ASDs, nonlinear loads	Acoustic noise in power equipment
	Notching	THD, harmonic spectrum	Power electronic converters	Damage to capacitive components
	Noise	THD, harmonic spectrum	Arc furnaces, arc lamps, power converter	Capacitor overloading, disturbance to appliances
Voltage flicker		Frequency of occurrence, modulating frequency	Arc furnaces, arc lamps	Human health, irritation, headache, migraine
Voltage fluctuations		Intermittent	Load changes	Protection malfunction, light intensity changes
Power frequency variations			Faults, disturbances in isolated customer-owned systems and islanding operations	Damage to generator and turbine shafts

## CHAPTER THREE

### D-STATCOM AND CONTROL METHODS

#### 3.1 D-STATCOM

D-STATCOM is one of the Custom Power Devices used in distribution systems, it is normally shunted colligated solid state device, in order to offer regulation for disturbances at load side. It is actually a STATCOM (static compensator), a member of a FACTS devices that is used in transmission systems. When this STATCOM is used for distribution system it is known as DSTATCOM (Distribution STATCOM).

DSTATCOM is employed at the distribution level for improving power factor and regulating voltage. Figure 3.1 demonstrates line diagram of DSTATCOM.

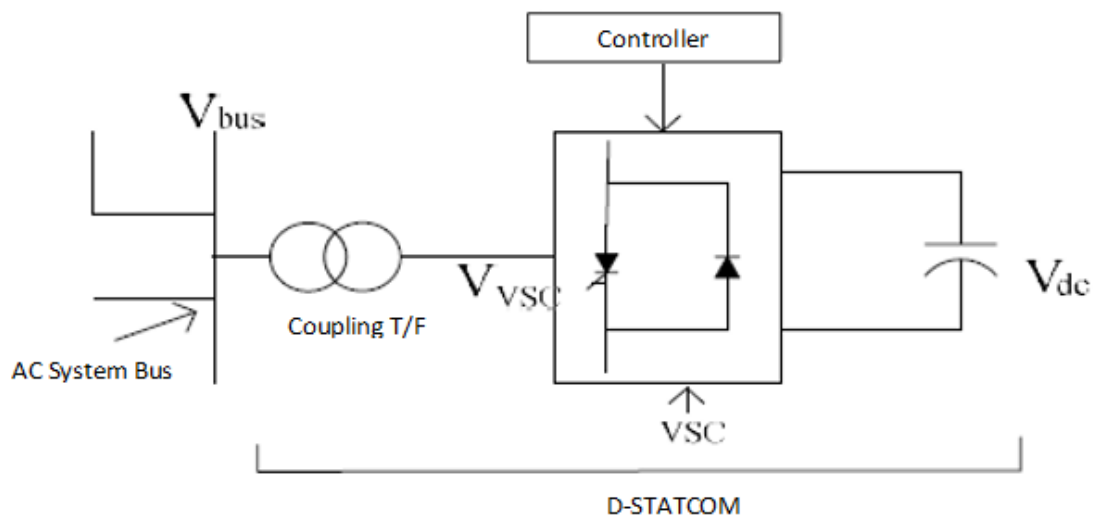


**Figure 3.1:** D-STATCOM.

DSTATCOM is power electronics technology based VSC which is itself a versatile device which counterbalances the reactive power in AC systems. The reactive power compensation is attained through regulation of a VSC behind leakage impedance of a transformer. It analyses the waveform with reference to a reference AC signal and therefore, it provides nearly the accurate amount of leading or lagging reactive compensation to reduce fluctuations in voltage.

It is also termed as a shunt active filter that mitigates Voltage sags and swells and brings down total harmonic distortion level and also compensates for unbalancing or distortions in the current at source.

DSTATCOM is colligated to the system at PCC (point of common coupling) in order to deliver current to the coupled system at the instant of connection of unbalanced or non-linear load. The positioning of DSTATCOM is in shunt to the distribution system. It is a device with lower capital cost, better dynamics, and absence of inertia, lowers operating and maintenance cost.

### **3.2 Basic Elements of DSTATCOM**

The basic configuration of DSTATCOM consists of:

- 1) Voltage Source Converter.
- 2) L-C Passive Filter.
- 3) Coupling Transformer.
- 4) Control Block.
- 5) Energy Storage Device (it may be a large capacitor or a combination of batteries, or distributed generators with a bank of capacitors).

Figure 3.2 demonstrates different components of DSTATCOM as shown below. All components are marked and briefed explanation of them presented in this chapter.

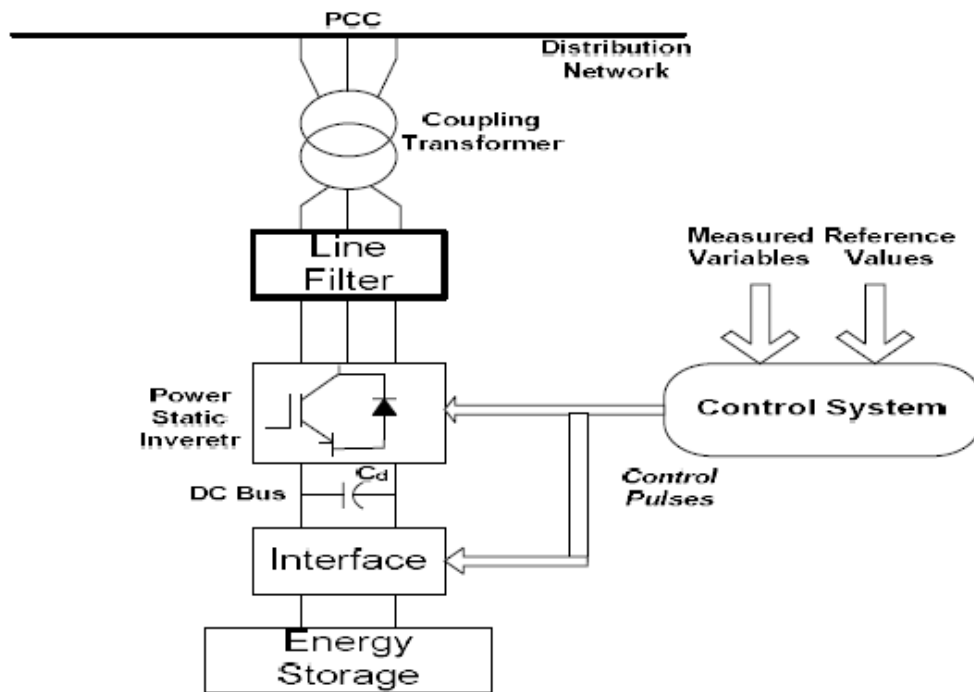


**Figure 3.2:** Components of D-STATCOM.

### 3.2.1 Voltage Source Converter

A voltage-source converter (VSC) according to the compensation required offers the regulated output voltage in terms of magnitude and phase angle to result in either leading or lagging reactive current. It uses semiconductor technology to perform its operation. It helps in conversion of DC voltage stored in the storage device to three phase AC output.

Features of VSC-based transmission [30]:

- Independent control of reactive and active power.
- Reactive control independent of another terminal(s).
- Simpler interface with AC system.
- Provides continuous AC voltage regulation.
- Operation in extremely weak systems.
- No commutation failures.
- No polarity reversal needed to reverse power.
- Variable frequency.

### 3.2.1.1 Distribution Static Synchronous Compensator (D-STATCOM) based on Six-Pulse VSI

The Distribution Static COMPensators (D-STATCOM) the device has the capability to generate and absorb active and reactive power, the main use of this device is applied in the field of reactive power exchange to compensate the required reactive power that needed in AC system.

The distribution static synchronous compensator (D-STATCOM) depend on six-pulse VSI, figure 3.3, and is the major building block of high power static VAR compensator. The configuration six-pulse has no a proper performance in high power applications, because it shows a high rate of harmonic. Accordingly, the current analysis aims to give an important insight into the analysis of higher pulse arrangements that are more sophisticated.

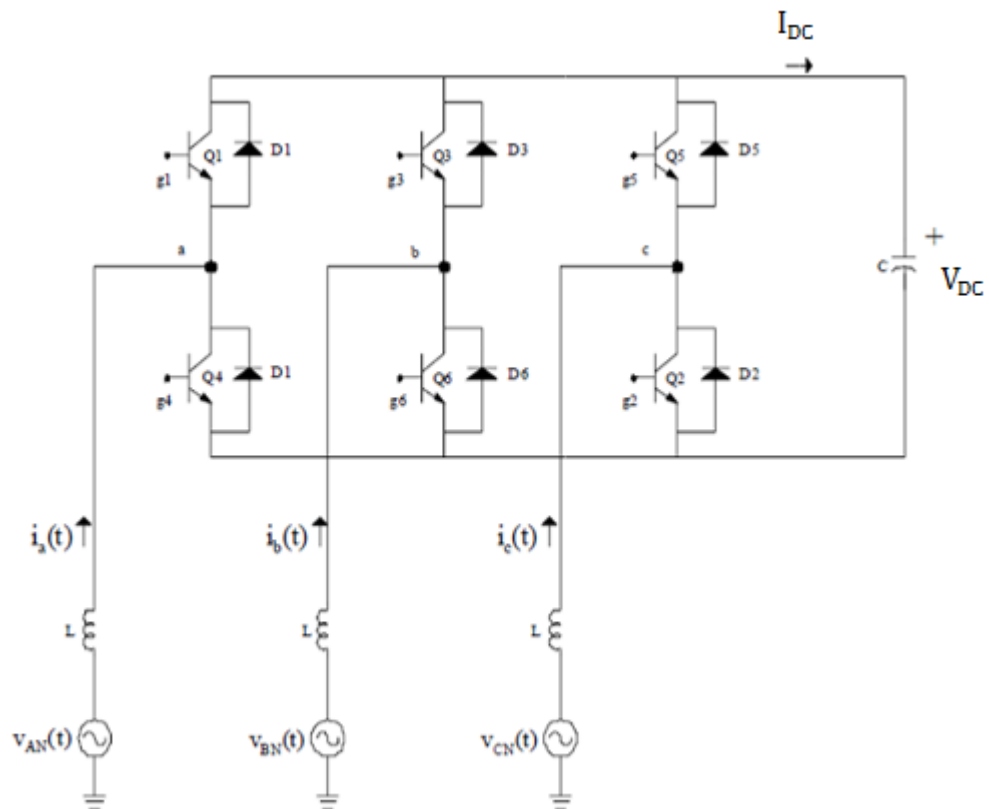


Figure 3.3: Six-pulse VSI D-STATCOM.

### 3.2.1.1.1 Reactive Power Exchange

The exchange of reactive power between the compensator and AC system is under control by changing and varying the magnitude of the essential part of the inverter's voltage below and above the AC system's magnitude.

Control of the compensator is managed by small variations done in the switching angle of the semiconductor devices, thus the essential part of the voltage created by the inverter is enforced to lag or lead the AC system voltage by a few degrees. This results in the flowing of active power into or out of the inverter adjusting the value of the DC capacitor voltage, and then the resultant reactive power, and the inverter terminal voltage's magnitude. In case of providing only reactive power by the compensator, the active power of the DC capacitor is zero. Therefore, the capacitor does not change its voltage. Accordingly, the capacitor has no role in the generation of reactive power [31].

#### 3.2.1.1.1.1 Analysis of the AC current signals

The voltage across the tie inductor governs the current passing through the compensator and the AC system. When the AC voltage is approximately pure sinusoidal function,  $e_{an}(t) = V_m \sin(\omega t)$ , then the fundamentals magnitude and harmonic elements are shown by equations (3.1) and (3.2). An instantaneous phase voltage is obtained as:

$$v_{an}(t) = 0.6366V_{DC} \sin(\omega t) \quad , \text{ then:}$$

$$i_a(t)_1 = -\frac{V_m - 0.6366 V_{DC}}{\omega L} \cos(\omega t) ; \quad (\text{fundamental component})$$

$$i_a(t)_n = \frac{0.6366 V_{DC}}{n^2 \omega L} \cos(n\omega t) ; \quad (nth \text{ harmonic component})$$

The fundamental current is also called fundamental reactive current  $I_q$ .

$$I_{a_1} = I_q = \frac{V_m - 0.6366 V_{DC}}{\omega L} \quad (3.1)$$

$$I_{a_n} = I_{q_n} = \frac{0.6366 V_{DC}}{n^2 \omega L}, \quad n > 1 \quad (3.2)$$

The basic current will be leading when  $V_m < 0.6366V_{DC}$ ; that is, if the voltage magnitude of the inverter is rise above the voltage of the AC system (the current drifts from converter toward the AC system); the AC system showed the compensator as a capacitor. The basic current is considering lagging when  $V_m > 0.6366V_{DC}$ , that is, if the voltage magnitude of the inverter is reduced below the voltage of the AC system (the current drifts from the AC system to the compensator); as such, AC system considers the compensator as a inductor, Figure 3.4.

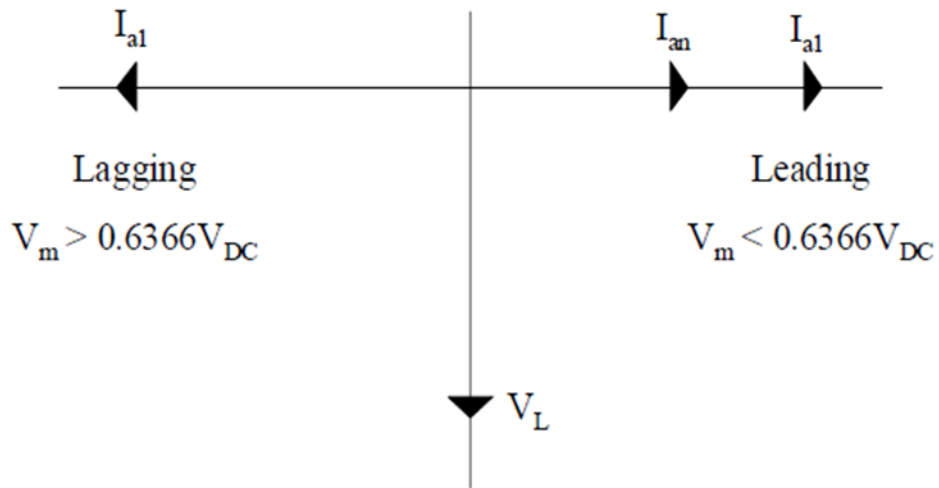


**Figure 3.4:** Phase relationship between the inductor voltage  $V_L$  and the essential current  $I_{a_1}$ .

From equation (3.2) can be deduced that the harmonic currents only flow from the compensator to the AC system. Figure 3.5 represent the relation between the DC voltage ( $V_{DC}$ ) and the essential reactive current. The lower-order harmonic currents as a function of the fundamental reactive current are shown too.

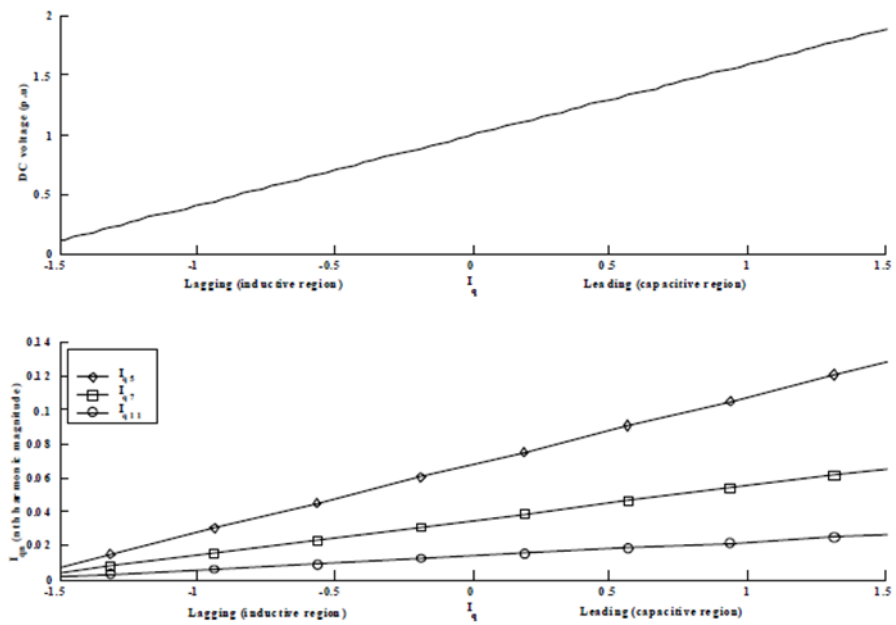


**Figure 3.5:** Relationship between DC voltage, fundamental, and harmonics current.

Considering the voltage across the tie inductor over each  $60^\circ$  conduction interval, figure 3.6.

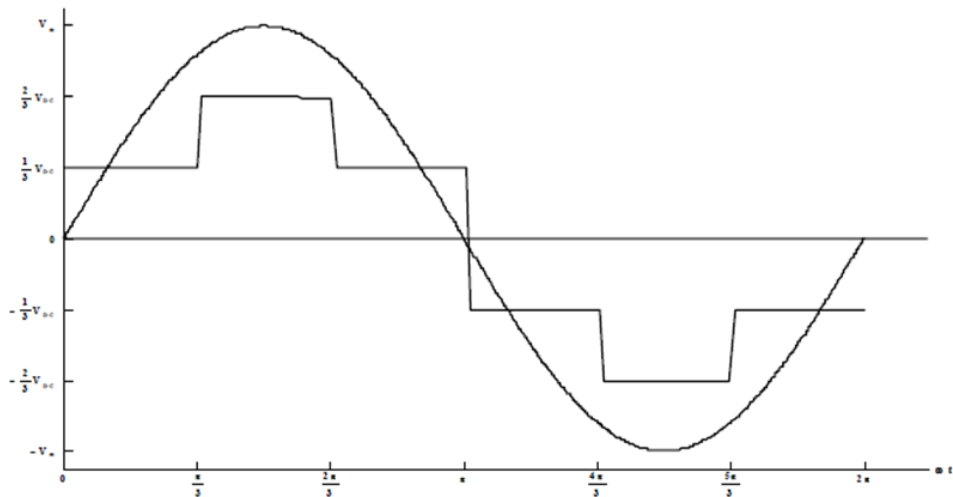


**Figure 3.6:** AC system voltage and voltage compensator  $v_{an}(t)$ .



The relation portraying the AC current  $i_a(t)$  is inferred. The other two-phase currents,  $i_b(t)$  and  $i_c(t)$ , phase are shifted by  $120^\circ$  and  $240^\circ$ , respectively, from  $i_a(t)$ . At any time  $v_L(t) = L \frac{d}{dt} i_a(t)$ , where  $v_L(t)$  is the instantaneous voltage of inductor, which is the instantaneous difference across the AC system voltage,  $e_{an}(t)$ , and the compensator voltage  $v_{an}(t)$ . The differential equations of  $60^\circ$  conduction interval can be expressed for the inductor voltage and current of phase (a).

- Interval:  $0 \leq \omega t \leq \pi/3$

$$v_L(t) = V_m \sin(\omega t) - \frac{1}{3} V_{DC} = L \frac{d}{dt} i_a(t)$$

$$i_a(t) = -\frac{V_m}{\omega L} (\cos(\omega t) - 1) - \frac{1}{3L} V_{DC} t + I_0 \quad (3.3)$$

Where ( $I_0$ ): Stands to the initial condition at  $t = 0$ ;  $i_a(0) = I_0$ .

Interval:  $\pi/3 \leq \omega t \leq 2\pi/3$

$$v_L(t) = V_m \sin(\omega t) - \frac{2}{3} V_{DC} = L \frac{d}{dt} i_a(t)$$

$$i_a(t) = -\frac{V_m}{\omega L} (\cos(\omega t) - 0.5) - \left( \frac{2}{3L} t - \frac{2\pi}{9\omega L} \right) V_{DC} + I_1 \quad (3.4)$$

Where:

$$I_1 = i_a \left( \frac{\pi}{3\omega} \right)$$

- Interval:  $2\pi/3 \leq \omega t \leq \pi$

$$v_L(t) = V_m \sin(\omega t) - \frac{1}{3} V_{DC} = L \frac{d}{dt} i_a(t)$$

$$i_a(t) = -\frac{V_m}{\omega L} (\cos(\omega t) - 0.5) - \left( \frac{1}{3L} t - \frac{2\pi}{9\omega L} \right) V_{DC} + I_2 \quad (3.5)$$

Where:

$$I_2 = i_a \left( \frac{2\pi}{3\omega} \right)$$

It is common that the AC current waveform is symmetric in the steady state, therefore,

$$i_a\left(\frac{\pi}{2\omega}\right) = 0$$

Taking into account the above property, the steady state initial condition  $I_0$  can be estimated as expressed below:

$$i_a\left(\frac{\pi}{2\omega}\right) = -\frac{V_m}{\omega L}\left(\cos\left(\frac{\pi}{2}\right) - 0.5\right) - \left(\frac{2}{3L} \cdot \frac{\pi}{2\omega} - \frac{2\pi}{9\omega L}\right)V_{DC} + I_1 = 0$$

$$I_1 = -\frac{V_m}{\omega L}0.5 + \frac{\pi}{9\omega L}V_{DC} \quad (3.6)$$

$$I_1 = i_a\left(\frac{\pi}{3\omega}\right) = -\frac{V_m}{\omega L}\left(\cos\left(\frac{\pi}{3}\right) - 1\right) - \frac{1}{3L}V_{DC} \cdot \frac{\pi}{3\omega} + I_0$$

$$I_1 = \frac{V_m}{\omega L}0.5 - \frac{\pi}{9\omega L}V_{DC} + I_0 \quad (3.7)$$

Equating equations (3.6) and (3.7), the steady state condition is estimated:

$$I_0 = -\frac{V_m}{\omega L} + \frac{2\pi}{9\omega L}V_{DC} \quad (3.8)$$

Substituting equation (3.8) into equation (3.3) the steady state equations are derived:

$$i_a(t) = -\frac{V_m}{\omega L}\cos(\omega t) - \left(\frac{1}{3L}t - \frac{2\pi}{9\omega L}\right)V_{DC} \quad (3.9)$$

Where:

$$0 \leq \omega t \leq \pi/3$$

$$i_a(t) = -\frac{V_m}{\omega L}\cos(\omega t) - \left(\frac{2}{3L}t - \frac{\pi}{3\omega L}\right)V_{DC} \quad (3.10)$$

$$\pi/3 \leq \omega t \leq 2\pi/3$$

$$i_a(t) = -\frac{V_m}{\omega L} \cos(\omega t) - \left(\frac{1}{3L}t - \frac{\pi}{9\omega L}\right) V_{DC} \quad (3.11)$$

$$2\pi/3 \leq \omega t \leq \pi$$

During the interval  $\pi \leq \omega t \leq 2\pi$  the AC current signal is the negative respect to the one explained in the above-mentioned equations. AC current signal is represented in figure 3.7. For the leading state  $V_{DC} = 6$  V,  $V_m = 2.5$  V, and  $L = 3$  mH were utilized; and  $V_{DC} = 6$  V,  $V_m = 4.5$  V, and  $L = 3$  mH for the lagging state.

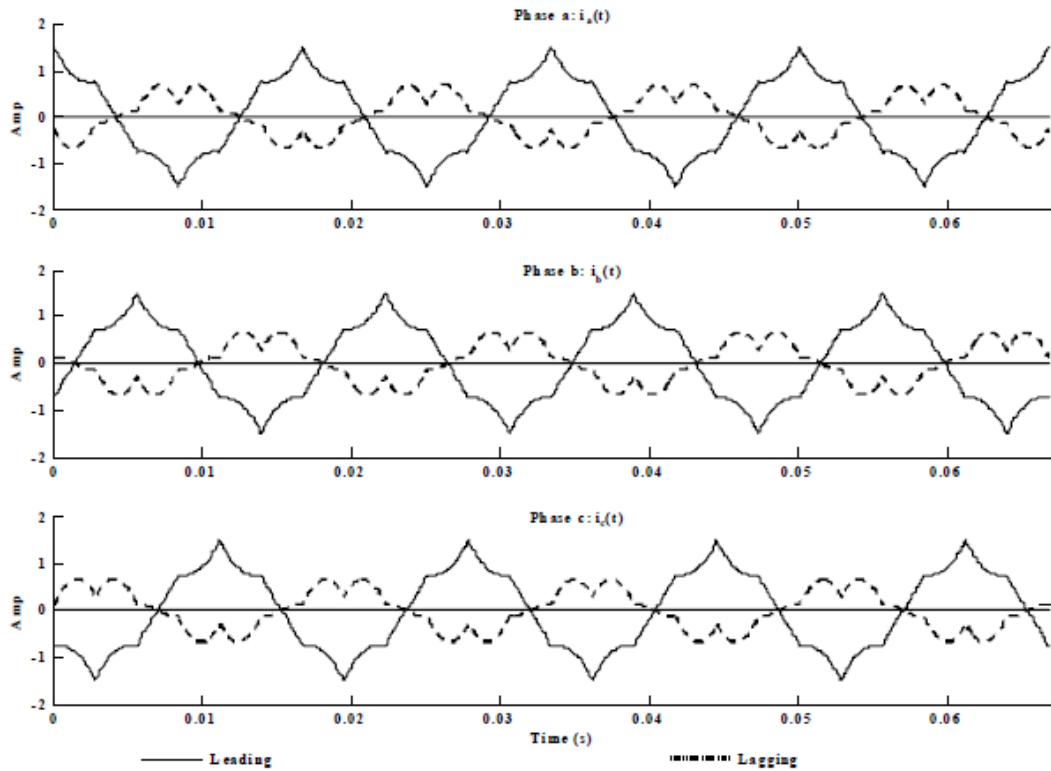


**Figure 3.7:** AC current waveform.

### 3.2.1.1.1.2 Conduction period transistors and diodes

With the above-mentioned AC current equations, it is likely to expect the conduction interval of each transistor and diode. In generating only reactive power (zero power factor), both transistors and diodes of the inverter circuit conduct for  $90^\circ$ .

In case of absorbing the reactive power by the compensator, the transistors regularly turn off at zero current and in case of generating reactive power, the transistors turn off at the peak of the AC current signal. So, the following algorithm suggests a way to limit the conduction interval of each device at any power factor depend on the firing control signals and the AC current signals.

1) Leg 1:

Pulse  $g_1$  on:

- If  $i_a(t)$  is positive,  $D_1$  will conduct.
- If  $i_a(t)$  is negative,  $Q_1$  will conduct.

Pulse  $g_4$  on:

- If  $i_a(t)$  is positive,  $Q_4$  will conduct.
- If  $i_a(t)$  is negative,  $D_4$  will conduct.

2) Leg 2:

Pulse  $g_3$  on:

- If  $i_b(t)$  is positive,  $D_3$  will conduct.
- If  $i_b(t)$  is negative,  $Q_3$  will conduct.

Pulse  $g_6$  on:

- If  $i_b(t)$  is positive,  $Q_6$  will conduct.
- If  $i_b(t)$  is negative,  $D_6$  will conduct.

3) Leg 3:

Pulse  $g_5$  on:

- If  $i_c(t)$  is positive,  $D_5$  will conduct.
- If  $i_c(t)$  is negative,  $Q_5$  will conduct.

Pulse  $g_2$  on:

- If  $i_c(t)$  is positive,  $Q_2$  will conduct.
- If  $i_c(t)$  is negative,  $D_2$  will conduct.

The  $Q_1$  and  $D_1$  conduction period for leading and lagging current are presented in Figure 3.8.

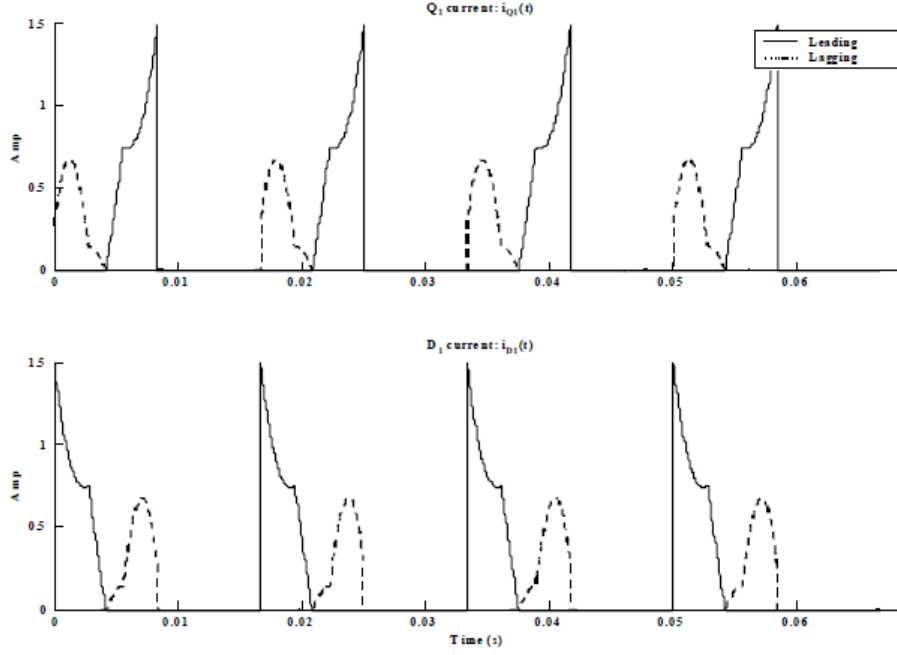


**Figure 3.8:**  $Q_1$  and  $D_1$  conduction period.

### 3.2.1.1.3 Capacitor Current

The capacitor current consists of segments of the three AC phase currents and is reliant on which semiconductor devices are conducting over each  $60^\circ$  interval. The deduction of capacitor current can be drawn in the following way:

$$i_{D_1}(t) + i_{D_3}(t) + i_{D_5}(t) + i_{DC}(t) = i_{Q_1}(t) + i_{Q_3}(t) + i_{Q_5}(t)$$

So that:

$$i_{DC}(t) = i_{Q_1}(t) + i_{Q_3}(t) + i_{Q_5}(t) - (i_{D_1}(t) + i_{D_3}(t) + i_{D_5}(t)) \quad (3.12)$$

- Interval:  $0 \leq \omega t \leq \pi/3$

$$i_{DC}(t) = i_a(t) + i_c(t)$$

Where:

$$i_c(t) = -\frac{V_m}{\omega L} \cos\left(\omega t + \frac{2\pi}{3}\right) - \left(\frac{1}{3L}t + \frac{\pi}{9\omega L}\right)V_{DC}$$

So that:

$$i_{DC}(t) = \frac{V_m}{\omega L} \sin\left(\omega t - \frac{\pi}{6}\right) - \left(\frac{2}{3L}t - \frac{\pi}{9\omega L}\right)V_{DC} \quad (3.13)$$

- Interval:  $\pi/3 \leq \omega t \leq 2\pi/3$

$$i_{DC}(t) = i_a(t)$$

$$i_{DC}(t) = \frac{V_m}{\omega L} \sin\left(\omega t - \frac{\pi}{2}\right) - \left(\frac{2}{3L}t - \frac{\pi}{3\omega L}\right)V_{DC} \quad (3.14)$$

- Interval:  $2\pi/3 \leq \omega t \leq \pi$

$$i_{DC}(t) = i_a(t) + i_b(t)$$

Where:

$$i_b(t) = -\frac{V_m}{\omega L} \cos\left(\omega t - \frac{2\pi}{3}\right) - \left(\frac{1}{3L}t - \frac{4\pi}{9\omega L}\right)V_{DC}$$

So that,

$$i_{DC}(t) = \frac{V_m}{\omega L} \sin\left(\omega t - \frac{5\pi}{6}\right) - \left(\frac{2}{3L}t - \frac{5\pi}{9\omega L}\right)V_{DC} \quad (3.15)$$

These relations are equivalent excluding phase shifted by  $60^\circ$  among them; hence, the capacitors current signals over each of the residual three conduction intervals is matching to that defined by equation (3.13) and yields, in a repetitive signal, six times the corresponding AC power system frequency.

#### 3.2.1.1.1.4 DC Capacitor Voltage

The earlier analysis assumes a steady DC voltage; it is equivalent to take into account an infinite capacitor, therefore zero DC ripple voltage. If a finite capacitor is considerate, a DC ripple voltage exists which relies on the capacitor's values and the capacitor's current.

If the capacitor current stays significantly unchanged from the one mentioned in equation (3.13), an estimation can be done to the capacitor voltage; in which a minimum DC ripple voltage can be gained [32]. The capacitor voltage over the first 60° interval is given by the following:

$$v_{cap}(t) = \frac{1}{C} \int_0^t i_{DC}(t) dt + V_0 \quad (3.16)$$

Where ( $V_0$ ): Stand to the initial condition at  $t = 0$ ;  $V_0 = v_{cap}(0)$ . Substituting equation (3.13) into equation (3.16):

$$v_{cap}(t) = -\frac{V_m}{\omega^2 LC} \cos\left(\omega t - \frac{\pi}{6}\right) - \frac{1}{3LC} V_{DC} t^2 + \frac{\pi}{9\omega LC} V_{DC} t + \frac{\sqrt{3}V_m}{2\omega^2 LC} + V_0 \quad (3.17)$$

The value of ( $V_0$ ) is estimated from the average element of equation (3.17) with the period  $T = \pi/3\omega$ . Simultaneously, the DC voltage level  $V_{DC}$  is limited.

$$V_{DC} = \frac{1}{T} \int_0^{\pi/3\omega} v_{cap}(t) dt \quad (3.18)$$

$$V_{DC} = \frac{3\omega}{\pi} \left( -\frac{V_m}{\omega^3 LC} - \frac{\pi^3}{243\omega^3 LC} V_{DC} + \frac{\pi^3}{162\omega^3 LC} + \frac{\sqrt{3}\pi}{6\omega^3 LC} V_m + \frac{\pi}{3\omega} V_0 \right)$$

Simplifying this expression results:

$$V_0 = 0.0889 \frac{V_m}{\omega^2 LC} - 0.0609 \frac{1}{\omega^2 LC} V_{DC} + V_{DC} \quad (3.19)$$

The current and voltage signals of the capacitor gained by the use of the relations (3.13) and (3.17) are seen in figures (3.9, 3.10). Figure 3.10 explains that the peak capacitor voltage  $V_{pk}$ , exist when a reactive power is generated by the compensator (leading current),  $\omega t = 30^\circ$ .

$$\begin{aligned}
V_{pk} &= v_{cap}\left(\frac{\pi}{6\omega}\right) \\
&= -\frac{V_m}{\omega^2 LC} - \frac{1}{3LC} V_{DC} \left(\frac{\pi}{6\omega}\right)^2 + \frac{\pi}{9\omega LC} V_{DC} \left(\frac{\pi}{6\omega}\right) + \frac{\sqrt{3}}{2\omega^2 LC} V_m \\
&\quad + 0.0889 \frac{V_m}{\omega^2 LC} - 0.0609 \frac{1}{\omega^2 LC} V_{DC} + V_{DC}
\end{aligned}$$

Simplifying, gives rises to:

$$V_{pk} = -0.0451 \frac{V_m}{\omega^2 LC} + 0.0305 \frac{1}{\omega^2 LC} V_{DC} + V_{DC} \quad (3.20)$$

The above peak voltage is important because of the direct application of the capacitor voltage to the semiconductor devices, thus they should be capable of supporting that voltage. Figure 3.11 shows the phase voltage,  $v_{an}(t)$ , and the line to line voltage,  $v_{ab}(t)$ , when the compensator is run with a finite capacitor as a DC source. This figure represents the effect of capacitor ripple voltage. Figure 3.12 introduces the capacitor voltage and current signals.

If the compensator only exchanges reactive power the voltage capacitor does not vary, thus the capacitor current is the one shown in figure 3.9. Based on Fourier analysis it is given by:

$$i_{DC}(t) = \sum_{n=1}^{\infty} I_{DCn} \sin(n\omega t) \quad (3.21)$$

Where:

$$i_{DCn} = \frac{2}{T} \int_0^T i_{DC}(t) \sin(n\omega t) dt$$

$$T = \frac{\pi}{3\omega}$$

Thereby the capacitor voltage is made up only by sinusoidal functions with fixed amplitude and a DC offset as illustrated in figure 3.10.



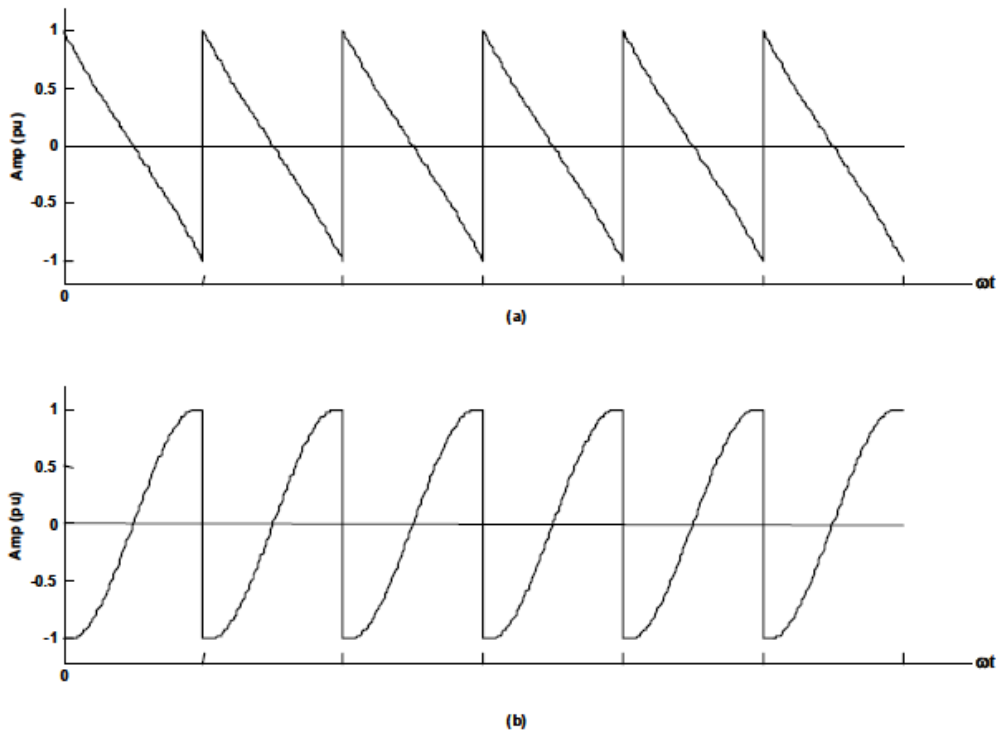


**Figure 3.9:** Capacitor current; a) generating reactive power; b) absorbing reactive power.

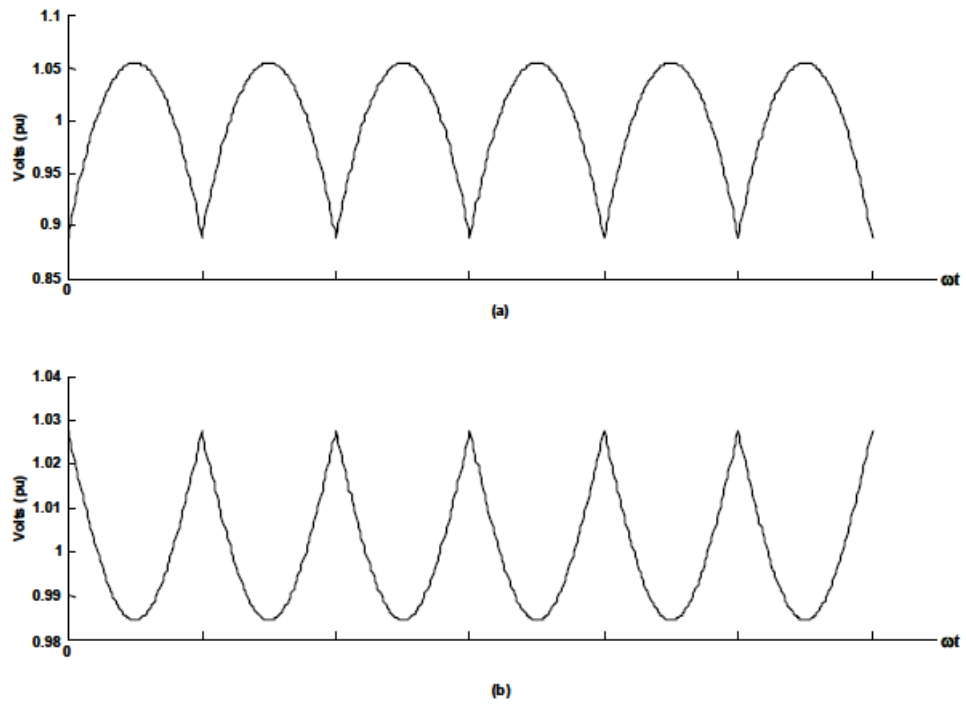


**Figure 3.10:** DC capacitor voltage; a) generating reactive power; b) absorbing reactive power.

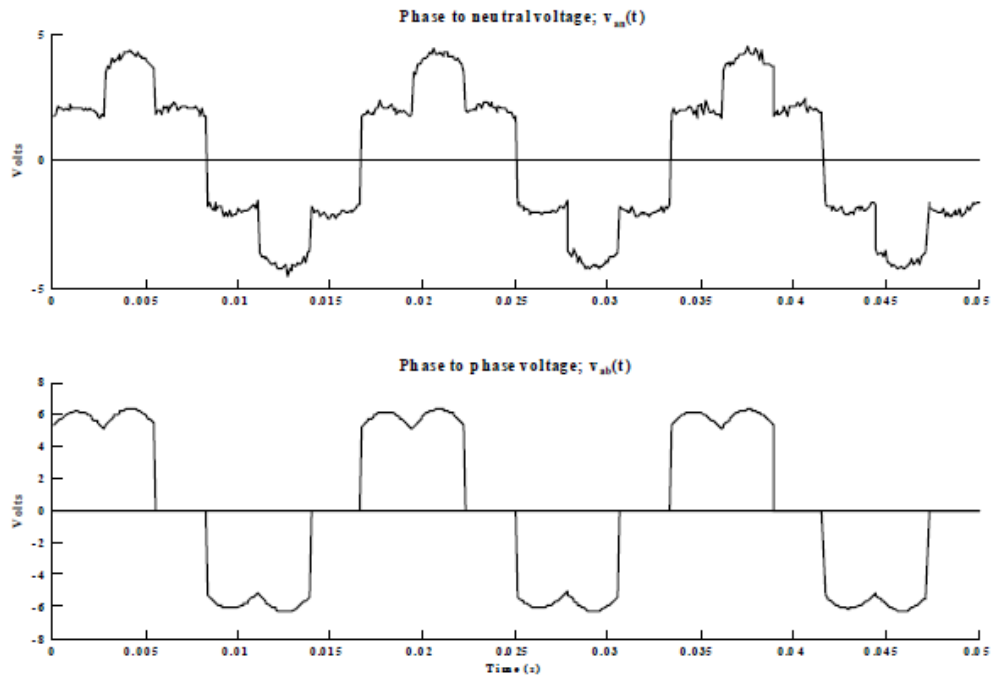


**Figure 3.11:** Voltage waveforms with a finite DC capacitor.

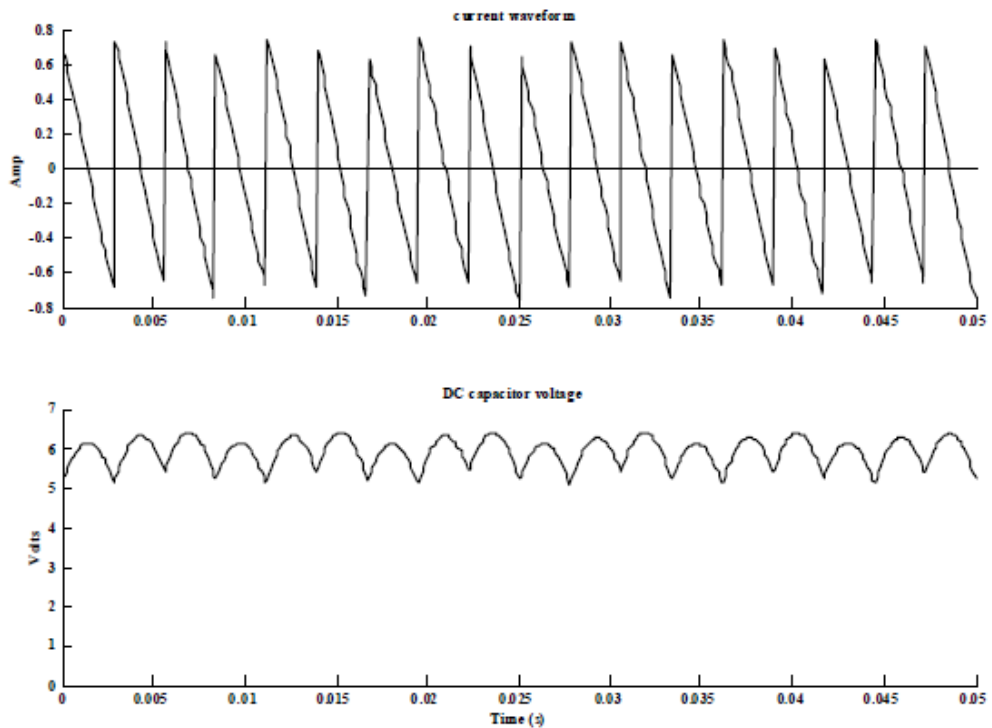


**Figure 3.12:** Capacitor current and DC capacitor voltage waveform.

### 3.2.1.1.2 Reactive and active power exchange

Considering a phase shift  $\phi$  across the AC power system and the essential compensator voltage, figure 3.13, shows the exchange of both reactive and active power. In order to get the AC current relations, the same procedure conducted in the section 3.2.1.1.1 is carried out.

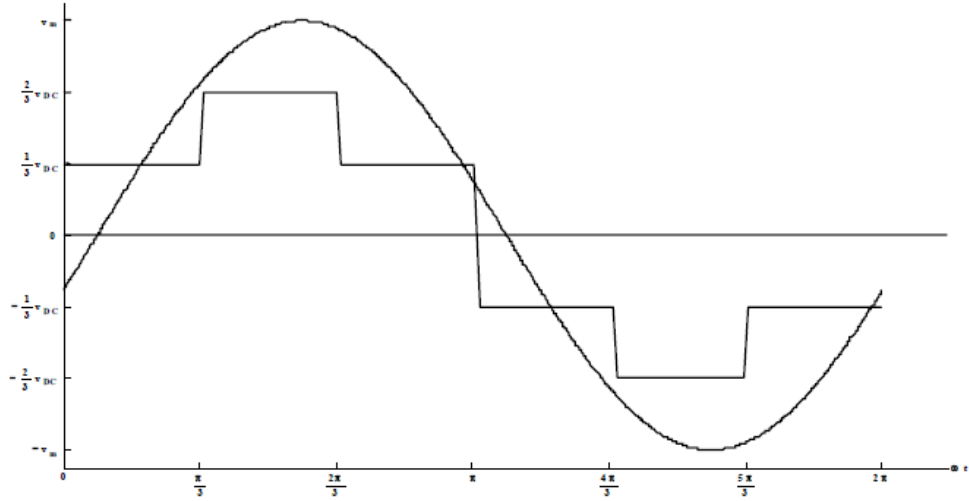


**Figure 3.13:** AC system voltage and compensator voltage;  $v_{an}(t)$ .

- Interval:  $0 \leq \omega t \leq \pi/3$

$$v_L(t) = V_m \sin(\omega t - \phi) - \frac{1}{3} V_{DC} = L \frac{d}{dt} i_a(t)$$

$$i_a(t) = -\frac{V_m}{\omega L} (\cos(\omega t - \phi) - \cos(\phi)) - \frac{1}{3L} V_{DC} t + I_0 \quad (3.22)$$

Where ( $I_0$ ) : Stands to the initial condition at  $t = 0$ ;  $i_a(0) = I_0$ .

- Interval:  $\pi/3 \leq \omega t \leq 2\pi/3$

$$v_L(t) = V_m \sin(\omega t - \phi) - \frac{2}{3} V_{DC} = L \frac{d}{dt} i_a(t)$$

$$i_a(t) = -\frac{V_m}{\omega L} \left( \cos(\omega t - \phi) - \cos\left(\frac{\pi}{3} - \phi\right) \right) - \left( \frac{2}{3L} t - \frac{2\pi}{9\omega L} \right) V_{DC} + I_1 \quad (3.23)$$

Where:

$$I_1 = i_a\left(\frac{\pi}{3\omega}\right)$$

- Interval:  $2\pi/3 \leq \omega t \leq \pi$

$$v_L(t) = V_m \sin(\omega t - \phi) - \frac{1}{3}V_{DC} = L \frac{d}{dt} i_a(t)$$

$$i_a(t) = -\frac{V_m}{\omega L} \left( \cos(\omega t - \phi) - \cos\left(\frac{2\pi}{3} - \phi\right) \right) - \left( \frac{1}{3L}t - \frac{2\pi}{9\omega L} \right) V_{DC} + I_2 \quad (3.24)$$

Where:

$$I_2 = i_a\left(\frac{2\pi}{3\omega}\right)$$

Taking into account that  $i_a(0) = -i_a\left(\frac{\pi}{\omega}\right)$ , the steady state initial condition  $I_0$  can be calculated:

$$I_0 = -i_a\left(\frac{\pi}{\omega}\right) = \frac{V_m}{\omega L} \left( \cos(\pi - \phi) - \cos\left(\frac{2\pi}{3} - \phi\right) \right) + \left( \frac{1}{3L} \frac{\pi}{\omega} - \frac{2\pi}{9\omega L} \right) V_{DC} - I_2$$

So that,

$$I_0 = \frac{V_m}{\omega L} \left( \cos(\pi - \phi) - \cos\left(\frac{2\pi}{3} - \phi\right) \right) + \frac{\pi}{9\omega L} V_{DC} - I_2 \quad (3.25)$$

Where:

$$I_2 = -\frac{V_m}{\omega L} \left( \cos\left(\frac{2\pi}{3} - \phi\right) - \cos\left(\frac{\pi}{3} - \phi\right) \right) - \frac{2\pi}{9\omega L} V_{DC} + I_1 \quad (3.26)$$

$$I_1 = i_a\left(\frac{\pi}{3\omega}\right) = -\frac{V_m}{\omega L} \left( \cos\left(\frac{\pi}{3} - \phi\right) - \cos(\phi) \right) - \frac{\pi}{9\omega L} V_{DC} + I_0 \quad (3.27)$$

Replacing equations (3.26) and (3.27) into equation (3.25) yields:

$$I_0 = -\frac{V_m}{\omega L} \cos(\phi) + \frac{2\pi}{9\omega L} V_{DC} \quad (3.28)$$

Using equation (3.28) the steady state equations are:

$$i_a(t) = -\frac{V_m}{\omega L} \cos(\omega t - \phi) - \left(\frac{1}{3L}t - \frac{2\pi}{9\omega L}\right)V_{DC} \quad (3.29)$$

$$0 \leq \omega t \leq \pi/3$$

$$i_a(t) = -\frac{V_m}{\omega L} \cos(\omega t - \phi) - \left(\frac{2}{3L}t - \frac{\pi}{\omega L}\right)V_{DC} \quad (3.30)$$

$$\pi/3 \leq \omega t \leq 2\pi/3$$

$$i_a(t) = -\frac{V_m}{\omega L} \cos(\omega t - \phi) - \left(\frac{1}{3L}t - \frac{\pi}{9\omega L}\right)V_{DC} \quad (3.31)$$

$$2\pi/3 \leq \omega t \leq \pi$$

Over the interval  $\pi \leq \omega t \leq 2\pi$  the AC current signal is the negative of the one explained in the above-mentioned equations. As the phase shift  $\phi$  increases the AC current changes regarding to the one shown in Figure 3.7. Figure 3.14 illustrates the AC current with  $\phi = 15^\circ$ .

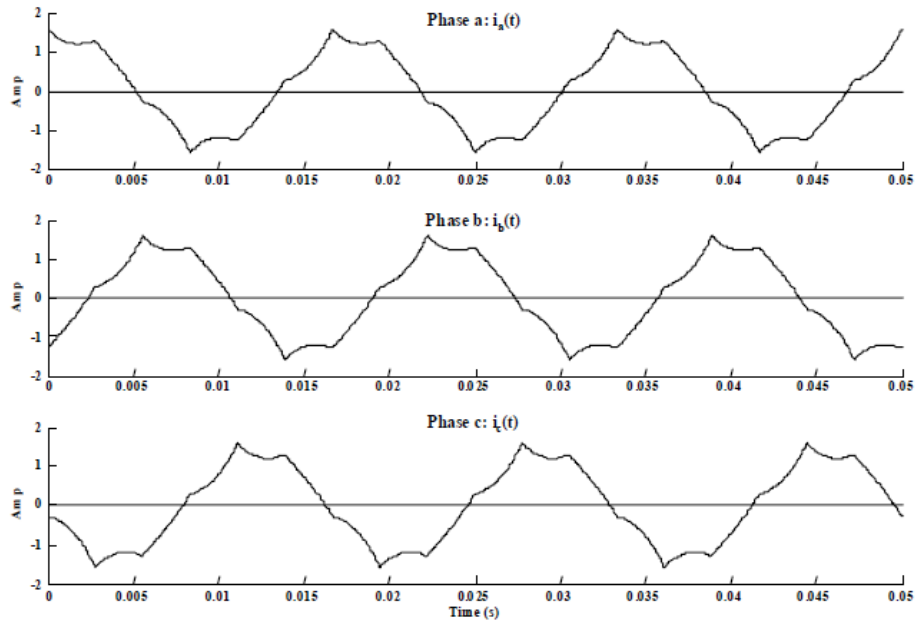


**Figure 3.14:** AC current waveform with  $\phi = 15^\circ$ .

### 3.2.1.1.2.1 Capacitor current

The capacitor current is obtained in a similar manner to that presented previously and has a similar behavior, a waveform made up by six segments where each segment can be represented by equation (3.32) with a phase shifted by  $60^\circ$  from each other.

$$i_{DC}(t) = \frac{V_m}{\omega L} \sin\left(\omega t - \phi - \frac{\pi}{6}\right) - \left(\frac{2}{3L}t - \frac{\pi}{9\omega L}\right)V_{DC} \quad (3.32)$$

$$0 \leq \omega t \leq \pi/3$$

It is important that if the angle  $\phi$  rises the capacitor current would have a greater DC level, as shown in figure 3.15 where  $i_{DC}(t)$  is presented taking into account  $\phi = 2^\circ$  and  $\phi = 15^\circ$ .

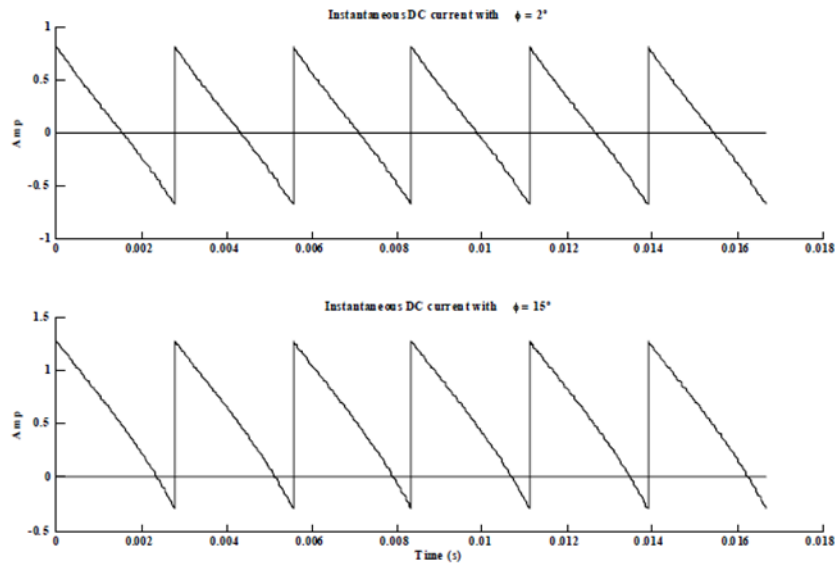


**Figure 3.15:** Instantaneous capacitor current.

If an angle  $\phi$  exists between the AC power system voltage and the fundamental compensator voltage the instantaneous capacitor voltage and current, depend on Fourier analysis are given by:

$$i_{DC}(t) = I_{DC_0} + \sum_{n=1}^{\infty} I_{DC_n} \sin(n\omega t)$$

$$v_{cap}(t) = V_{DC_0} + \sum_{n=1}^{\infty} V_{DC_n} \cos(n\omega t)$$

The above-mentioned expressions indicate that a DC power or active power flows through the DC side, thus an increase or decrease will occur in the capacitor voltage, based on whether the  $I_{DC_0}$  is negative or positive. To reveal this effect consider the circuit shown in figure 3.16.

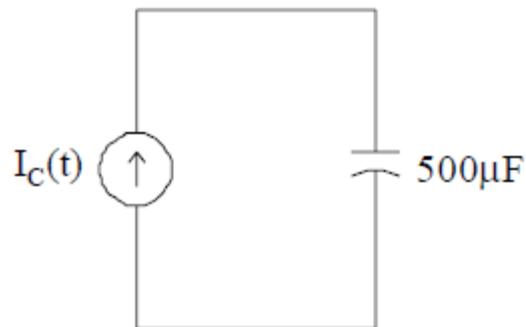


**Figure 3.16:** Test circuit.

The circuit is primarily at steady state, then with  $\phi = 0^\circ$ , at time  $t = 0.0333 \text{ s}$ , Angle  $\phi$  was stepped from  $0^\circ$  to  $-0.5^\circ$ . Figure 3.17 illustrates the capacitor voltage. The figure shows the phase shift  $\phi$  affect the capacitor voltage, as a result of the DC component into  $i_{DC}(t)$ , then, the exchange of active power, and that the dynamic of phase angle tuning is employed to get control over the VAR generation or absorption through the increase or decrease of the capacitor voltage, and in so doing the amplitude of the output voltage formed by the converter.

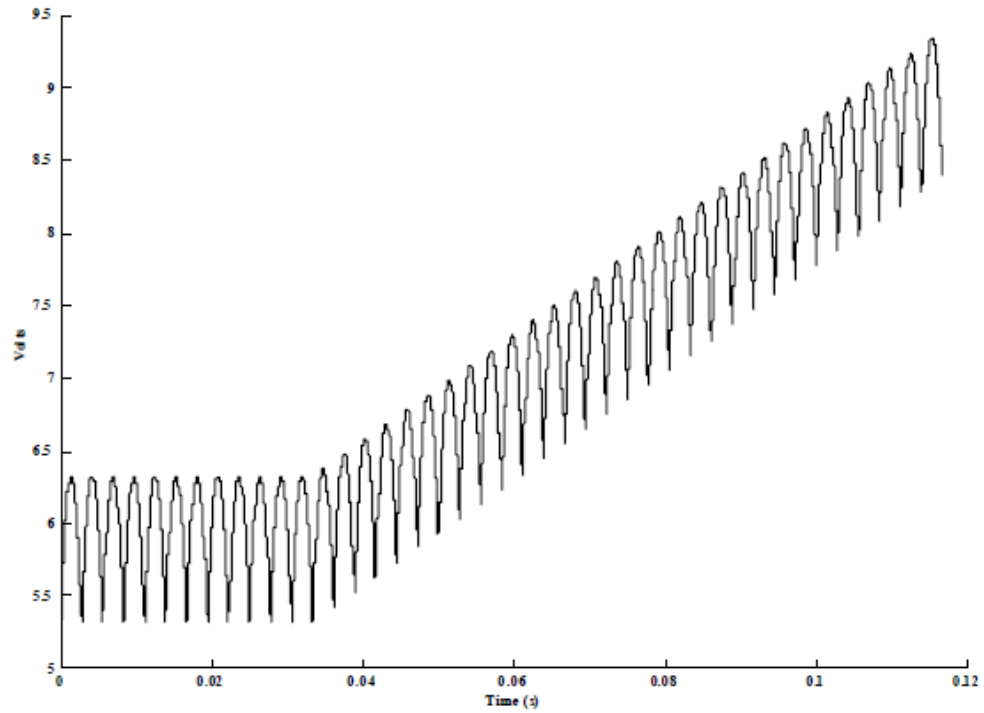


**Figure 3.17:** Instantaneous capacitor voltage.

The steady state DC component of the capacitor current is explained as below:

$$I_{DC_0}(t) = \frac{1}{T} \int_0^T i_{DC}(t) dt$$

Where  $i_{DC}(t)$  is given by equation (3.32) and  $T = \pi/3\omega$ , so that:

$$I_{DC_0} = -\frac{3V_m}{\pi\omega L} \sin(\phi) \quad (3.33)$$

When the converter only provides reactive power, the voltage of AC power system and the essential converter voltage, both in phase, considering there is an ideal converter (no losses). In practical converters, however, the semiconductor switches have some losses, and thus the energy stored in the DC capacitor would be utilized by the internal losses.

Anyhow, these losses can be also provided from the alternating current system by allowing the output voltages of the converter to be lag the AC system voltages by a slight angle; this makes an active power pass from the alternating current system to



the D-STATCOM converter, which works on compensating the converter losses and keeping the preferred level for the capacitor voltage.

The above concept is explained in figure 3.18. The system works in steady state with a constant direct current source at  $t = 0.1$  s. A direct current capacitor act to change the magnitude of the direct current source. In figure 3.18(a) each one of the AC system and the compensator voltages are in the same phase, thus the energy stored in the DC capacitor is consumed by the internal losses. In figure 3.18(b), if the difference angle between the AC system and the compensator voltages is a slightly small, the losses are provided from the AC system and the capacitor voltage, thus keeping the capacitor voltage at the preferred level.

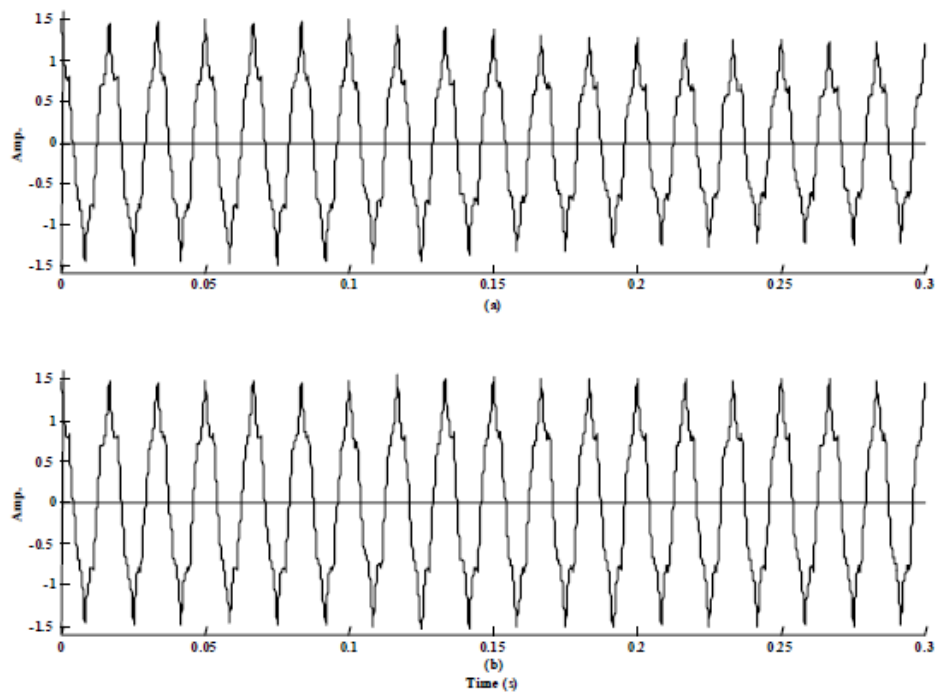


**Figure 3.18:** AC instantaneous current with: a)  $\phi = 0^\circ$  ; b)  $\phi = -0.5^\circ$ .

### 3.2.1.2 Twelve Pulse Converter

The six-pulse D-STATCOM is the easiest procedure employed in such kind of devices. In high power applications, it does not provide a good performance because of the high harmonic content. Combining two six-pulse converters, a better performance is obtained. This new arrangement is termed twelve-pulse D-STATCOM.

This arrangement is practically the lowest pulse-numbered configuration for power system application to provide an acceptable harmonic behavior [32].

The six-pulse converter output are the line-to-line voltages,  $v_{ab}(t)$ ,  $v_{bc}(t)$ , and  $v_{ca}(t)$ .  $v_{ab}(t)$  can be illustrated it by its Fourier series results:

$$\begin{aligned} v_{ab}(t) = & V_{ab_1} \sin(\omega t + 30^\circ) + V_{ab_5} \sin(5\omega t + 150^\circ) + V_{ab_7} \sin(7\omega t + 210^\circ) \\ & + V_{ab_{11}} \sin(11\omega t + 330^\circ) + V_{ab_{13}} \sin(13\omega t + 30^\circ) \\ & + V_{ab_{17}} \sin(17\omega t + 150^\circ) + V_{ab_{19}} \sin(19\omega t + 210^\circ) \\ & + V_{ab_{23}} \sin(23\omega t + 330^\circ) + \dots \end{aligned} \quad (3.34)$$

When connecting the compensator to a Y-Y transformer with a 1:1 turn ratio; the phase voltage,  $v_{an}(t)$  is given by:

$$\begin{aligned} v_{an}(t) = & \frac{1}{\sqrt{3}} (V_{ab_1} \sin(\omega t) - V_{ab_5} \sin(5\omega t) - V_{ab_7} \sin(7\omega t) + V_{ab_{11}} \sin(11\omega t) \\ & + V_{ab_{13}} \sin(13\omega t) - V_{ab_{17}} \sin(17\omega t) - V_{ab_{19}} \sin(19\omega t) \\ & + V_{ab_{23}} \sin(23\omega t) + \dots) \end{aligned} \quad (3.35)$$

$$v_{an}(t) = \frac{1}{3} \sum_{n=1}^{\infty} \frac{V_{ab_n}}{(-1)^r} \sin(n\omega t) \quad (3.36)$$

$$\forall n = 6r \pm 1, r = 0,1,2, \dots$$

From equations (3.34) and (3.35) could be noted that the line-to-line voltage amplitudes are  $\sqrt{3}$  by the phase voltage amplitudes and the harmonic components not mentioned in the set  $n = 12r \pm 1$ , where  $r = 0,1,2, \dots$ , are in phase opposition. This feature is useful to cancel the harmonic components not mentioned in the set  $n = 12r \pm 1$ .

Assuming that a second six-pulse converter supplies line-to-line voltages, they are lagging by  $30^\circ$  in relation to the other converter and with similar magnitude. That is:

$$\begin{aligned}
v_{ab}(t)_2 &= V_{ab_1} \sin(\omega t) + V_{ab_5} \sin(5\omega t) + V_{ab_7} \sin(7\omega t) + V_{ab_{11}} \sin(11\omega t) \\
&+ V_{ab_{13}} \sin(13\omega t) + V_{ab_{17}} \sin(17\omega t) + V_{ab_{19}} \sin(19\omega t) \\
&+ V_{ab_{23}} \sin(23\omega t) + \dots
\end{aligned} \tag{3.37}$$

$$v_{ab}(t)_2 = \sum_{n=1}^{\infty} V_{ab_n} \sin(n\omega t) \tag{3.38}$$

In connecting the second converter is to a  $\Delta - Y$  transformer with a  $1: 1/\sqrt{3}$  turn ratio, the phase voltage in the Y-side, the voltage of the secondary would be:

$$\begin{aligned}
v_{anY}(t)_2 &= \frac{1}{\sqrt{3}} (V_{ab_1} \sin(\omega t) + V_{ab_5} \sin(5\omega t) + V_{ab_7} \sin(7\omega t) + V_{ab_{11}} \sin(11\omega t) \\
&+ V_{ab_{13}} \sin(13\omega t) + V_{ab_{17}} \sin(17\omega t) + V_{ab_{19}} \sin(19\omega t) \\
&+ V_{ab_{23}} \sin(23\omega t) + \dots)
\end{aligned} \tag{3.39}$$

$$v_{anY}(t)_2 = \frac{1}{\sqrt{3}} \sum_{n=1}^{\infty} V_{ab_n} \sin(n\omega t) \tag{3.40}$$

$$\forall n = 6r \pm 1, r = 0, 1, 2, \dots$$

As well as, the line-to-line voltage in the wye-side can be written as:

$$\begin{aligned}
v_{abY}(t)_2 &= V_{ab_1} \sin(\omega t + 30^\circ) - V_{ab_5} \sin(5\omega t + 150^\circ) - V_{ab_7} \sin(7\omega t + 210^\circ) \\
&+ V_{ab_{11}} \sin(11\omega t + 330^\circ) + V_{ab_{13}} \sin(13\omega t + 30^\circ) \\
&- V_{ab_{17}} \sin(17\omega t + 150^\circ) - V_{ab_{19}} \sin(19\omega t + 210^\circ) \\
&+ V_{ab_{23}} \sin(23\omega t + 330^\circ) + \dots
\end{aligned} \tag{3.41}$$

$$v_{abY}(t)_2 = \frac{1}{3} \sum_{n=1}^{\infty} \frac{V_{ab_n}}{(-1)^r} \sin\left(n\omega t + \frac{\pi}{6}n\right) \tag{3.42}$$

$$\forall n = 6r \pm 1, r = 0, 1, 2, \dots$$

That can be expressed in another form:

$$v_{abY}(t)_2 = \sqrt{3} \sum_{n=1}^{\infty} V_{an_n} \sin\left(n\omega t + \frac{\pi}{6}n\right) \quad (3.43)$$

$$\forall n = 6r \pm 1, r = 0, 1, 2, \dots$$

The both waveforms are summed together by using a transformer to provide a third waveform  $v_{ab}(t)_{12}$  similar to being a sine wave; this voltage is named twelve-pulse voltage:

$$v_{ab}(t)_{12} = v_{ab}(t) + v_{abY}(t)_2 \quad (3.44)$$

$$v_{ab}(t)_{12} = 2(V_{ab_1} \sin(\omega t + 30^\circ) + V_{ab_{11}} \sin(11\omega t + 330^\circ) + V_{ab_{13}} \sin(13\omega t + 30^\circ) + V_{ab_{23}} \sin(23\omega t + 330^\circ) + \dots) \quad (3.45)$$

Thus,  $v_{ab}(t)_{12}$  is the line-to-line voltage of a twelve-pulse converter. Figure 3.19 shows these waveforms. In the configuration seen in figure 3.20, the two six-pulse converters are coupled in shunt to the DC bus, the two converter working as a twelve-pulse VSI-D-STATCOM.

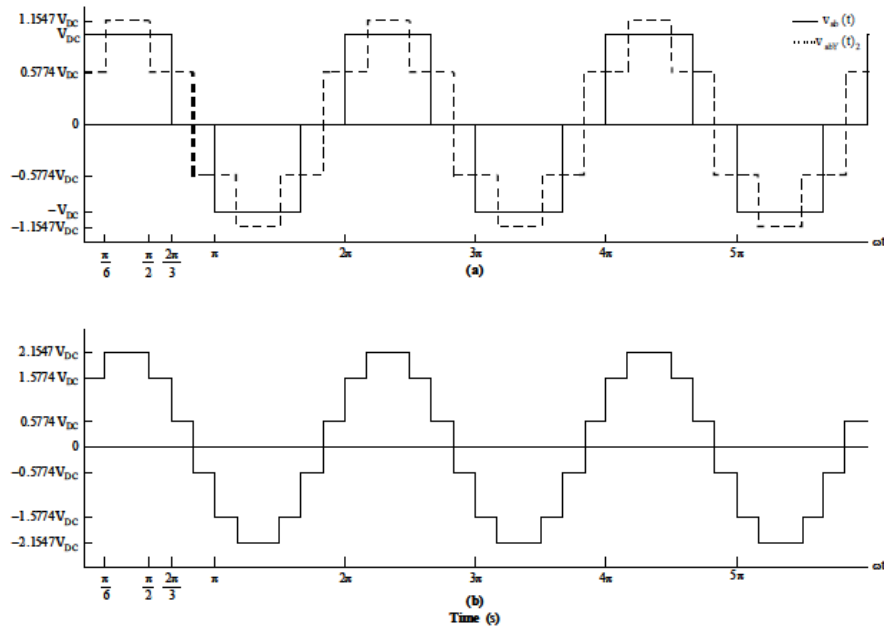


**Figure 3.19:** a)  $v_{ab}(t)$  and  $v_{abY}(t)_2$  ; b) 12-pulse voltage.

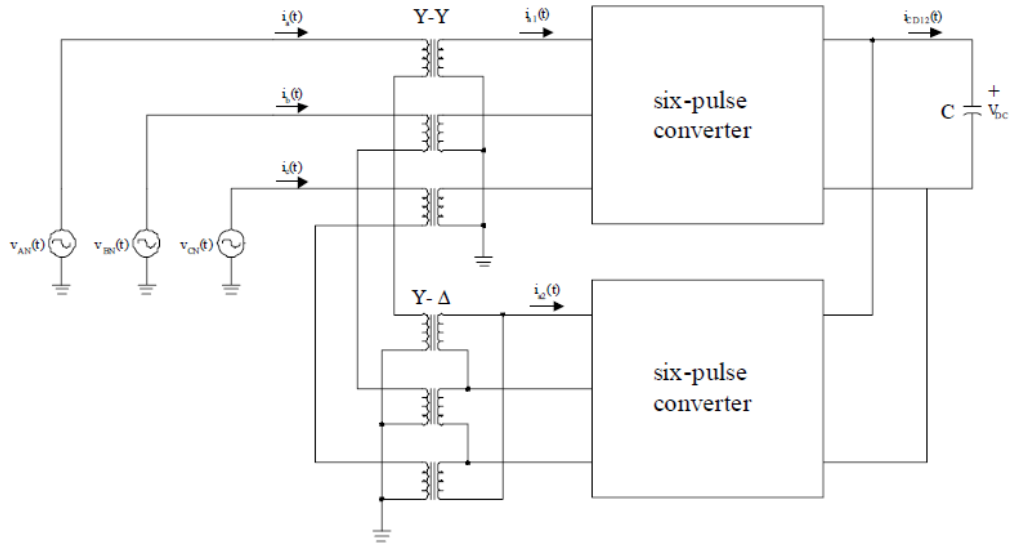


**Figure 3.20:** 12-pulse VSI D-STATCOM.

The twelve-pulse voltage given by eq. (2.61) expressed as a Fourier series is given by:

$$v_{ab}(t)_{12} = \sum_{n=1}^{\infty} V_{ab12n} \sin\left(n\omega t + \frac{\pi}{6}n\right) \quad (3.46)$$

$$\forall n = 12r \pm 1, r = 0, 1, 2, \dots$$

Where:

$$V_{ab12n} = V_{abn} + \sqrt{3}V_{an_n}$$

$$V_{ab12n} = \sqrt{3} \frac{4}{n\pi} V_{DC} , \forall n = 12r \pm 1, r = 0, 1, 2, \dots \quad (3.47)$$

The line-to-neutral voltages are illustrated in figure 3.21.

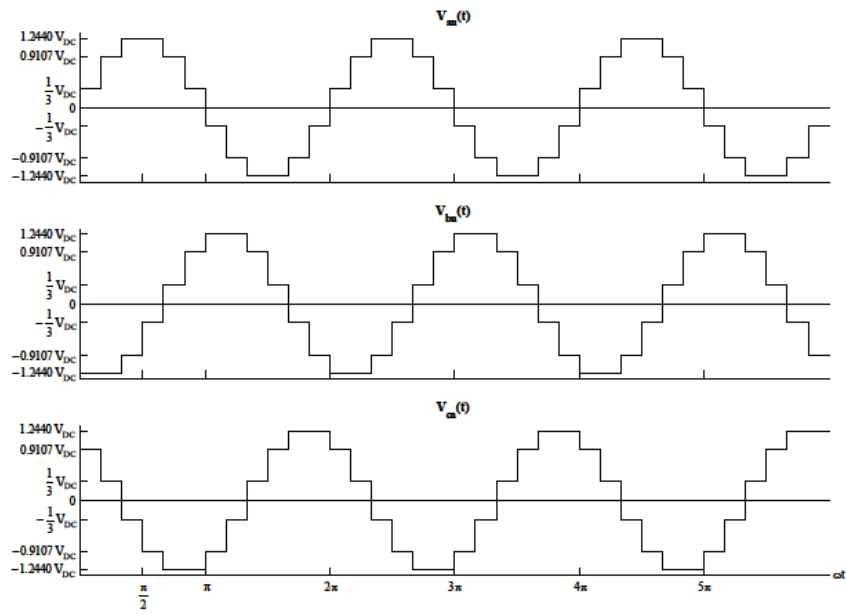


**Figure 3.21:** 12-pulse D-STATCOM line-to-neutral voltages.

Figure 3.22 shows that the twelve-pulse voltage  $v_{ab}(t)_{12}$ , contain only harmonics of orders  $n = 12r \pm 1$ , where  $r$  is any positive integer, that is,  $n = 11th, 13th, 23th, 25th \dots$ , with amplitudes  $1/11th, 1/13th, 1/23th, 1/25th \dots$ , respectively.

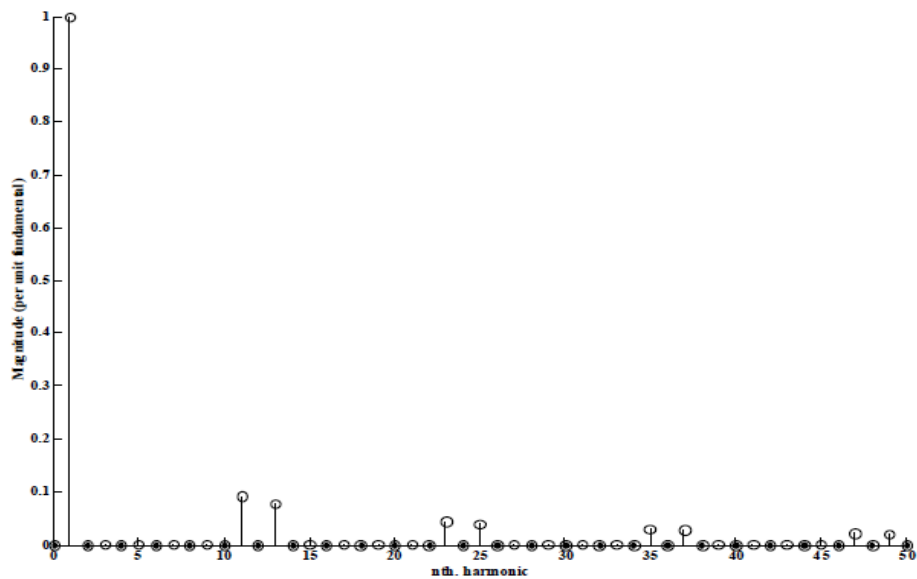


**Figure 3.22:**  $v_{ab}(t)_{12}$  voltage Fourier spectrum.

### 3.2.1.2.1 AC Current Signals

When a similar procedure conducted in the earlier section is applied, the alternating current analysis is done. Let the AC voltage be a pure sinusoidal function,  $e_{an}(t) = V_m \sin(\omega t)$ , then the level of the fundamental and harmonics elements are provided by equation (2.65) and equation (2.66), where  $v_{an_1}(t) = 1.2732V_{DC} \sin(\omega t)$ .

$$i_a(t)_1 = -\frac{V_m - 1.2732V_{DC}}{\omega L} \cos(\omega t) \quad ; (\text{fundamental component})$$

$$i_a(t)_n = \frac{1.2732V_{DC}}{n^2 \omega L} \cos(n\omega t) \quad , \forall n > 1 ; (nth \text{ harmonic component})$$

So that,

$$I_{a_1} = I_q = \frac{V_m - 1.2732V_{DC}}{\omega L} \quad (3.48)$$

$$I_{a_n} = I_{q_n} = \frac{1.2732V_{DC}}{n^2 \omega L} \quad , \forall n > 1 \quad (3.49)$$

From now on, voltages  $v_{ab}(t)$ ,  $v_{bc}(t)$  and  $v_{ca}(t)$  will be referred as the twelve-pulse D-STATCOM line-to-line voltages and the voltages  $v_{an}(t)$ ,  $v_{bn}(t)$  and  $v_{cn}(t)$  as the twelve-pulse STATCOM line-to-neutral voltages.

The fundamental current will be led when  $V_m < 1.2732 V_{DC}$ ; thus, the AC system regards the compensator as a capacitor and the current passes from the compensator to the AC system. When  $V_m > 1.2732 V_{DC}$ , the fundamental current will be lagging, therefore, the compensator acts as an inductor by the AC system and the current passes from the AC system to the compensator. Figure 3.23 exhibits the phasorial diagram over the tie inductor and the AC current.

Figure 3.24 represented the relation between the fundamental reactive current and the DC voltage (VDC). The lower-order harmonic currents as a function of the fundamental reactive current are displayed too.

In order to get the AC current equations, the procedure is done in the way as that of the six-pulse circuit, taking into consideration that the width across each conduction interval is  $30^\circ$ , figure 3.25.

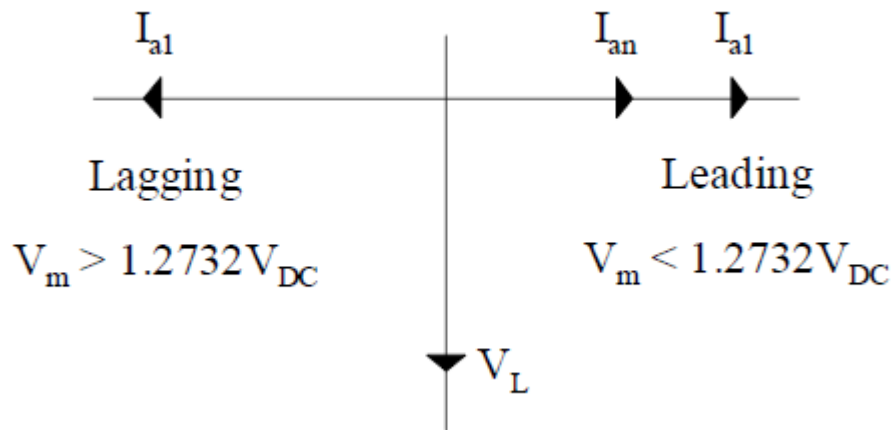


Figure 3.23: Phasorial diagram.

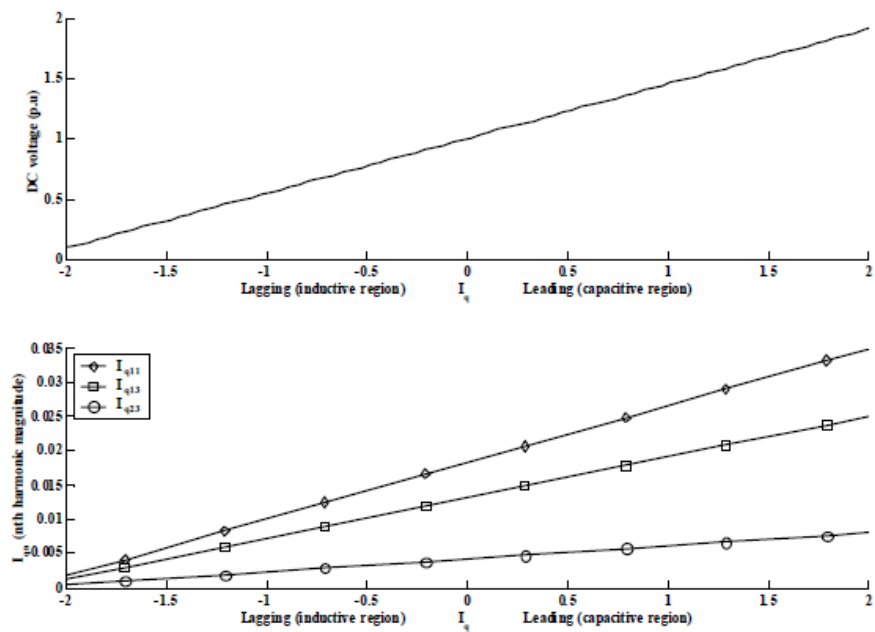
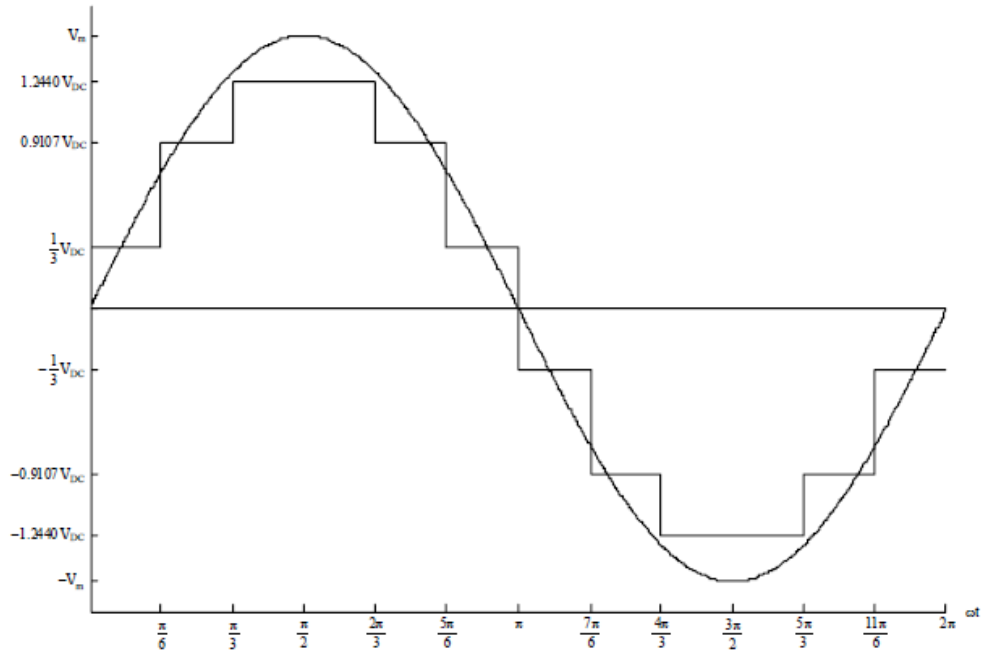


Figure 3.24: Relationship between the DC voltage, the fundamental and harmonics current.





**Figure 3.25:** AC system voltage and fundamental voltage compensator  $v_{an}(t)$ .

- Interval:  $0 \leq \omega t \leq \pi/6$

$$v_L(t) = V_m \sin(\omega t) - \frac{1}{3} V_{DC} = L \frac{d}{dt} i_a(t)$$

$$i_a(t) = -\frac{V_m}{\omega L} (\cos(\omega t) - 1) - \frac{1}{3L} V_{DC} t + I_0 \quad (3.50)$$

Where ( $I_0$ ): Stands to the initial condition at  $t = 0$ ;  $i_a(0) = I_0$ .

- Interval:  $\pi/6 \leq \omega t \leq \pi/3$

$$v_L(t) = V_m \sin(\omega t) - 0.9107 V_{DC} = L \frac{d}{dt} i_a(t)$$

$$i_a(t) = -\frac{V_m}{\omega L} \left( \cos(\omega t) - \frac{\sqrt{3}}{2} \right) - \left( \frac{0.9107}{L} t - \frac{0.9107\pi}{6\omega L} \right) V_{DC} + I_1 \quad (3.51)$$

Where:

$$I_1 = i_a\left(\frac{\pi}{6\omega}\right)$$

- Interval:  $\pi/3 \leq \omega t \leq \pi/2$

$$v_L(t) = V_m \sin(\omega t) - 1.2440 V_{DC} = L \frac{d}{dt} i_a(t)$$

$$i_a(t) = -\frac{V_m}{\omega L} (\cos(\omega t) - 0.5) - \left( \frac{1.2440}{L} t - \frac{1.2440\pi}{3\omega L} \right) V_{DC} + I_2 \quad (3.52)$$

Where:

$$I_2 = i_a \left( \frac{\pi}{3\omega} \right)$$

In steady state  $i_a \left( \frac{\pi}{2\omega} \right) = 0$ , then the steady state initial condition  $I_0$  is computed

as:

$$i_a \left( \frac{\pi}{2\omega} \right) = -\frac{V_m}{\omega L} (-0.5) - \left( \frac{1.2440}{L} \cdot \frac{\pi}{2\omega} - \frac{1.2440\pi}{3\omega L} \right) V_{DC} + I_2 = 0$$

$$I_2 = -\frac{V_m}{2\omega L} + \frac{1.2440\pi}{6\omega L} V_{DC} \quad (3.53)$$

$$I_2 = i_a \left( \frac{\pi}{3\omega} \right) = -\frac{V_m}{\omega L} \left( \frac{1}{2} - \frac{\sqrt{3}}{2} \right) - \left( \frac{0.9107}{L} \cdot \frac{\pi}{3\omega} - \frac{0.9107\pi}{6\omega L} \right) V_{DC} + I_1$$

$$I_1 = -\sqrt{3} \frac{V_m}{2\omega L} + \frac{2.1547\pi}{6\omega L} V_{DC} \quad (3.54)$$

$$I_1 = i_a \left( \frac{\pi}{6\omega} \right) = -\frac{V_m}{\omega L} \left( \frac{\sqrt{3}}{2} - 1 \right) - \frac{1}{3L} \cdot \frac{\pi}{6\omega} V_{DC} + I_0$$

$$I_0 = -\frac{V_m}{\omega L} + \frac{7.4641\pi}{18\omega L} V_{DC} \quad (3.55)$$

Substituting equation (3.55) into equation (3.50) the  $i_a(t)$  steady state equations are:

$$i_a(t) = -\frac{V_m}{\omega L} \cos(\omega t) - \left( \frac{1}{3L} t - \frac{7.4641\pi}{18\omega L} \right) V_{DC} \quad (3.56)$$

$$0 \leq \omega t \leq \pi/6$$

$$i_a(t) = -\frac{V_m}{\omega L} \cos(\omega t) - \left( \frac{0.9107}{L} t - \frac{3.0654\pi}{6\omega L} \right) V_{DC} \quad (3.57)$$

$$\pi/6 \leq \omega t \leq \pi/3$$

$$i_a(t) = -\frac{V_m}{\omega L} \cos(\omega t) - \left( \frac{1.2440}{L} t - \frac{3.7320\pi}{6\omega L} \right) V_{DC} \quad (3.58)$$

$$\pi/3 \leq \omega t \leq 2\pi/3$$

$$i_a(t) = -\frac{V_m}{\omega L} \cos(\omega t) - \left( \frac{0.9107}{L} t - \frac{2.3988\pi}{6\omega L} \right) V_{DC} \quad (3.59)$$

$$2\pi/3 \leq \omega t \leq 5\pi/6$$

$$i_a(t) = -\frac{V_m}{\omega L} \cos(\omega t) - \left( \frac{1}{3L} t + \frac{1.4641\pi}{18\omega L} \right) V_{DC} \quad (3.60)$$

$$5\pi/6 \leq \omega t \leq \pi$$

Across the interval  $\pi \leq \omega t \leq 2\pi$  the AC current signal comes to be the negative of the one explained for the above-mentioned expressions. Figure 3.26 shows the  $i_a(t)$  AC current signal. Hence, for the leading case  $V_{DC} = 3 V$ ;  $V_m = 2.5 V$  and  $L = 3 mH$  were employed;  $V_{DC} = 3 V$ ;  $V_m = 4.5 V$  and  $L = 3 mH$  for lagging.

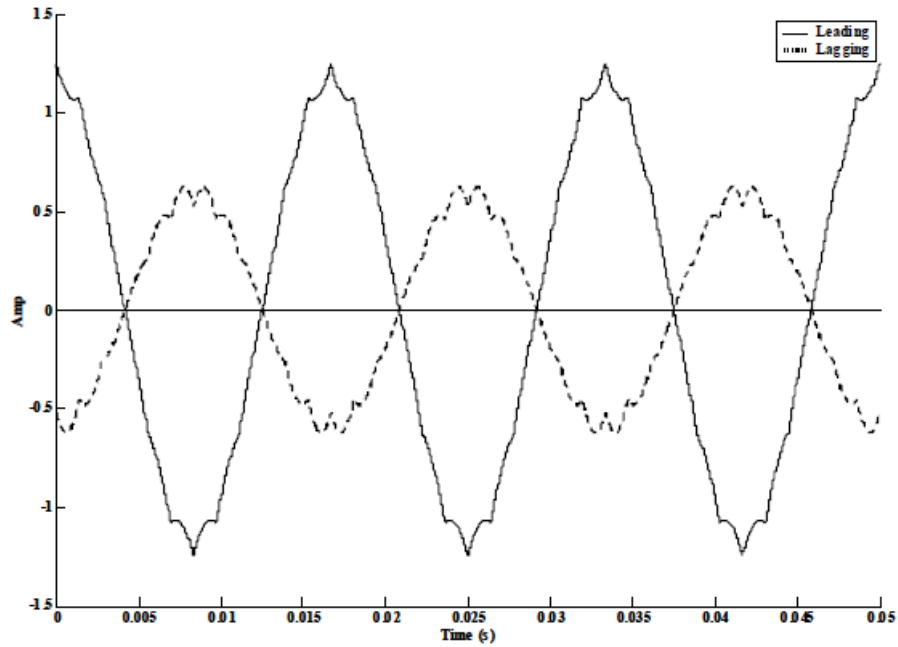


**Figure 3.26:** AC current waveform,  $i_a(t)$ .

### 3.2.1.2.1.1 Six-pulse AC current

The current that flows into the wye-side secondary of both transformers (Y – Y and  $\Delta$  – Y) is equal to the current of AC line, this is due to both secondary windings are connected in series. Using the instantaneous power  $P(t)$  the AC current of each six-pulse VSI can be obtained.

#### Y – Y connection

- $0 \leq \omega t \leq \pi/6$

$$P_a(t)_s = v_{an}(t)_s i_a(t) \quad (3.61)$$

Where:

$P_a(t)_s$  : Is the phase "a" instantaneous power in the secondary winding.

$v_{an}(t)_s = \frac{1}{3}V_{DC}$ : is the line-to-neutral voltage in the secondary winding.

So that,

$$P_a(t)_s = \frac{1}{3}V_{DC} \left( -\frac{V_m}{\omega L} \cos(\omega t) - \left( \frac{1}{3L} t - \frac{7.4641\pi}{18\omega L} \right) V_{DC} \right) \quad (3.62)$$

At the primary side the instantaneous power is:

$$P_a(t)_p = v_{an}(t)_p i_{a_1}(t) \quad (3.63)$$

Where:

$P_a(t)_p$ : Is the phase "a" instantaneous power in the primary winding.

$v_{an}(t)_p = \frac{1}{3}V_{DC}$  , is the line-to-neutral voltage in the primary winding.

$i_{a_1}(t)$  : Is the AC current in the primary winding.

Then,

$$P_a(t)_p = \frac{1}{3}V_{DC} i_{a_1}(t) \quad (3.64)$$

Neglecting losses, the instantaneous power in both windings is equal, then the AC current in the primary winding is:

$$i_{a_1}(t) = -\frac{V_m}{\omega L} \cos(\omega t) - \left( \frac{1}{3L} t - \frac{7.4641\pi}{18\omega L} \right) V_{DC} \quad (3.65)$$

Therefore the wye-side primary current and the AC line current are equal.

#### $\Delta - Y$ connection

The instantaneous phase "a" power of the  $\Delta - Y$  transformer is expressed as:

$$P_a(t)_s = v_{an}(t)_s i_a(t) = P_{ab}(t) = v_{ab}(t)_p i_{ba}(t) \quad (3.66)$$

Where:

$v_{ab}(t)_p$  : Is the line-to-line voltage in the primary winding ( $\Delta$ ).

$i_{ba}(t)$  : Is the current in the primary winding.

$v_{an}(t)_s$  : Is the phase voltage in the secondary winding (Y).

Due to,

$$v_{ab}(t)_p = \sqrt{3} v_{an}(t)_s \quad (3.67)$$

Then,

$$i_{ba}(t) = \frac{1}{\sqrt{3}} i_a(t) \quad (3.68)$$

$$i_{cb}(t) = \frac{1}{\sqrt{3}} i_b(t) \quad (3.69)$$

$$i_{ac}(t) = \frac{1}{\sqrt{3}} i_c(t) \quad (3.70)$$

The AC current of the second VSI  $i_a(t)_p$  is given by:

$$i_{a_2}(t) = i_{ba}(t) - i_{ac}(t) \quad (3.71)$$

Over the interval  $0 \leq \omega t \leq \pi/6$  the phase current of the second six-pulse VSI is given by equation (3.72).

$$i_{a_2}(t) = -\frac{V_m}{\omega L} \cos\left(\omega t - \frac{\pi}{6}\right) + \left(\frac{1}{3L}t + \frac{6.4641\pi}{18\omega L}\right)V_{DC} \quad (3.72)$$

From the above analysis can be concluded that the flowing of the current into the delta-side primary is shifted by  $30^\circ$  in relation to the wye-side primary. Figure 3.27 describe the AC current signal of each six-pulse VSI and the current across the diode and transistor one,  $D_1$ ,  $Q_1$  of the first six-pulse VSI is shown in figure 3.28.

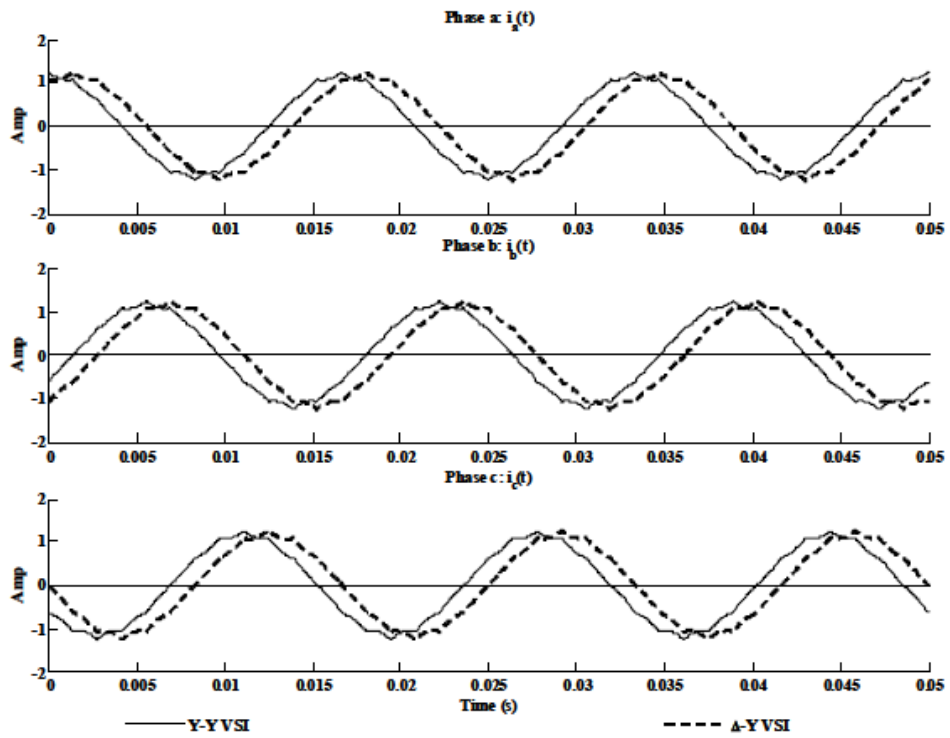


Figure 3.27: AC current of each six-pulse VSI.

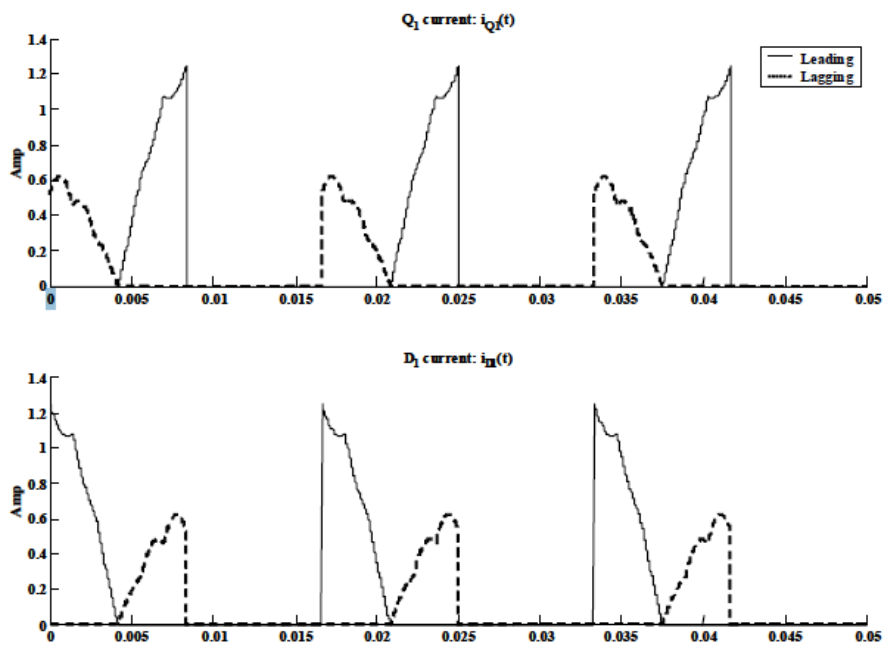


Figure 3.28:  $Q_1$  and  $D_1$  currents.

### 3.2.1.2.2 Capacitor Current

It is comprised of the DC currents participate between the two six-pulse converters. It is offered by,

$$i_{DC}(t)_{12} = i_{DC}(t)_1 + i_{DC}(t)_2 \quad (3.73)$$

Where;

$i_{DC}(t)_{12}$  : Is the twelve-pulse capacitor current.

$i_{DC}(t)_1$  : Is the 1<sup>st</sup> compensator capacitor current.

$i_{DC}(t)_2$  : Is the 2<sup>nd</sup> compensator capacitor current.

To obtain the current of the DC side, the same procedure is conducted as in the case of six pulse circuit, having into consideration that each conduction period's width is 30°. The current of the first six-pulse compensator at the DC side  $i_{DC}(t)_1$ , during the first 60° is calculated as follows. In all time  $t$ ,  $i_{DC}(t)_1$  is given by,

$$i_{DC}(t)_1 = i_{a_1}(t) + i_{c_1}(t)$$

Taking into account that the conduction interval is 30° yields:

$$i_{DC}(t)_1 = -\frac{V_m}{\omega L} \cos\left(\omega t + \frac{\pi}{3}\right) - \frac{1.2440}{L} \left(t - \frac{\pi}{6\omega}\right) V_{DC} \quad (3.74)$$

$$0 \leq \omega t \leq \pi/3$$

Therefore, equation (3.74) gives the first six-pulse compensator current at the DC side of during the first 60° interval. The current of the second compensator  $i_{DC}(t)_2$  presents a similar behavior lagged 30°. Figures 3.29 and 3.30 exhibit these waveforms for both cases lagged and leading.

$$i_{DC}(t)_2 = -\frac{V_m}{\omega L} \cos\left(\omega t + \frac{\pi}{6}\right) - \frac{1.2440}{L} \left(t - \frac{\pi}{3\omega}\right) V_{DC} \quad (3.75)$$

$$\pi/6 \leq \omega t \leq \pi/2$$



Substitute equations (3.74) and (3.75) into equation (3.73), then we get:

$$i_{DC}(t)_{12} = -1.9319 \frac{V_m}{\omega L} \cos\left(\omega t + \frac{5\pi}{12}\right) - \frac{2.4880}{L} \left(t - \frac{\pi}{12\omega}\right) V_{DC} \quad (3.76)$$

$$0 \leq \omega t \leq \pi/6$$

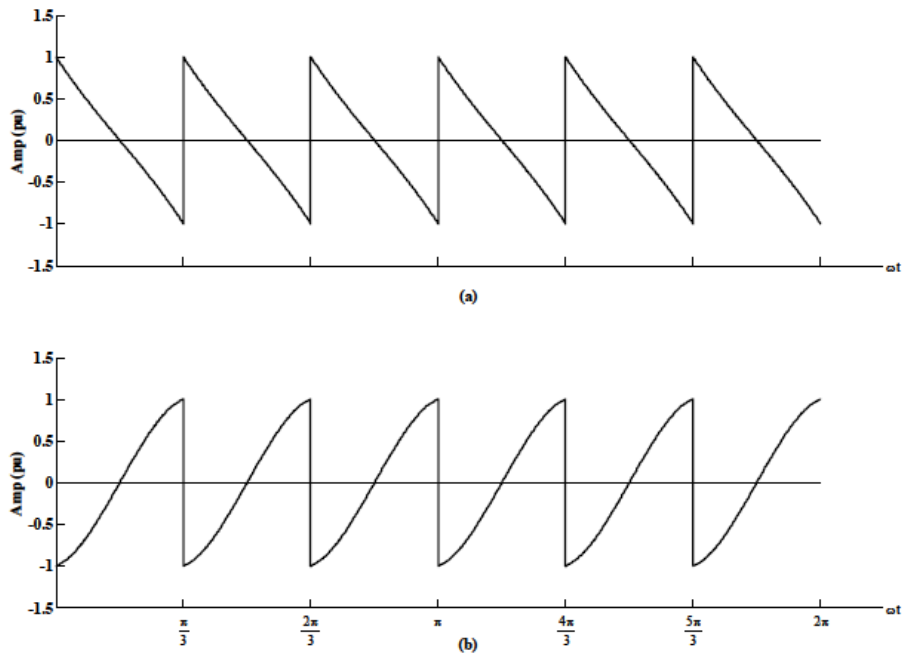


**Figure 3.29:** First converter capacitor current; a) generate reactive power; b) absorb reactive power.

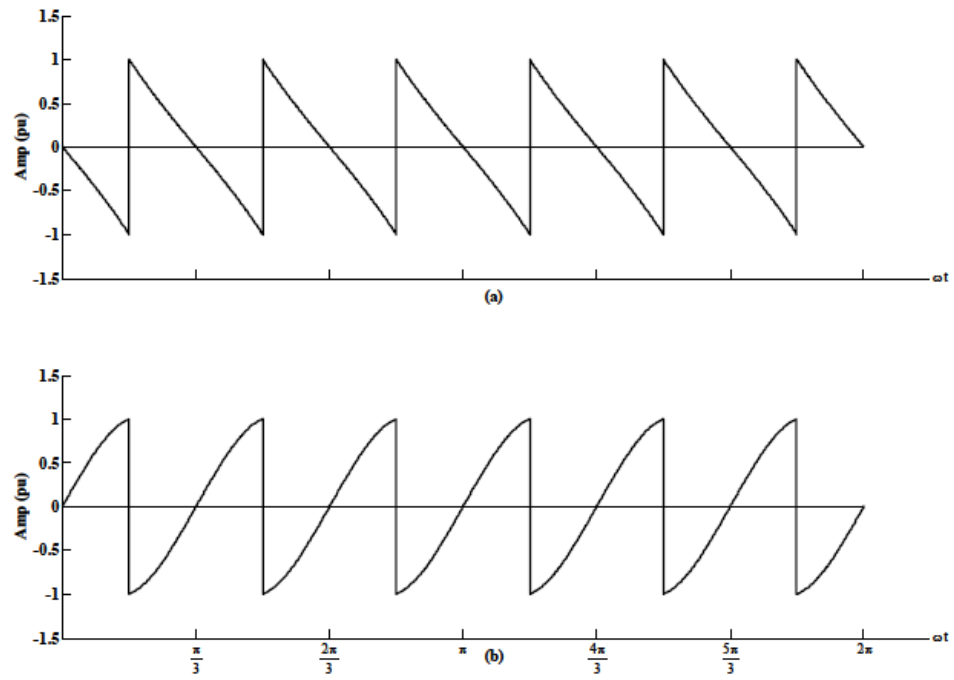


**Figure 3.30:** Second converter capacitor current: a) generate reactive power; b) absorb reactive power.

The capacitor current signal over the residual 11 conduction intervals is equal to that mentioned in equation (3.76) and results in a frequent signal at twelve times the frequency of the AC power system. Figure 3.31 presents the twelve-pulse capacitor current.

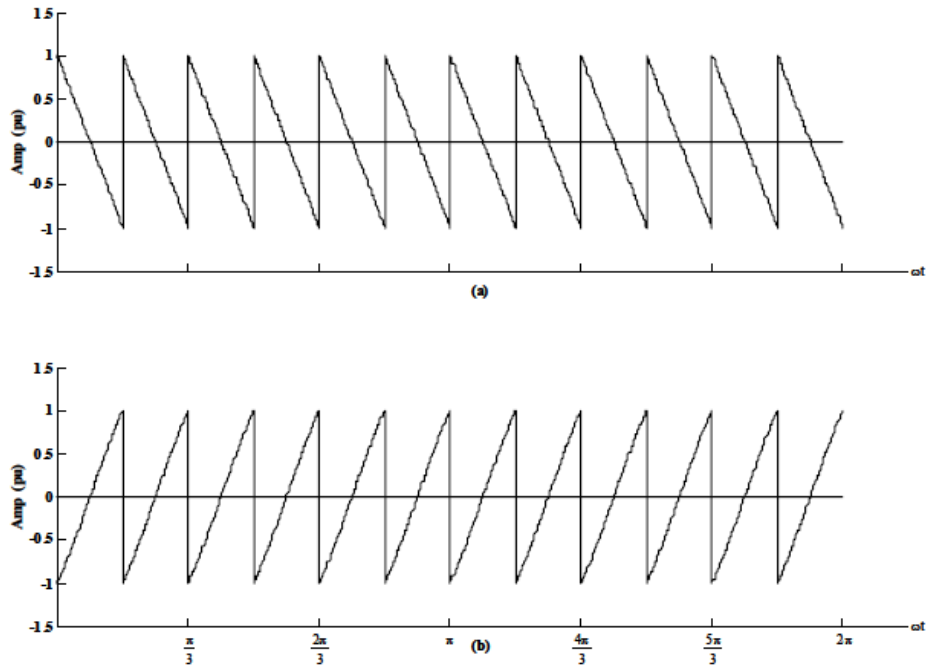


**Figure 3.31:** Capacitor current; a) generate reactive power; b) absorb reactive power.

### 3.2.1.2.3 DC Capacitor Voltage

The capacitor voltage can be expressed for the first 30° conduction interval as:

$$v_{cap}(t)_{12} == -1.9312 \frac{V_m}{\omega^2 LC} \sin\left(\omega t + \frac{5\pi}{12}\right) + 1.8681 \frac{V_m}{\omega^2 LC} - \frac{1.2440}{LC} V_{DC} t^2 + \frac{1.2440\pi}{6\omega LC} V_{DC} t + V_0 \quad (3.77)$$

Where ( $V_0$ ) : Stands to the initial condition at  $t = 0$ ;  $V_0 = v_{cap}(0)$ . The calculation of the initial condition is done using the average component  $V_{DC}$  of equation (3.77) with  $T = \pi/6\omega$ ; therefore,

$$V_{DC} = -\frac{6}{\pi\omega^2 LC} V_m + \frac{1.8681}{\omega^2 LC} V_m + \frac{0.4147\pi^2}{72\omega^2 LC} V_{DC} + V_0 \quad (3.78)$$

Simplifying,

$$V_0 = -0.04180 \frac{1}{\omega^2 LC} V_m + 0.05680 \frac{1}{\omega^2 LC} V_{DC} + V_{DC} \quad (3.79)$$

Figure 3.32 depicts the twelve-pulse DC-capacitor voltage. It also explains the occurrence of the peak capacitor voltage at  $\omega t = 15^\circ$  when the compensator generates reactive power. Equation (3.80) gives the peak voltage,

$$V_{pk} = -0.0220 \frac{1}{\omega^2 LC} V_m + 0.0284 \frac{1}{\omega^2 LC} V_{DC} + V_{DC} \quad (3.80)$$

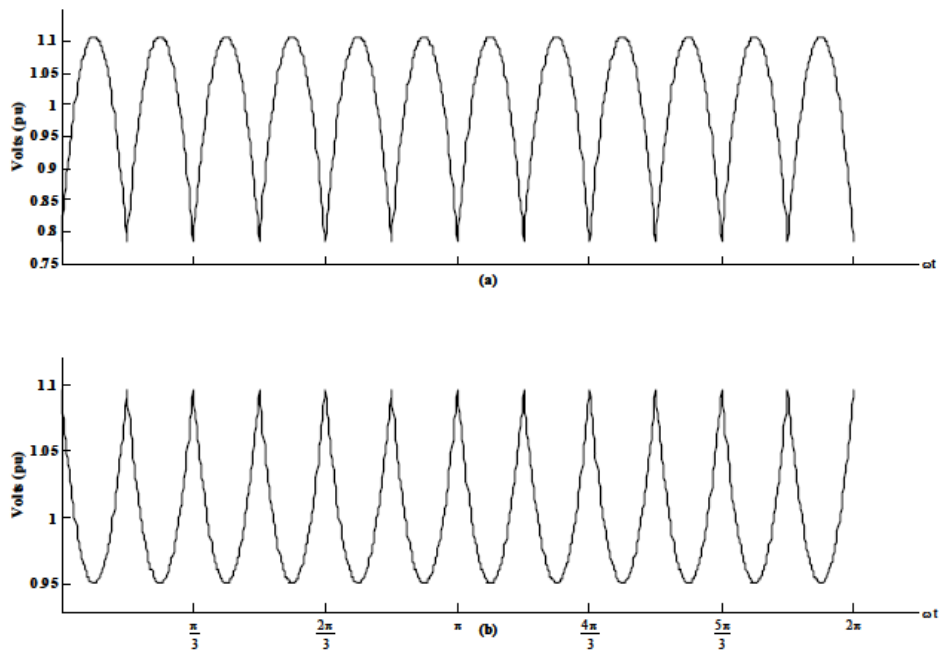


**Figure 3.32:** DC capacitor voltage: a- generate, b- absorb reactive power.

### 3.2.2 L-C Passive Filter

The LC filter helps in suppressing harmonics and also couples inverter output impedance to that of the inverter in order to partake current. The choice of LC filter is established on the grounds of the character of the system and the anticipated harmonics.

### **3.2.3 Coupling Transformer**

The coupling transformer is the medium to couple resultant voltage of VSC to the AC system. This purpose is served by the coupling transformer reactance.

### **3.2.4 Control Block**

The Control block performs the function of recognizing Power Quality problems like sags and swells in voltage due to load disturbance or fault and compensate for those problems by generating trigger pulses and terminating triggers when the disturbance instant has ended. These trigger pulses are fed to power electronics based PWM inverter.

Various control theories and algorithms are the basis of control blocks designing. The main objective of the control configuration is to sustain voltage at magnitude has a constant level at the instant whenever a sensitive load is joined that leads to system disturbances.

Control technique is measuring the voltage at the PCC that is to be compensated as per the requirement. The switching pulses for the inverter are derived from the PWM hysteresis control technique. The input to the controller consists of an error waveform achieved from the comparison of terminal voltage and the reference voltage. A PI controller is using to process such this error, the output is the angle  $\delta$ , which is delivered to the PWM waveform generator.

In this case, the important note we should care about is that, the convertor is indirect controlled, both, active and reactive power are exchanging with the network instantaneously: an error waveform is gotten by applied the reference voltage and the RMS voltage measured at the load point to a comparator. The controller is deal with the error waveform and generates the necessary angle to draw the error signal to zero, i.e., the load RMS voltage is carried out to match the reference voltage.

### 3.2.4.1 Basic Hysteresis Controller

Among various PWM techniques the hysteresis current controller is more used according to its simple execution. It does not need any information regarding any load parameters. Its implementation is entirely based on deriving of switching signals from the fixed tolerance band and current error comparison [33].

In this, the actual phase current is compared with the predefined tolerance band. In this, the switching frequency can be varied depending upon the load conditions leading to inverter operations as irregular.

### 3.2.4.2 Design of Hysteresis Controller

For tracking the reference current. The comparison between Instantaneous source current and reference current are done within the small hysteresis band and the resultant error signal is 1-5% of the current magnitude. Here by using the logic below:

$$I_{Sa} < i_{Sa}^* - h_b$$

For better track down of source currents, a narrow hysteresis band is preferred with the condition of the higher switching frequency. Figure 3.33 shows Hysteresis Controller as below.

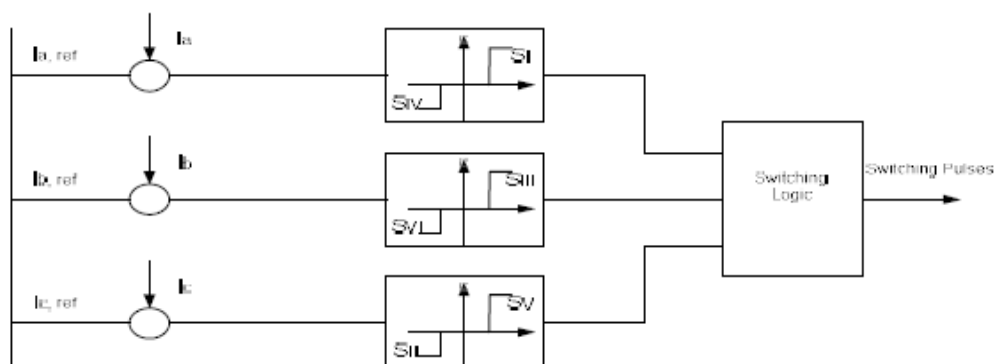


**Figure 3.33:** Hysteresis Controller.

### **3.2.5 Energy Storage Device**

Units of energy storage such as batteries, flywheels, super conducting magnetic energy storage (SMES) and supercapacitors store energy [34]. DC source and the DC capacitor is the general device that stores reactive power. It is plugged in parallel to the system and holds the converter's ripple current.

A battery is separately employed for the charging of DC capacitor or converter charges itself. The energy demand by the VSC for the voltage generation to be injected in the system is met with the help of storage devices.

### **3.3 Main Features of DSTATCOM**

- 1) Power factor correction.
- 2) Eliminating the harmonics presents in source current.
- 3) Compensating and regulating the voltage and reactive power respectively.

### **3.4 Basic Principle of DSTATCOM**

A DSTATCOM consists of a switching device like IGBT or GTO get along with storage device such as a capacitor, flywheel ... etc. and a controller to inject the controlled switching pulses for the semiconductor device and a coupling transformer that connects the whole system to an AC system. D-SATCOM's basic operating principle is similar to the synchronous machine's one. Synchronous machine will supply leading current when over excited and lagging current when under excited. Similarly, DSTATCOM generates and absorbs reactive power and interchange real power in case external DC source is provided [35].

The DSTATCOM is connected to the power system at a PCC, in which problems in the voltage quality are serious [36]. All the requisite currents and voltages are gauged and are supplied to the controller and then compared corresponding to the reference values. Then the feedback is performed by the controller, the result is a set of switching pulses and used to drive the main semiconductor devices of the power converter.

VSC based on IGBT changes the DC voltage to a three-phase AC voltages from the storage device. Such voltages are in phase and tied with the AC system via the coupling transformer's reactance. Possible alterations of the magnitude and phase of the DSTATCOM output voltages permits to control effectively reactive and active power and allow to exchange them between the DSTATCOM and the main bus system.

### 3.4.1 Reactive Power Exchange

Amplitude regulation is used to control the exchange of reactive power of the D-STATCOM with the AC system, D-STATCOM's reactive power is described as:

$$Q = \frac{(V_i - V_s) \cdot V_s}{X} \quad (3.81)$$

Where:

$Q$  : stands for reactive power.

$V_i$  : stands magnitude of D-STATCOM output voltage.

$V_s$  : is the system voltage's magnitude.

$X$  : stands for the equivalent impedance between DSTATCOM and the system.

Exchange of power within DSTATCOM and AC system is known by:

**Case I:**  $V_i = V_s$

The reactive current is zero. There is no generating or absorbing of reactive power by DSTATCOM.

**Case II:**  $V_i > V_s$  (capacitive mode)

Flowing of lagging current occurs via the transformer reactance from the DSTATCOM to the AC system.

**Case III:**  $V_i < V_s$  (inductive mode)

Then, the flow of leading current occurs from the AC system to the DSTATCOM.



### **3.4.2 Active Power Exchange**

It is required by a DC capacitor to supply real power to the switching devices employed in the DSTATCOM. In case there is a demand of direct voltage control, exchange of real power is required by an AC system to achieve and keep constancy of capacitor voltage. When there is a very low voltage or faults in the distribution system, external DC source is supplied in DSTATCOM for the sake of regulating voltage when a real power exchange exists in the AC system. If the system voltage lags the VSC voltage, then real power from the DC source will be injected into the AC system in order to obtain regulation for system voltage or to keep capacitor voltage constant.

### **3.5 Control Algorithms**

In order to compensate reactive power, a DSTATCOM supplies reactive power as required by the load, and thus, the source current keeps unity power factor (UPF). Since the source provides real power only, load balancing will be obtained by balancing the source reference current. Reference source current achieved to determine the switching of the DSTATCOM has real fundamental frequency element of the load current, which is being taken out by these techniques.

#### **3.5.1 IRP Theory**

Akagi proposed the IRP theory [37]. This theory is depend on the transformation from three-phase to two-phase quantities in  $\alpha$ - $\beta$  pattern and calculate the instantaneous active and reactive power in this pattern [37], [38]. Figure 3.34 showed the basic block diagram of the mentioned theory.

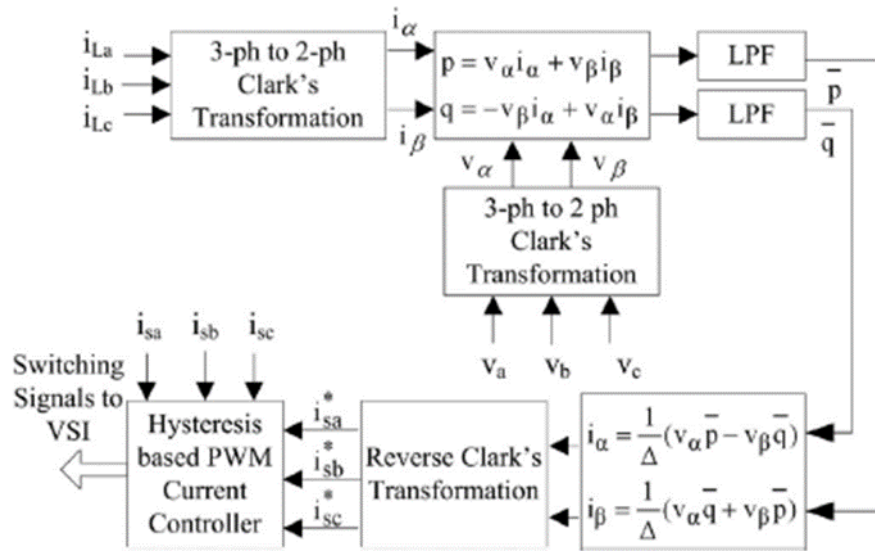


**Figure 3.34:** Block diagram of the reference current extraction using IRP theory.

The inputs  $v_a$ ,  $v_b$ , and  $v_c$  and  $i_{La}$ ,  $i_{Lb}$ , and  $i_{Lc}$  are supplied to the controller, and the processing of these quantities is conducted to produce reference current which used to give commands ( $i_{sa}^*$ ,  $i_{sb}^*$ , and  $i_{sc}^*$ ), these signals are supplied to a hysteresis-based pulse width modulated (PWM) as seen in figure 3.34 to create the final switching signals supplied to the DSTATCOM; thus, figure 3.35 shows that this block functions as a DSTATCOM's controller.

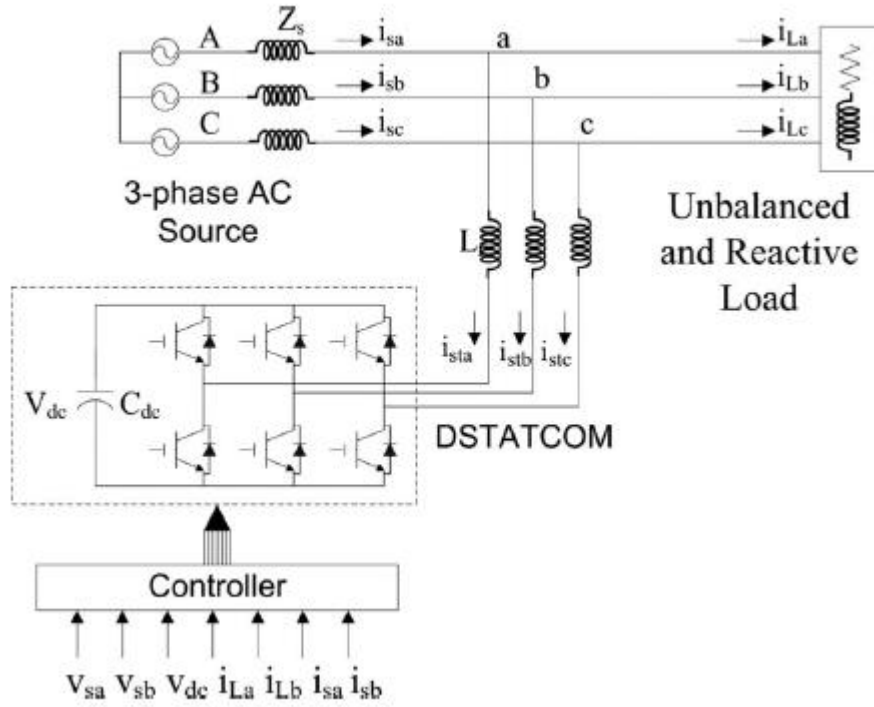


**Figure 3.35:** Basic circuit diagram of the DSTATCOM system.

The terminal voltages of the system are expressed as:

$$v_a = V_m \sin(\omega t) \quad (3.82)$$

$$v_b = V_m \sin(\omega t - 2\pi/3) \quad (3.83)$$

$$v_c = V_m \sin(\omega t - 4\pi/3) \quad (3.84)$$

The respective currents of the load are expressed as:

$$i_{La} = \sum I_{Lan} \sin\{(n\omega) - \theta an\} \quad (3.85)$$

$$i_{Lb} = \sum I_{Lbn} \sin\{(n\omega - 2\pi/3) - \theta bn\} \quad (3.86)$$

$$i_{Lc} = \sum I_{Lcn} \sin\{(n\omega - 4\pi/3) - \theta cn\} \quad (3.87)$$

In a–b–c coordinates, the axis are putted in the same plane at a distance of  $2\pi/3$  from each other. The instantaneous space vectors  $v_a$  and  $i_{La}$  are set on the "a" axis, and their amplitude has been varying with time to take positive and negative directions. The same case is true for the other two phases. The transformation of these phasors into  $\alpha$ – $\beta$  coordinate can be done via using Clark's transformation as illustrated:

$$\begin{bmatrix} v_\alpha \\ v_\beta \end{bmatrix} = \sqrt{\frac{2}{3}} \begin{bmatrix} 1 & -1/2 & -1/2 \\ 0 & \sqrt{3}/2 & -\sqrt{3}/2 \end{bmatrix} \begin{bmatrix} v_a \\ v_b \\ v_c \end{bmatrix} \quad (3.88)$$

$$\begin{bmatrix} i_\alpha \\ i_\beta \end{bmatrix} = \sqrt{\frac{2}{3}} \begin{bmatrix} 1 & -1/2 & -1/2 \\ 0 & \sqrt{3}/2 & -\sqrt{3}/2 \end{bmatrix} \begin{bmatrix} i_{La} \\ i_{Lb} \\ i_{Lc} \end{bmatrix} \quad (3.89)$$

Where  $\alpha$  and  $\beta$  axes are the perpendicular coordinates. For the three-phase the conventional instantaneous power circuit can be expressed as:

$$p = v_\alpha i_\alpha + v_\beta i_\beta \quad (3.90)$$

Where  $p$  is equal to conventional equation

$$ip = v_a i_a + v_b i_b + v_c i_c \quad (3.91)$$

Similarly, the IRP has defined as:

$$q = -v_\beta i_\alpha + v_\alpha i_\beta \quad (3.92)$$

The instantaneous real and reactive powers are expressed in matrix shape as:

$$\begin{bmatrix} p \\ q \end{bmatrix} = \begin{bmatrix} v_\alpha & v_\beta \\ -v_\beta & v_\alpha \end{bmatrix} \begin{bmatrix} i_\alpha \\ i_\beta \end{bmatrix} \quad (3.93)$$

The  $\alpha$ – $\beta$  currents can be written as:

$$\begin{bmatrix} i_\alpha \\ i_\beta \end{bmatrix} = \frac{1}{\Delta} \begin{bmatrix} v_\alpha & -v_\beta \\ v_\beta & v_\alpha \end{bmatrix} \begin{bmatrix} p \\ q \end{bmatrix} \quad (3.94)$$

Where:

$$\Delta = v_\alpha^2 + v_\beta^2 \quad (3.95)$$

Instantaneous active and reactive powers  $p$  and  $q$  can be analyzed to an average (dc) and an oscillatory components.

$$p = \bar{p} + \tilde{p} \quad (3.96)$$

$$q = \bar{q} + \tilde{q} \quad (3.97)$$

Where  $\bar{p}$  and  $\bar{q}$  are the average (dc) portion and  $\tilde{p}$  and  $\tilde{q}$  are the oscillatory (ac) portion of these real and reactive instantaneous powers. Reference source currents are estimated to find compensation for the IRP and the oscillatory component of the instantaneous active power. Hence, only the non-oscillating component of the active power is transmitted by source. Thus, the expression of the reference source currents  $i_{s\alpha}^*$  and  $i_{s\beta}^*$  in  $\alpha$ - $\beta$  coordinate will be as follows:

$$\begin{bmatrix} i_{s\alpha}^* \\ i_{s\beta}^* \end{bmatrix} = \frac{1}{\Delta} \begin{bmatrix} v_\alpha & -v_\beta \\ v_\beta & v_\alpha \end{bmatrix} \begin{bmatrix} \bar{p} \\ 0 \end{bmatrix} \quad (3.98)$$

By using reverse Clark's transformation, these currents can be transformed in  $a$ - $b$ - $c$  quantities to find the reference currents in  $a$ - $b$ - $c$  coordinates as states below:

$$\begin{bmatrix} i_{sa}^* \\ i_{sb}^* \\ i_{sc}^* \end{bmatrix} = \frac{2}{\sqrt{3}} \begin{bmatrix} 1/\sqrt{2} & 1 & 0 \\ 1/\sqrt{2} & -1/2 & \sqrt{3}/2 \\ 1/\sqrt{2} & -1/2 & -\sqrt{3}/2 \end{bmatrix} \begin{bmatrix} i_0^* \\ i_{s\alpha}^* \\ i_{s\beta}^* \end{bmatrix} \quad (3.99)$$

Where ( $i_0^*$ ): Stands to the zero sequence component, it has value equal to zero in three-phase three-wire system.

### 3.5.2 SRF Method

SRF theory depends on the current's transformation in rotating  $d$ - $q$  frame that rotates in a synchronous way [39], [40]. Figure 3.36 shows the basic blocks diagram of SRF method. Each of the inputs  $v_a$ ,  $v_b$ ,  $v_c$ ,  $i_{La}$ ,  $i_{Lb}$ , and  $i_{Lc}$  are sensed and fed to the controller. The voltage signals are processing by using a phase-locked loop (PLL) [41] to help generating unit voltage templates (signals of cosine and sine).

Transformation of current signals to  $d$ - $q$  frame is done, that they have been filtered and transformed back to  $abc$  frame ( $i_{sa}$ ,  $i_{sb}$ , and  $i_{sc}$ ), the outputs of this stage

are supplied to a unit of hysteresis-based PWM signal modulator [42] to produce final switching signals that were supplied to the DSTATCOM. Figure 3.35 shows that this block again functions as a DSTATCOM's controller.

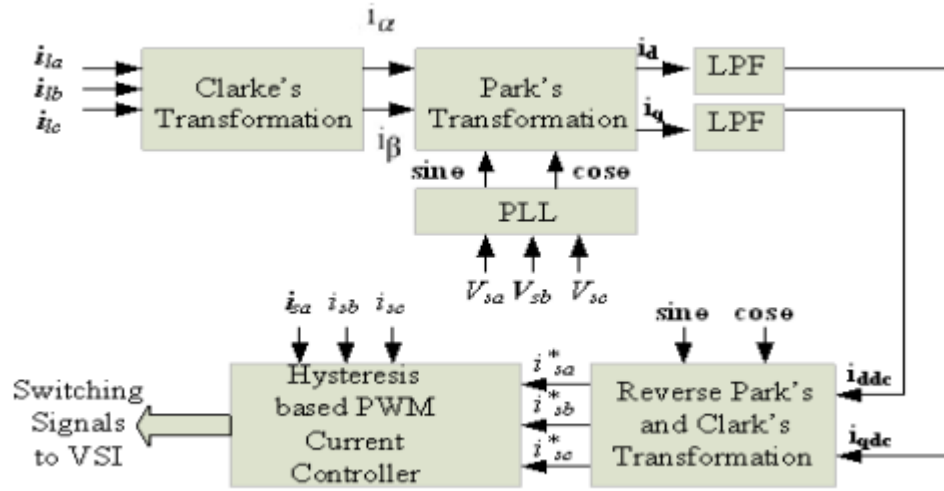


**Figure 3.36:** Block diagram: reference current extraction employing SRF theory.

As same as the  $p-q$  theory, by using  $\alpha-\beta$  coordinates, the current components are produced and utilizing  $\theta$  as a transformation angle. Their transformation from  $\alpha-\beta$  to  $d-q$  frame known as (Park's transformation).

$$\begin{bmatrix} i_d \\ i_q \end{bmatrix} = \begin{bmatrix} \cos \theta & \sin \theta \\ -\sin \theta & \cos \theta \end{bmatrix} \begin{bmatrix} i_\alpha \\ i_\beta \end{bmatrix} \quad (3.100)$$

SRF isolator makes an extraction for the dc component via the use of low-pass filters (LPFs) for both  $i_d$  and  $i_q$  which are realized by moving averager at 100 Hz. The extraction results of dc components ( $i_{ddc}$  and  $i_{qdc}$ ) are reversely transformed into  $\alpha-\beta$  frame via the use of reverse Park's transformation.

$$\begin{bmatrix} i_{\alpha dc} \\ i_{\beta dc} \end{bmatrix} = \begin{bmatrix} \cos \theta & \sin \theta \\ -\sin \theta & \cos \theta \end{bmatrix} \begin{bmatrix} i_{ddc} \\ i_{qdc} \end{bmatrix} \quad (3.101)$$

The transformation is done using these currents to gain three-phase reference source currents in  $a-b-c$  coordinates using (3.99). Also, reactive power compensation can be supplied by gripping  $i_q$  component to zero value for the getting of reference source currents.

### 3.5.3 Adaline-Based Control Algorithm

The basic theory of the suggested Adaline decomposer was depend on LMS algorithm and its done by Adaline, which works on tracking the unit vector templates to maintain lowest error signal. Figure 3.37 shows a block diagram of Adaline based control diagram. The theory can be easily understood by taking into account the analysis in single-phase system, seen below.

The supply voltage can be given as follows:

$$v_s = V_1 \sin \omega t \quad (3.102)$$

Active current ( $i_p^+$ ) and reactive current ( $i_q^+$ ) for positive sequence as well as the negative sequence current ( $i^-$ ) are formed the sensed load current, these signals can be analyzed to as seen in the following equation:

$$i_L = i_p^+ + i_q^+ + i^- \quad (3.103)$$

This control depend on getting the current component and the unit voltage template in the same phase. In order to calculate the real component of load current of the fundamental frequency positive sequence, the unit voltage template should be in the same phase with the system voltage. Moreover, it should have unit amplitude, and be undistorted. To calculate the templates, the voltage at the PCC is sensed.

A band-pass filter is used to filter the sensed voltages, and their amplitude is calculated. The three-phase voltages that sensed in the input stage of the controller (see figure 3.35) went into division by this amplitude to obtain three-phase voltage templates ( $u_a$ ,  $u_b$ , and  $u_c$  see in figure 3.37).

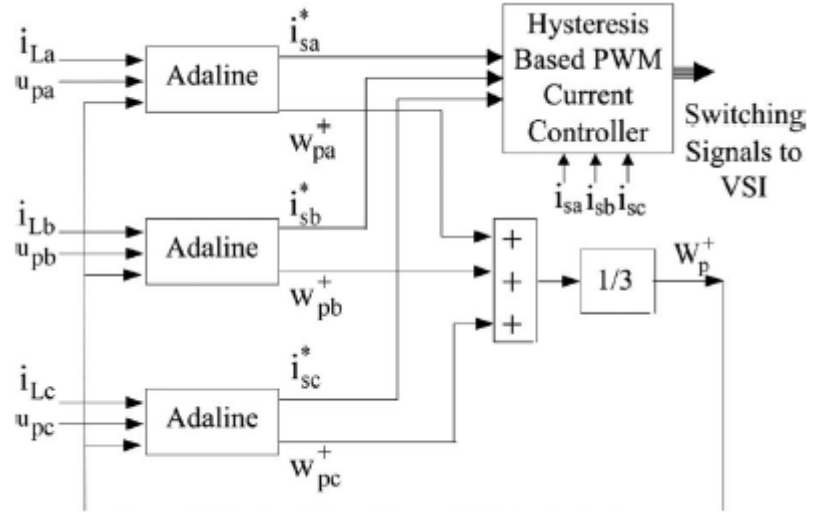


**Figure 3.37:** Block diagram of the reference current extraction via the use of Adaline-based theory.

A primary calculate of the active portion of current for single phase can be selected as:

$$i_p^+ = W_p \times u_p \quad (3.104)$$

For three-phase system, where, the Adaline technique is utilized to estimate weight ( $W_p$ ). The weight is variable. It also varies with the magnitude of phase voltage and load current. Estimating weight's scheme that correspond to the real component of current of the fundamental frequency, depend on LMS-algorithm-tuned Adaline, the unit voltage templates were tracked to keep the lowest error  $\{i_{L(k)} - W_{P(k)}u_{p(k)}\}$ .

Calculation of weight is expressed as a series or iterations [43]:

$$W_{P(k+1)} = W_{P(k)} + \eta \{i_{L(k)} - W_{P(k)} u_{p(k)}\} u_{p(k)} \quad (3.105)$$

The rate of convergence and the accuracy of estimation is decided by the value of  $\eta$  (convergence coefficient). Convergence coefficient lies practically in a range in between 0.1 and 1.0. The higher values of  $\eta$  supply fast convergence toward the final value with losing some a bit of accuracy. In order to get higher accuracy, the chosen  $\eta$  value here is regarded as 0.2 at the acceptable dynamic response.



Three-phase reference source currents that correspond to positive sequence real component of load current can be expressed as:

$$i_{sa}^* = W_p^+ u_{pa} ; i_{sb}^* = W_p^+ u_{pb} ; i_{sc}^* = W_p^+ u_{pc} \quad (3.106)$$

$$W_p^+ = (W_{pa}^+ + W_{pb}^+ + W_{pc}^+)/3 \quad (3.107)$$

To estimate the reference currents, an average of weights is used to compute an equivalent weight for positive sequence current component in the analyzed form. This averaging serves to remove the unbalance occur in the current components.

Reference source currents of three-phase are supplied to the hysteresis-based PWM current controller in order to control the source currents to track the reference source currents in UPF mode of operation.

Such currents are regarded as the reference source currents  $i_{ref}^*$  ( $i_{sa}^*$ ,  $i_{sb}^*$  and  $i_{sc}^*$ ), and together with the sensed source currents  $i_{act}$  ( $i_{sa}$ ,  $i_{sb}$ , and  $i_{sc}$ ), they are supplied to a hysteresis-based PWM current controller to get control over the source currents to get these reference currents followed.

The switching of signals that are produced by PWM current controller get control over the source currents that are close to the reference current. These switching signals are created by the logic as following, where  $h_b$  is the hysteresis band around the reference current  $i_{ref}$ .

- If  $(i_{act}) > (i_{ref} + h_b)$ , the leg's upper switch is ON, and the lower switch is OFF.
- If  $(i_{act}) < (i_{ref} - h_b)$ , the leg's upper switch is OFF, and the lower switch is ON.

The current control leads to get control over the slow changing source current (as compared to D-STATCOM currents) and thus demands less computational efforts. In addition, this scheme spontaneously helps compensating the processor's computational delay.

### 3.5.4 PI Controller for Maintaining Constant DC Bus Voltage of D-STATCOM

The operation of D-STATCOM system entails AC mains to provide the power required to the load and apart of losses such as dielectric losses of dc bus capacitor, switching losses of devices, and losses in the reactor in the D-STATCOM. Thus, the reference source current, employed to decide to switch of D-STATCOM, contains two components. The first component is the real fundamental frequency component of the load current that is extracted utilizing the SRF theory, Adaline technique, or  $p-q$  theory. The estimation of another component, which matches the loss in D-STATCOM, is done via the use a proportional–integral (PI) controller over the DSTATCOM dc bus voltage.

The second component of the reference active current is calculated via a reference dc bus voltage ( $v_{dc}^*$ ) which is compared with the sensed dc bus voltage ( $v_{dc}$ ) of DSTATCOM. The sensed dc bus voltage is compared to the reference dc bus voltage of VSC outcomes in a voltage error, which, in the  $n$ th sampling instant, is seen as:

$$v_{dc(n)} = v_{dc(n)}^* - v_{dc(n)} \quad (3.108)$$

A PI controller is processing this error signal  $v_{dcl(n)}$  in, and the output  $\{Ip_{(n)}\}$  at the  $n$ th sampling instant is given as:

$$Ip_{(n)} = Ip_{(n-1)} + K_{pdc}\{v_{dc(n)} - v_{dc(n-1)}\} + K_{idc} v_{dcl(n)} \quad (3.109)$$

Where ( $K_{pdc}$ ) and ( $K_{idc}$ ) are the gains of proportional and integral respectively of the PI controller. This PI controller's output accounts for the losses in D-STATCOM, and it is seen as the current's loss component. This component ( $Ip_{(n)}$ ) can be summed with the average real power to control D-STATCOM by  $p-q$  theory. If SRF theory facilitates the control, the PI regulator's output can be supplemented with  $d$ -axis component of the current signal. Using Adaline to control D-STATCOM, the PI controller's output is supplemented with the equivalent source currents.

## **CHAPTER FOUR**

### **CALCULATIONS AND RESULTS**

#### **4.1 Arrangement of Results**

This chapter presents the proposed system of DSTATCOM for 33 KV microgrid systems, explain in details the controller and give the MATLAB / SIMULINK of this system. All the calculations required determining the parameters related to the proposed system of DSTATCOM have been done. The model has been implemented in MATLAB /SIMULINK software. All results have been obtained and organized and discussed.

#### **4. 2 DSTATCOMs Analysis and Design**

Design and analysis of DSTATCOM contain a detailed analysis conducted to derive the design equations needed for the sake of finding the calculation for the different components values that are used in their circuit configurations. As discussed earlier, the design of three-phase three-wire DSTATCOM containing the VSC design and its passive components is introduced in the next sections. The DSTATCOM contains a VSC, a ripple filter, and interfacing inductors. The VSC design contains the DC bus voltage level, rating of IGBTs and the DC capacitance.

The DSTATCOM topology of a three-phase three-wire is taken into consideration for thorough analysis. Figure 4.6 illustrations a planning diagram of one of the DSTATCOMs for this topology in distribution system. It is achieved by a three-leg VSC. Design of DSTATCOM is explained in the next sections [29].

### 4.2.1 Design of a Three-Phase Three Wire DSTATCOM

The DSTATCOM design includes estimating and selecting several components of the VSC of the DSTATCOM like DC capacitor value, a ripple filter, interfacing AC inductor and DC bus voltage. A ripple filter is employed to get filtration of the switching ripples from the voltage at PCC.

The interfacing inductors and ripple filter's design is executed to limit the ripple in the voltages and the currents. DC bus capacitor's design relies on the capacity of energy storage required during transient conditions. The DSTATCOM rating relies on the compensation of needed reactive power and degree of the load's unbalance.

Therefore, the current rating of the DSTATCOM is influenced by the rating of load power while its voltage rating relies on the DC bus voltage. The next sections show with the design equations for estimating and selecting the VSC components of the DSTATCOM and the voltage levels.

### 4.2.2 Three-Phase Three-Leg VSC Based DSTATCOM's Design

The use of a three leg VSC as a distribution static compensator and this topology has six IGBTs, DC capacitor and three AC inductors is explained in figure 4.6. The DSTATCOM supplies the compensation needed to decide the rating of VSC components. The design of VSC is done to compensate a reactive power, in 33KV 50HZ, three phase distribution system. The choice of an interfacing inductor a ripple filter, and a DC capacitor is explained in the next parts.

#### 4.2.2.1 Selection of the DC Bus Voltage

The VSC DC bus voltage level should have at least two times of phase voltage of distributing system. The following formula used to estimate it:

$$V_{DC} = \frac{2\sqrt{2} V_{LL}}{(\sqrt{3}m)} \quad (4.1)$$

Where ( $m$ ) stands to the modulation index. It is regarded as 1 and  $V_{LL}$  is the AC line output voltage of the DSTATCOM.

#### 4.2.2.2 Selection of a DC Bus Capacitor

The DC capacitor ( $C_{DC}$ ) value of the system relies on available amount of the instantaneous energy to the DSTATCOM for the period of transient. Energy conservation's principle can be given as:

$$\frac{1}{2} C_{DC} (V_{DC}^2 - V_{DC1}^2) = k_1 3 V a I t \quad (4.2)$$

Where ( $V_{DC}$ ) stands to the nominal DC voltage value that has a same value of the reference DC voltage, ( $V_{DC1}$ ) stands to the lowest level of DC bus voltage, ( $a$ ) stands to the over loading factor, ( $V$ ) stands to the phase voltage, ( $I$ ) stands to the phase current, ( $k_1$ ) stands to the variation of energy during dynamics, and ( $t$ ) stands to the recovery time that needed to recover the voltage of the DC bus.

#### 4.2.2.3 AC Inductor Selection

Selecting the AC inductance ( $L_r$ ) of a VSC relies on the DC bus voltage ( $V_{DC}$ ), switching frequency  $f_s$ , and current ripple  $i_{cr,pp}$ . The AC inductor can be calculated by using the following formula:

$$L_r = \sqrt{3} m V_{DC} / (12 a f_s i_{cr,pp}) \quad (4.3)$$

Where ( $m$ ) represents the modulation index and ( $a$ ) stands for the overloading factor.

#### 4.2.2.4 Ripple Filter Selection

In order to filter out the noise from the voltage at PCC, a high-pass first-order filter tuned to half the switching frequency has been utilized. The filter should have a short time constant compared with the fundamental time interval ( $T$ ),  $R_f C_f \leq T_f$ , considering  $R_f C_f = T_s / 10$ , where ( $R_f$ ) stands for the ripple filter resistance, ( $C_f$ ) stands to the ripple filter capacitance, and ( $T_s$ ) stands to the switching time.

#### 4.2.2.5 Voltage and Current Ratings of the Solid-State Switches

The calculation of the rating of voltage ( $V_{sw}$ ) of the device can be done under dynamic states and can be expressed as:

$$V_{sw} = V_{DC} + V_d \quad (4.4)$$

Where  $V_d$  represents the 10% overshoot in the DC link voltage under dynamic states, with a suitable safety factor, 3.3 KV, IGBTs are chosen for the VSC employed in the DSTATCOM.

The calculation of the current rating ( $I_{sw}$ ) of the device can be done under dynamic states and can be expressed as:

$$I_{sw} = 1.25 (i_{cr,pp} + I_{peak}) \quad (4.5)$$

In the light of such equations, estimation can be done to the voltage and current rating of the IGBT switches. Therefore, selection of a solid-state switch (IGBT) for the VSC is done with the next existing higher rating of IGBT switch [29].

### 4.3 Design of the 12-Pulse D-STATCOM

A typical 12-pulse inverter arrangement using two transformers with their primaries joined in series is shown in figure 4.1. The first inverter is linked to the system by using a Y-Y transformer, whereas the second one is connected through a Y- $\Delta$  connection. Each one of these inverters runs as a 6-pulse inverter, with the second inverter, a delay of  $30^\circ$  was gotten with respect to the first inverter [44]. The two inverters have the current flowing, determined by the transformer ratio, as the D-STATCOM draws the current from the system.

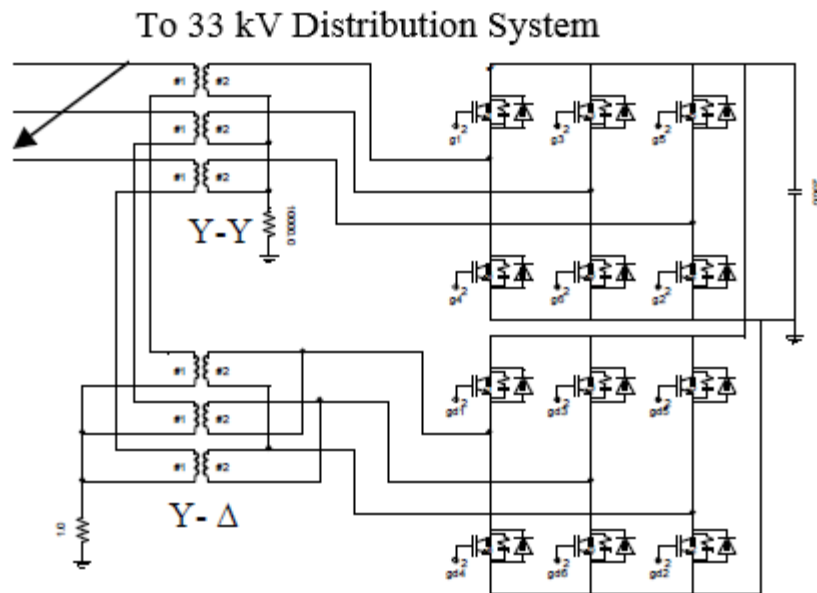


**Figure 4.1:** 12-pulse D-STATCOM

The proposed 12-pulse D-STATCOM configuration with the IGBT's utilized as power devices is shown in figure 4.1. The IGBTs are linked anti-parallel with diodes for commutation objectives and charging of the DC capacitor [45].

The DC side of D-STATCOM is linked in shunt to have the voltage on the DC side to the minimum level if possible in addition to improve using the DC side capacitor. The first transformer is in Y-Y link and the second transformer is in Y- $\Delta$  link in order to give a phase shift by  $30^\circ$  between the pulses and to decrease harmonics produced from the D-STATCOM. MATLAB/Simulink model for transformers combination illustrated in figure 4.2.

Figure 4.3 illustrates MATLAB/Simulink model of D-STATCOM system. Thus, both of these transformers are stepped down from 33kV to 1.25 KV, i.e. 33:1.25, the connection of D-STATCOM is done in parallel to the system.

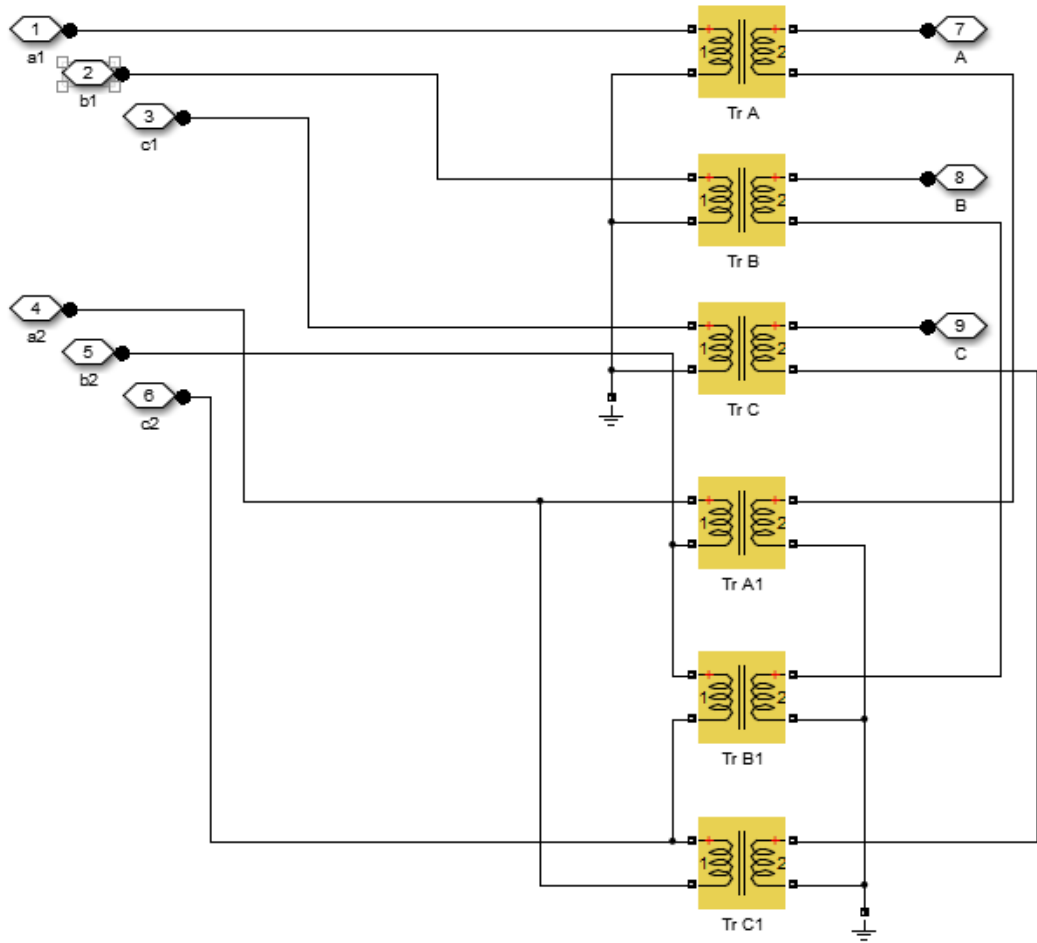


**Figure 4.2:** MATLAB/Simulink model of transformers combination

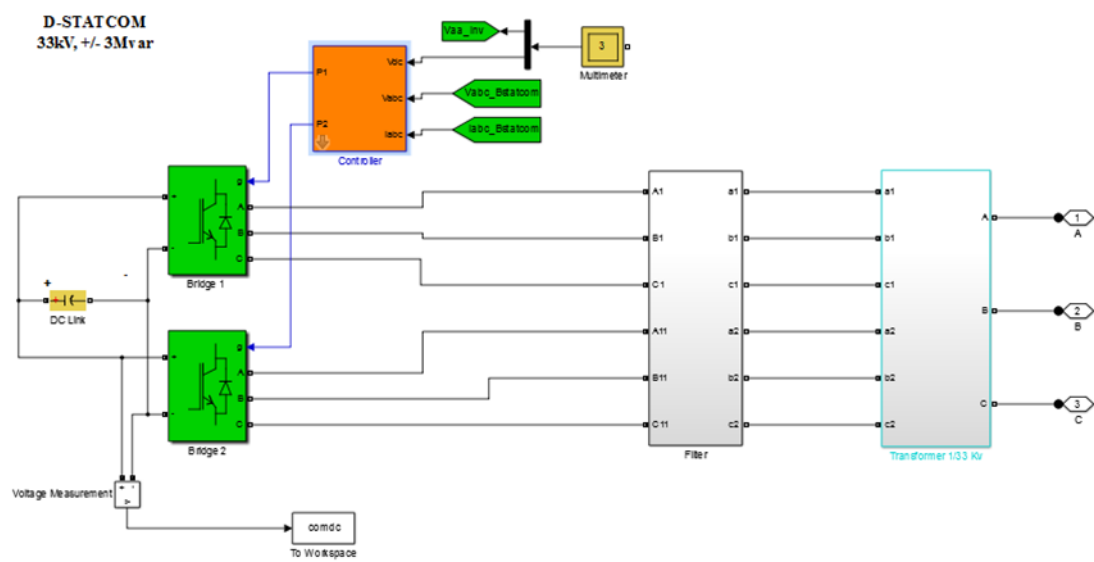


**Figure 4.3:** MATLAB/ Simulink model of the 12-pulse D-STATCOM



### 4.3.1 Inverter Design

To convert DC signal to AC signal by using the inverters, and it's represent the heart of the D-STSTCOM device. In this work a three-phase inverter has been designed. The DC capacitor represent the main source and supplied the system, which is located in shunt with the D-STATCOM, the capacitor's charging is indicates to the reactive power exchanged within the system.

The capacitor is charging if the current in the system is greater than the current produced from the DSTATCOM and it's discharged if the current of the D-STSTCOM is greater than the system current. For the inverter, the significant part is the sequences of operation of the IGBTs switches. The IGBTs waveforms are indicates to the Sinusoidal Pulse Width Modulation (SPWM) that will work on producing the pulses for driving the IGBTs.

### 4.3.2 Capacitor Sizing

It is indicates to the fault current occurring in the system. The difference between before and after fault in currents is regarded as current faults. In capacitor sizing, there should be an appropriate range of DC capacitor is required to store the energy in order to get the voltage sag's mitigation. If the voltage is in sag state, the DC capacitor,  $C_{DC}$  is employed to add reactive power to the D-STATCOM. In the scheme, the harmonic effects should be taken into consideration due to the inductive load which could influence the value of  $C_{DC}$ . The next equation is employed to have calculation for  $C_{DC}$  [45]:

$$1/2 C_{DC} [V_{C_{MAX}}^2 - V_{DC}^2] = 1/2 V_{SM} \cdot \Delta I_L \cdot T \quad (4.6)$$

Equation (4.6) is employed to mitigate harmonic in single phase system but for a three phase system the equation can be expressed as:

$$C_{DC} = 3 \times \frac{V_S \cdot \Delta I_L \cdot T}{V_{C_{max}}^2 - V_{DC}^2} \quad (4.7)$$

Where:

$V_S$  : Stands to the peak phase voltage.

$I_L$  : Stands to the step-drop of the load current.

$T$  : Stands to the period of one cycle of voltage and current.

$V_{C_{max}}$  : Stands to the pre-set upper limit of the energy storage capacitor (per-phase).

$V_{DC}$  : Stands to the voltage across the capacitor (per-phase).

The value of  $\Delta I_L$  can be calculated by measuring the load current before and during the voltage sag [45]. The value of  $V_{DC}$  can be expressed as:

$$V_{DC} = \frac{3\sqrt{3}.V_S.\cos\alpha}{\pi} \quad (4.8)$$

Where:

$\alpha$  : Stands to the delay angle ; if  $\alpha = 0$ , the expression can be written as:

$$V_{DC} = \frac{3\sqrt{3}.V_S}{\pi} \quad (4.9)$$

The value of  $V_{C_{max}}$  is represent the upper limit of  $C_{DC}$ , and is two or three times of the  $V_{DC}$ .

### 4.3.3 Transformer Configuration

In the case of 12-pulse operation, the first six-pulse inverter is shifted by  $30^\circ$  from the second one, they can supply the phase angle shift for an appropriate configuration. The connection of the transformers is done in shunt to each other for six pulse configuration for the 12-pulse D-STATCOM. The first inverter is linked in Y-Y to the system lagging  $30^\circ$  from the second one that is linked to the system in Y- $\Delta$  configuration. For Y- $\Delta$  link, it gives a phase shift of about  $30^\circ$ , which is required to prove the stable condition of the 12 pulse D-STATCOM.

### 4.3.4 Controller Configuration

The control employed to simulate the D-STATCOM in this work has aimed to control the AC voltage and control the reactive power. This kind of control has two parts. These are the sinusoidal pulse width modulation (SPWM) and reactive power control. The MATLAB/Simulink model of the controller that makes the regulation of the AC side of voltage sourced converter (VSC) or alternatively, reactive power into or out of the VSC and DC bus voltage is seen in figure 4.4. The PI controller's output is the angle order, employed to provide and keep maintaining the phase shift. The system's reactive power flowing is compared to the reference per-unit voltage that helps in changing the phase shift. The difference in phase shift will give the required reactive power from the DC link capacitor.

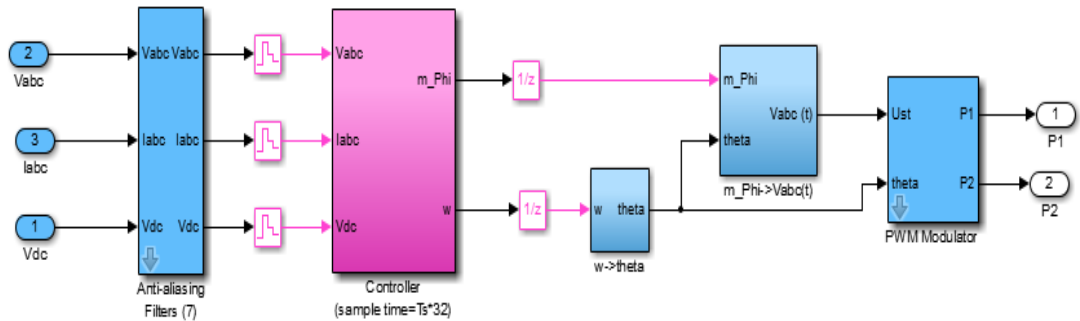


**Figure 4.4:** MATLAB/Simulink model of D-STATCOM controller

**Table 4.1:** Designing parameters

1	System voltage	33 KV
2	System frequency	50 Hz
3	D-STATCOM rating	3.3 MVAR
4	DC bus voltage	2500 V
5	DC capacitor	10000 $\mu$ F

**Table 4.1 (Continue):** Designing parameters

6	Passive filter	L=800 $\mu$ H
		C=100 $\mu$ F
		R=0.785 m $\Omega$
7	Transformers rating	33 KV/1250 V, 3.3 MVA
8	IGBT switches rating	3.3 KV, 1200 A
9	Inductive load	1 MW + 3 MVAR
10	Capacitive load	1 MW + 3 MVAR
11	Resistive load	1 MW

#### **4.4 Simulation Results of 33 KV System**

##### **4.4.1 MATLAB/ SIMULINK model of 33 KV Distribution System**

Figure 4.5 illustrates MATABL/Simulink model of the proposed 33 KV, 50 Hz micro- grid distribution system, this model consists of 33 KV power source and 33KV feeders with length of 30 Km, and four bus-bars. Three different loads (resistive, inductive, and capacitive) are connected to bus-bar B3 through step-down transformer (33/0.4 KV), the three loads are switched by three phase circuit breaker.

+3/-3 MVAR Distribution STATCOM is connected to the system on bus-bar named B-STATCOM through three phase circuit breaker, D-STATCOM composed of 12 pulse voltage source inverter and DC capacitor with LC filter and step-down transformers as shown in figure 4.6 controlled by a control unit that used SRF theory as shown in figure 4.4.

There are two cases illustrates the response of the system with and without D-STATCOM for voltage dip and voltage swell as indicates in the next sections.

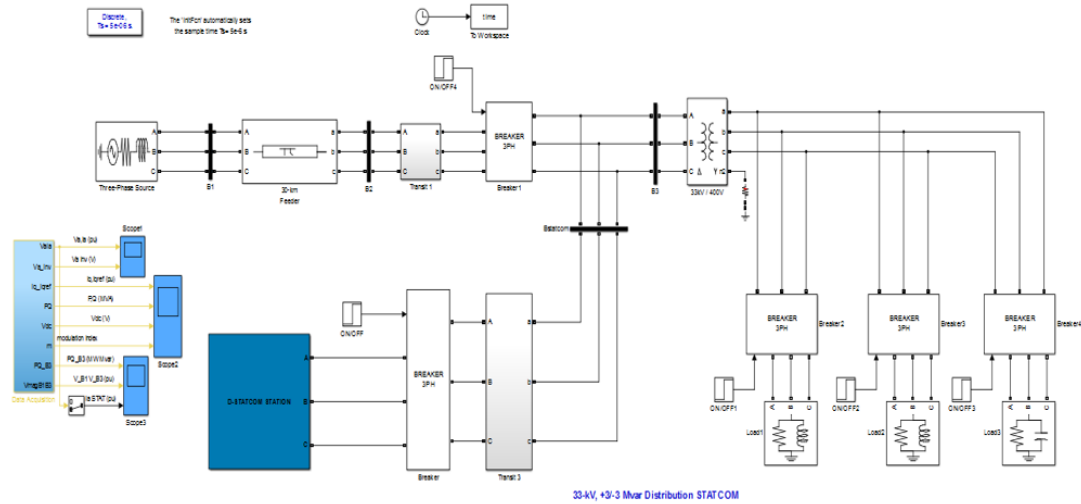


**Figure 4.5:** MATLAB/SIMULINK model of the proposed system

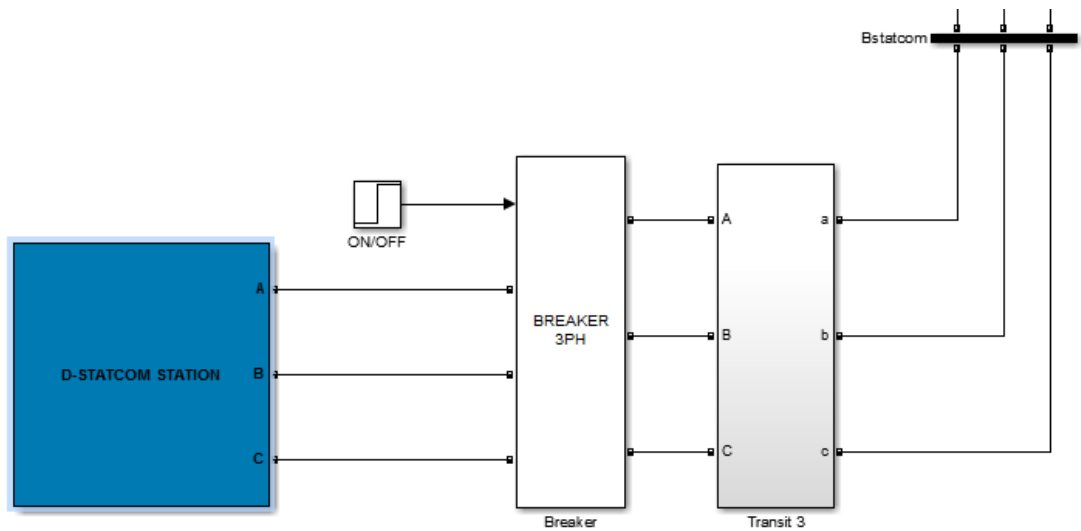


**Figure 4.6:** 33KV, +/- 3MVAR D-STATCOM (Simulink model)

#### 4.4.1.1 Voltage Dip of 33KV Microgrid System without D-STATCOM

For the testing system, we made the circuit breaker OFF to isolate the D-STATCOM from the system, in this case, we can test system for voltage dip (sag) by applying an inductive load for short time (0.4 s). From the simulation results we obtained the following waveforms. Figure 4.7 showed the voltage at PCC, figure 4.8 showed the active and reactive power of the system, and figure 4.9 indicates the active and reactive power at bus-bar B3 and the voltage at B1 and B3.

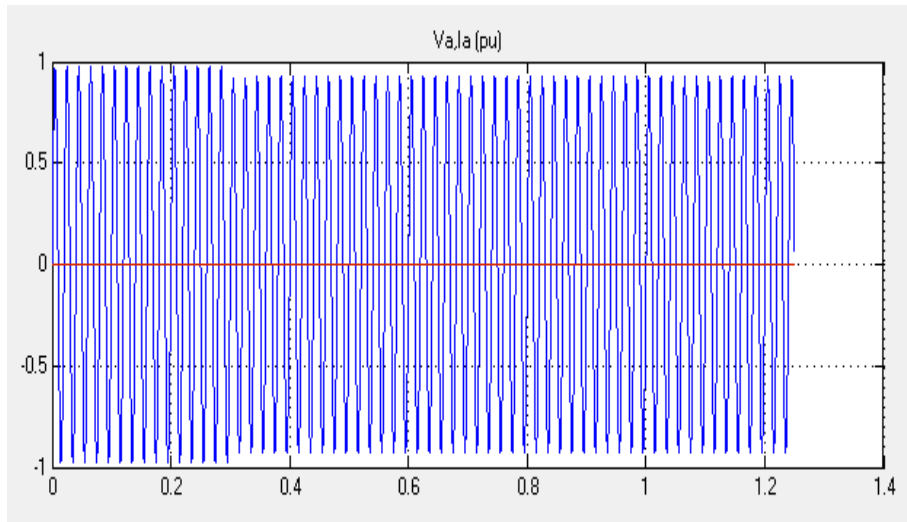


**Figure 4.7:** Voltage at PCC (without D-STATCOM)

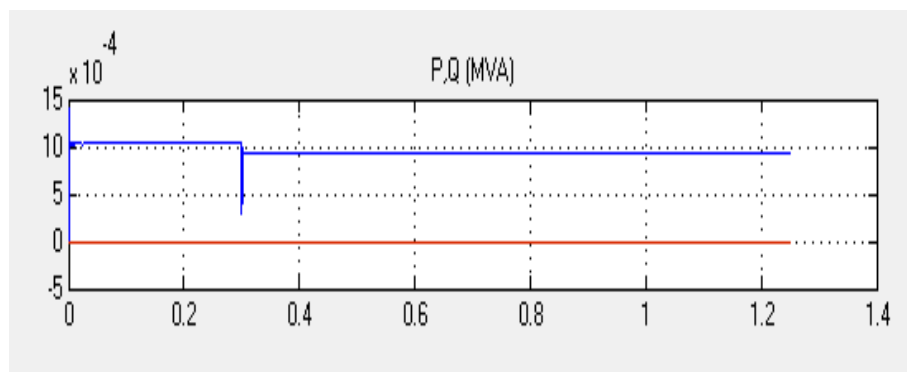


**Figure 4.8:** P, Q (without D-STATCOM)

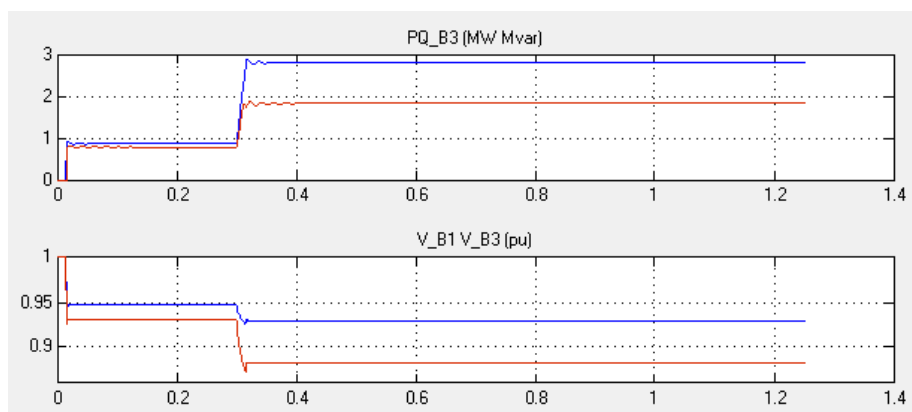


**Figure 4.9:** PQ\_B3, V\_B1, and V\_B3 (without D-STATCOM)

#### 4.4.1.2 Voltage Swell of 33KV System without D-STATCOM

For the testing system, we made the circuit breaker OFF to isolate the D-STATCOM from the system, in this case, we can test system for voltage swell by applying a capacitive load for short time (0.4 s). From the simulation results we obtained the following resulting waveforms. Figure 4.10 showed the voltage at PCC, figure 4.11 showed the active and reactive power of the system, and figure 4.12 indicates the active and reactive power at bus-bar B3 and the voltage at B1 and B3.

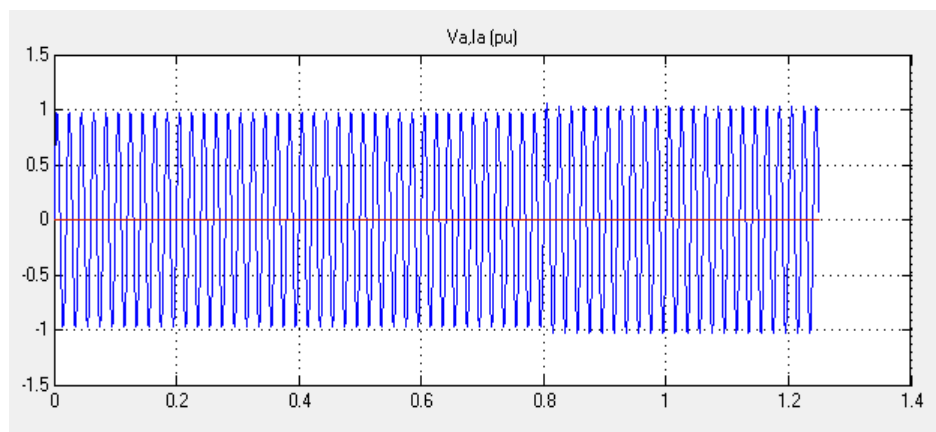


**Figure 4.10:** Voltage at PCC (without D-STATCOM)

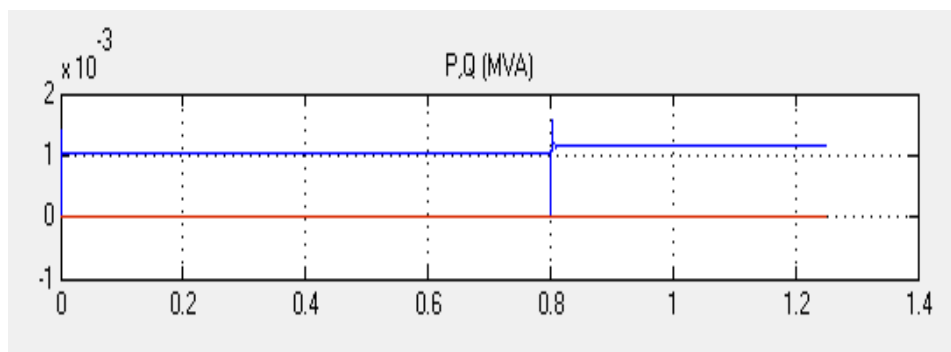


**Figure 4.11:** P, Q (without D-STATCOM)

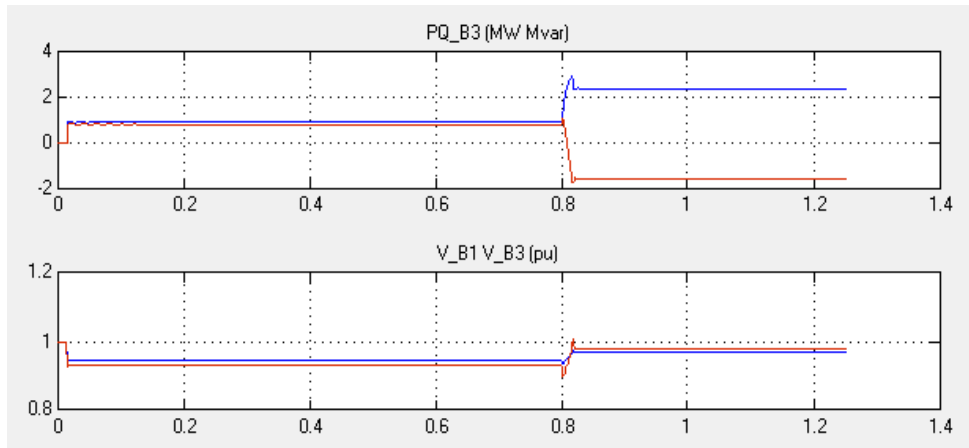


**Figure 4.12:** PQ\_B3, V\_B1, and V\_B3 (without D-STATCOM)

#### 4.4.1.3 Voltage Dip of 33KV System with D-STATCOM

For testing our proposed system, we made the circuit breaker ON to connect the D-STATCOM to the system, in this case, we can test system for voltage dip (sag) by applying an inductive load for short time (0.4 s). From the simulation results we obtained the following waveforms. Figure 4.13 showed the voltage and current at PCC, figure 4.14 showed the D-STATCOM inverter voltage, figure 4.15 indicates the  $I_q$ ,  $I_{qref}$  (pu), figure 4.16 indicates the active and reactive power of the system, figure 4.17 showed the voltage of the DC bus, figure 4.18 showed the modulation index of D-STATCOM, figure 4.19 showed the active and reactive power at bus-bar B3, figure 4.20 indicates the voltage at B1 and B3, and figure 4.21 showed  $I_a$  of D-STATCOM current.

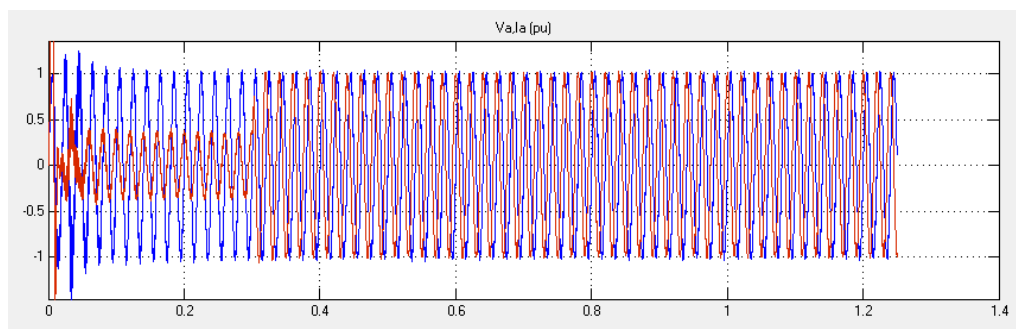


**Figure 4.13:** Voltage and current at PCC (with D-STATCOM)



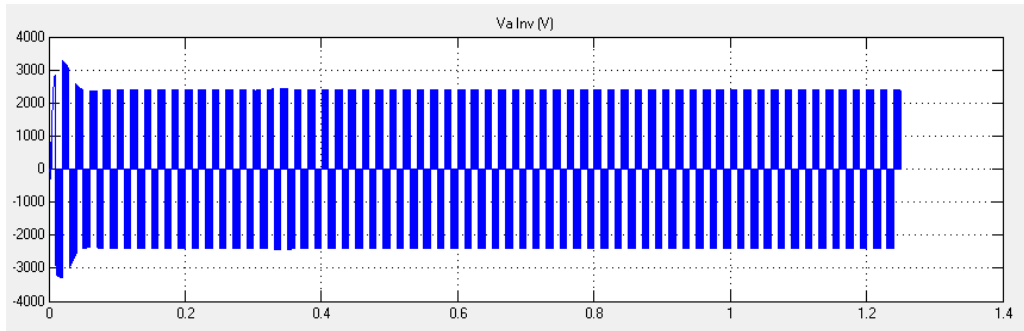


**Figure 4.14:** D-STATCOM inverter voltage

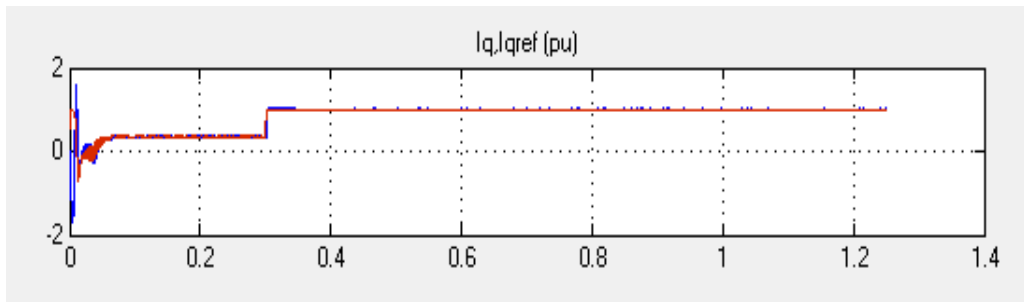


**Figure 4.15:**  $I_q$ ,  $I_{qref}$  (pu)

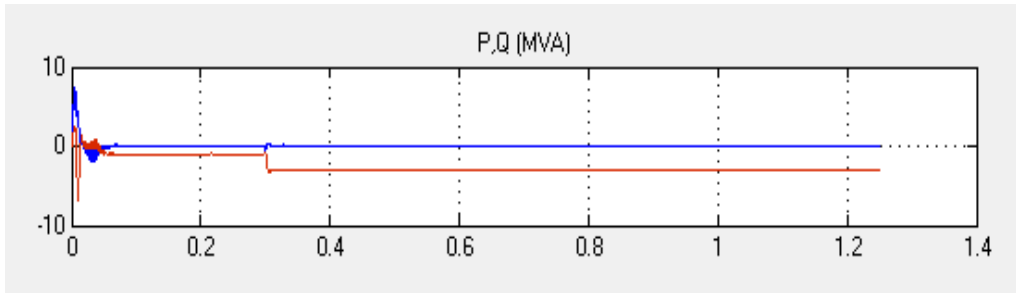


**Figure 4.16:** P, Q (with D-STATCOM)

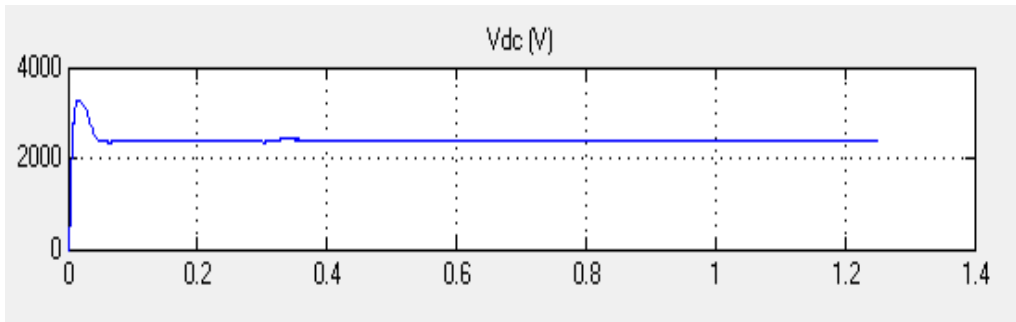


**Figure 4.17:**  $V_{dc}$  of D-STATCOM

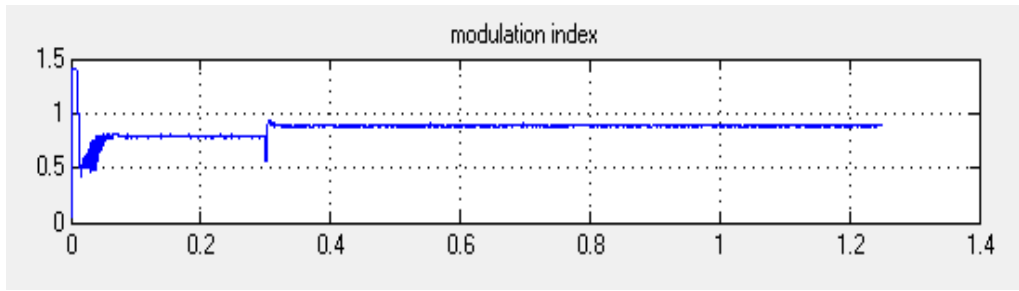


**Figure 4.18:** Modulation index of D-STATCOM

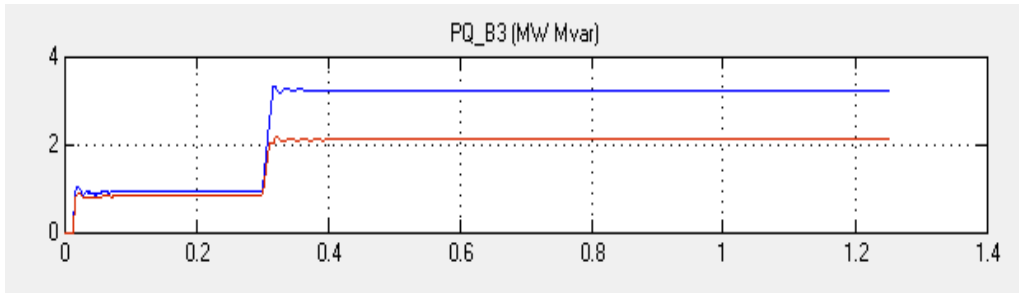


**Figure 4.19:** PQ\_B3 (with D-STATCOM)

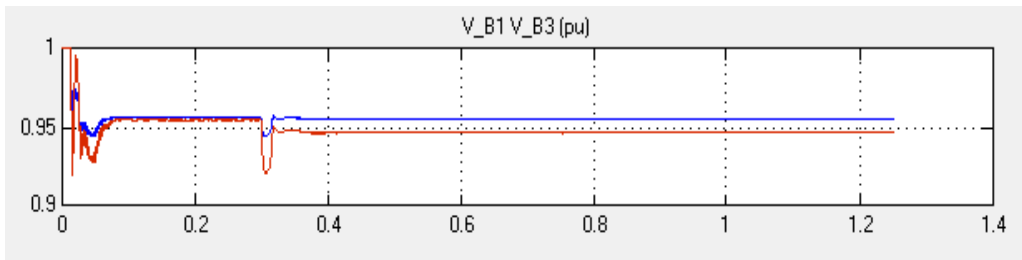


**Figure 4.20:** V\_B1 and V\_B3 (with D-STATCOM)

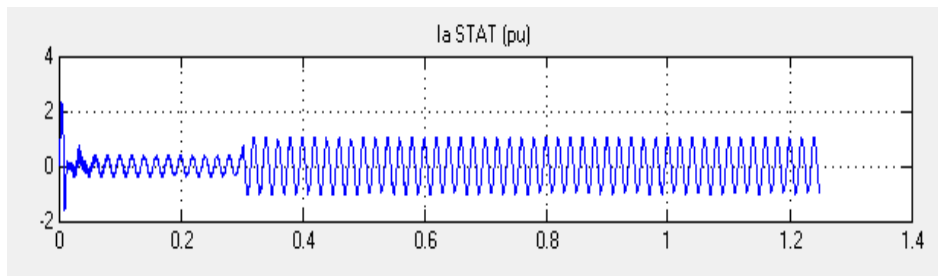


**Figure 4.21:** Ia of D-STATCOM

#### 4.4.1.4 Voltage Swell of 33KV System with D-STATCOM

For testing the system, we made the circuit breaker ON to connect the D-STATCOM to the system, in this case, we can test system for voltage swell by applying a capacitive load for short time (0.4 s). From the simulation results we obtained the following waveforms. Figure 4.22 showed the voltage and current at PCC, figure 4.23 showed the D-STATCOM inverter voltage, figure 4.24 indicates the  $I_q$ ,  $I_{qref}$  (pu), figure 4.25 indicates the active and reactive power of the system, figure 4.26 showed the voltage of the DC bus, figure 4.27 showed the modulation index of D-STATCOM, figure 4.28 showed the active and reactive power at bus-bar B3, figure 4.29 indicates the voltage at B1 and B3, and figure 4.30 showed  $I_a$  of D-STATCOM current.

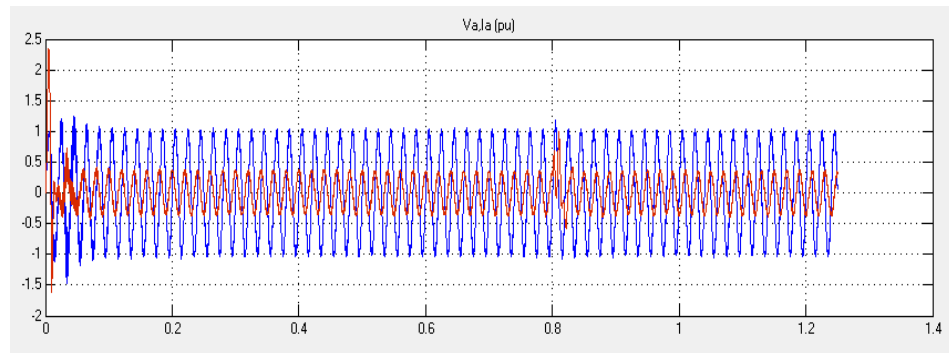


**Figure 4.22:** Voltage and current at PCC (with D-STATCOM)

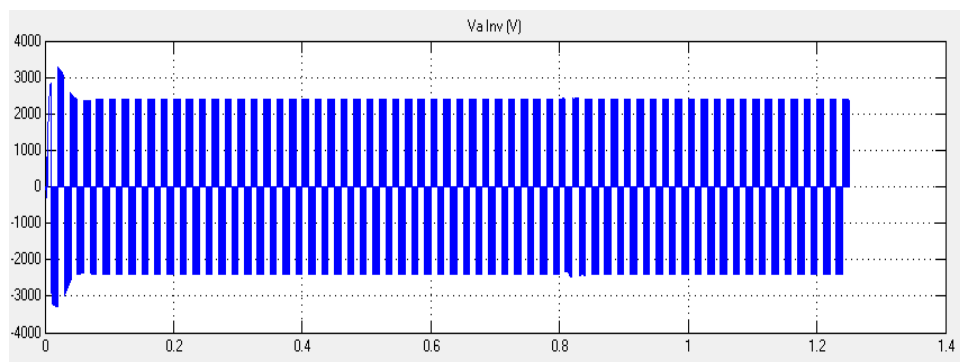


**Figure 4.23:** D-STATCOM inverter voltage

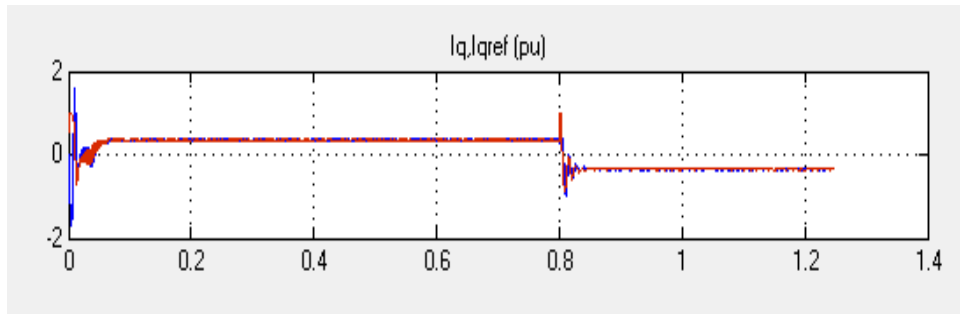


**Figure 4.24:**  $I_q, I_{qref}$  (pu)

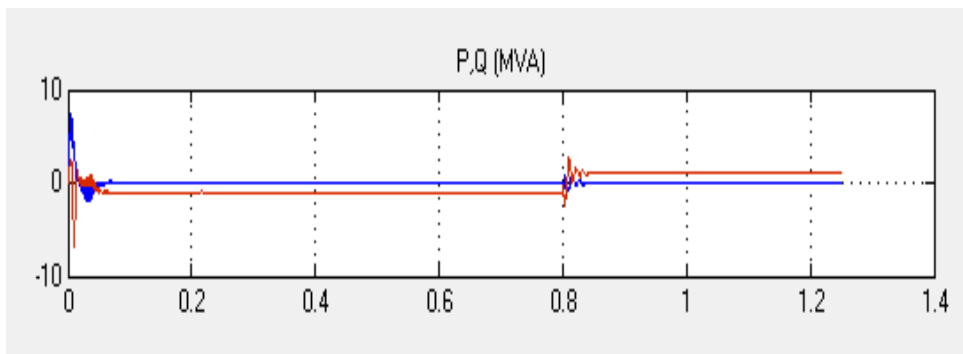


**Figure 4.25:**  $P, Q$  (with D-STATCOM)

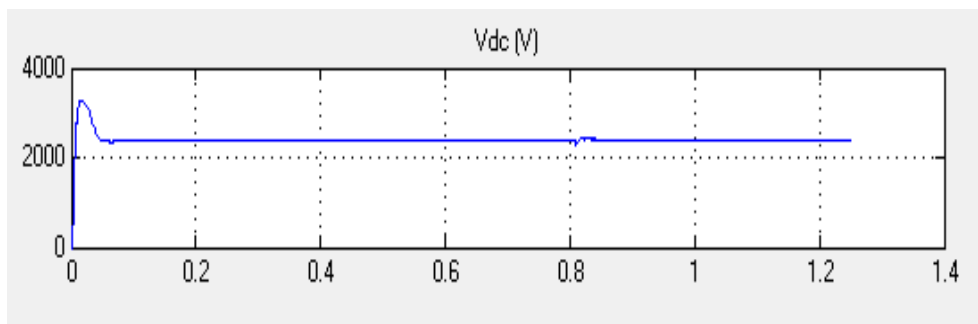


**Figure 4.26:**  $V_{dc}$  of D-STATCOM

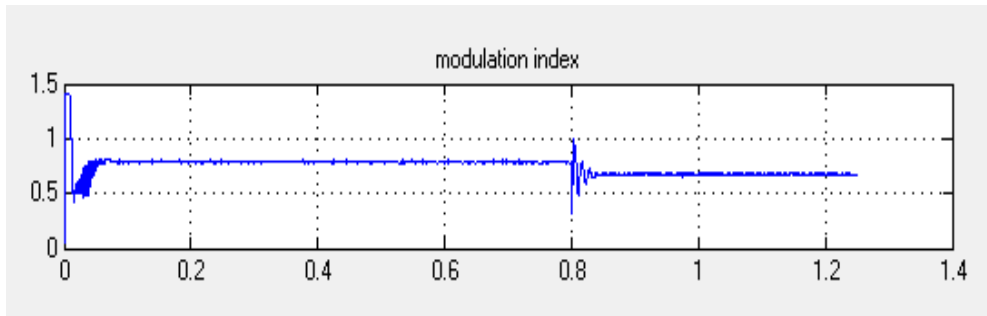


**Figure 4.27:** Modulation index of D-STATCOM

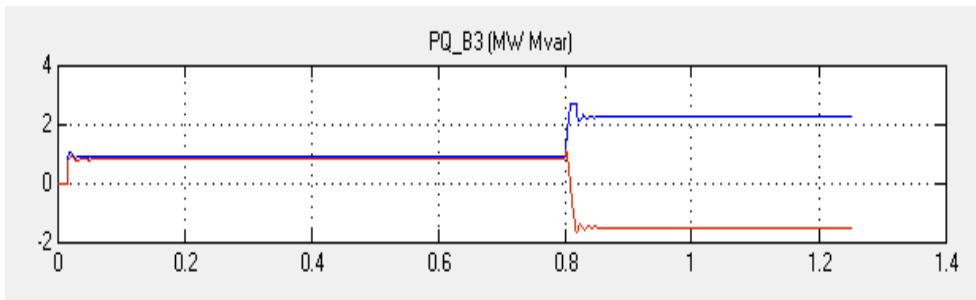


**Figure 4.28:** PQ\_B3 (with D-STATCOM)

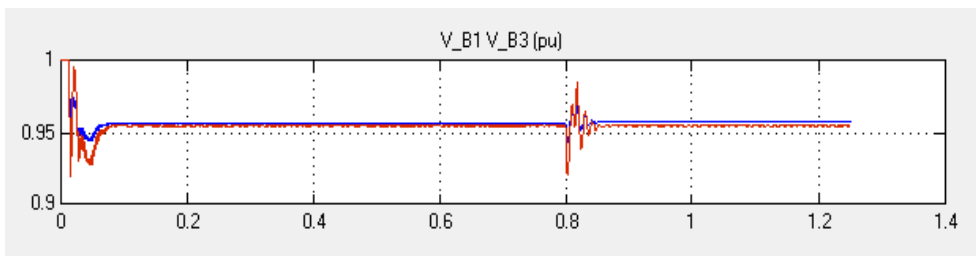


**Figure 4.29:** V\_B1 and V\_B3 (with D-STATCOM)

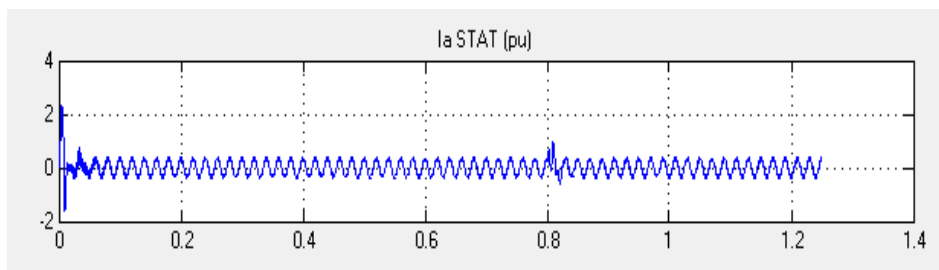


**Figure 4.30:** Ia of D-STATCOM

## CHAPTER FIVE

### CONCLOSIONS AND FUTURE WORKS

#### 5.1 Conclusions

This thesis has been present and studying D-STATCOM in terms of the problems that can be addressed and in terms of its components and methods of control used to control it, as well as this thesis has provided a mathematical analysis to the heart of this device, which is a VSC. Two common types of VSC that used especially in medium voltage systems are analyzed and presented in this thesis and a MATLAB model for a twelve pulse D-STATCOM in 33 KV system has been presented to mitigate voltage dip (sag) and voltage swell that yields when connecting or disconnecting a heavy loads or due to faults occurrence, to study the behavior of the system before and after connecting of D-STATCOM device. the results were discussed in terms of D-STATCOM ability to address these power quality problems.

In this thesis, D-STATCOM has been modeled in MATLAB/SIMULINK environment. The performance of DSTATCOM has been analyzed for inductive load and capacitive load. D-STATCOM has been found to regulate PCC current under varying load conditions. It is therefore, concluded that D-STATCOM has a huge scope in improving power quality levels in distribution systems.

A simulation model of the 12-pulse D-STATCOM has been designed using the MATLAB/SIMULINK program. An important aspect considered in the design is the control system. The control strategy for the D-STATCOM is the AC side voltage or reactive power control. PI controller is used to control the flow of reactive power to and from the DC capacitor. Phase Lock Loop components are used in the control to generate the switching signal, i.e. triangular waves, and reference signals, i.e. sinusoidal wave. PWM switching control is used to switch on and off the IGBT's.

The IGBT's are connected inversely and parallel to the diodes for commutation purposes and to charge the capacitor. IGBTs are used in this simulation because it is easy to control the switch on and off of their gates and suitable for the designed D-STATCOM. From the simulation results, the designed D-STATCOM responded well in mitigating voltage sag and voltage swell caused by connecting heavy inductive and capacitive load respectively.

The DC capacitor value is dependent on the percentage of voltage sag. The difference of step drop load current during sag is the amount of reactive current needed to be compensated. Lastly, the D-STATCOM is a promising device and will be a prominent feature in power systems in mitigating power quality related problems in the near future.

## **5.2 Future Works on D-STATCOM**

This thesis is shown that D-STATCOM can give an effective compensation of reactive power, keeping PCC voltage at desired magnitude even when applying inductive or capacitive loads. Thus meaning it help system to mitigate voltage dip and/or voltage swell.

The future work may be widened to study the effect of D- STATCOM to mitigate other power quality problems with developing the following parts:

- Controllers with using another advanced control methods like Adaline based control technique can be implemented with DSTATCOM to increase the effectiveness of DSTATCOM in distribution networks.
- The transformers combination to increase the effectiveness of DSTATCOM for mitigating power quality problems in distribution and enhance the performance against harmonics and to stabilize it with other types of non-linear loads like arc furnace, and so on.

## REFERENCES

- [1] D.G. Flinn, C. Gilker, and S.R. Mendis, "Methods for Identifying Potential Power Quality Problem", *Conference on Rural Electric Power*, February 3, 1991.
- [2] A. El Mofty and K. Youssef, "Industrial Power Quality Problems", *Conference on Electrical Distribution*, Vol.2, pp. 18-21, June 2001.
- [3] J. Sun, D. Czarkowski, and Z. Zabar, "Voltage Flicker Mitigation Using PWM-Based Distribution STATCOM", *Conference on Power Engineering Society Summer Meeting, Publication*, Vol.1 , pp. 616 – 621, 2002.
- [4] Walmir Freitas, Andre Morelato, Wilsun Xu, and Fujio Sato, "Impacts of AC Generators and DSTATCOM Devices on the Dynamic Performance of Distribution Systems", *Conference on IEEE Transactions on Power Delivery*, pp. 1493 – 1501, 2005.
- [5] Bhim Singh, Alka Adya, A.P. Mittal and J.R.P Gupta, "Modelling and Control of DSTATCOM for Three-Phase, Four-Wire Distribution Systems", *Conference, on Industry Applications Conference*, Vol. 4, pp: 2428 - 2434, 2005.
- [6] M. G. Molina and P. E. Mercado, "Dynamic Modelling and Control Design of DSTATCOM with Ultra-Capacitor Energy Storage for Power Quality Improvements", *Conference on Transmission and Distribution conference and Exposition: Latin America, IEEE/PES*, pp. 1 – 8, 2008.
- [7] Virulkar, V, and Aware, M, "Analysis of DSTATCOM with BESS for mitigation of flicker", *International Conference on Control, Automation, Communication and Energy Conservation, 2009. INCACEC 2009*, 4-6 June 2009.
- [8] Sepulveda, C.A, Espinoza, J.R., Landaeta, L.M., and Baier, C.R. "Operating Regions Comparison of VSC-based Custom Power Devices", *32nd Annual Conference on IEEE Industrial Electronics, IECON 2006*, 6-10 Nov. 2006.
- [9] Naetiladdanon Sumate, "Voltage Sag Compensation Performance by DSTATCOM with Series Inductor and Energy Storage", *7th International Conference on Power Electronics and Drive Systems, 2007. PEDS '07*, 27-30 Nov. 2007.



- [10] Aodsup, K., Boonchiam, P.N., Sode-Yome, A., Kongsuk, P. and Mithulananthan, N., "Response of DSTATCOM under Voltage Flicker in Farm Wind", *7th International 49 Conference on Power Electronics and Drive Systems, 2007. PEDS '07*, 27-30, Nov. 2007.
- [11] Naetiladdanon, S, "Design considerations of DSTATCOM for voltage sag compensation without interaction", *Electrical Engineering/Electronics, 5th International Conference on Computer, Telecommunications and Information Technology*, Vol. 2, 14-17 May 2008.
- [12] Molina, M.G. and Mercado, P.E., "Dynamic modelling and control design of DSTATCOM with ultra-capacitor energy storage for power quality improvements", *Transmission & Distribution Conference and Exposition: Latin America, 2006*, 15-18 Aug. 2006.
- [13] Molina, M.G. and Mercado, P.E., "Control Design and Simulation of DSTATCOM with Energy Storage for Power Quality Improvements", *Transmission & Distribution Conference and Exposition: Latin America, 2006*, 15-18 Aug. 2006.
- [14] Virulkar, V.B. and Aware, M, "Analysis of DSTATCOM with BESS for mitigation of flicker", *International Conference on Control, Automation, Communication and Energy Conservation, 2009. INCACEC 2009*, 27-29 Dec. 2009.
- [15] Molina, M.G. and Mercado, P.E., "Control of tie-line power flow of micro grid including wind generation by DSTATCOM-SMES controller", *Energy Conversion Congress and Exposition, 2009. ECCE 2009. IEEE*, 20-24 Sept. 2009.
- [16] Suvire, G.O. and Mercado P.E, "Improvement of power quality in wind energy applications using a DSTATCOM coupled with a Flywheel Energy Storage System", *Power Electronics Conference, 2009. COBEP '09. Brazilian*, Sept. 27 2009-Oct. 2009.
- [17] Satyanarayana, G. V R and Ganesh, S. N V, "Cascaded 5-level inverter type DSTATCOM for power quality improvement", *Students' Technology Symposium (TechSym), 2010 IEEE*, 3-4 April 2010.
- [18] Molina, M.G. and Mercado, P.E., "Power flow control of micro grid with wind generation using a DSTATCOM-UCES", *International Conference on Industrial Technology (ICIT), 2010 IEEE*, 14-17 March 2010.

- [19] Singh, A. Singh, B. and Singh, S., "Customized solution for real and reactive power compensation for small distribution systems", *Conference on the European Energy Market (EEM), 2010 7th International*, 23-25 June 2010.
- [20] Hosseini, S. H. and Nazarloo, A., "Application of D-STATCOM to improve distribution system performance with balanced and unbalanced fault conditions", *Electric Power and Energy Conference (EPEC), 2010 IEEE*, 25-27 Aug. 2010.
- [21] Suvire, G.O. and Mercado, P.E, "Active power control of a flywheel energy storage system for wind energy applications", *Renewable Power Generation, IET*, Vol. 6, issue-1, pp. 9-16, Jan 2012.
- [22] Annapoorna Chidurala, Tapan Kumar Saha and N. Mithulananthan, "Power Quality Enhancement in Unbalanced Distribution Network using Solar-DSTATCOM", *Australasian Universities Power Engineering Conference, AUPEC 2013, Hobart, TAS, Australia*, 29 September - 3 October 2013.
- [23] C. H. Lin, C. S. Chen, W. L. Hsieh, C. T. Hsu, H. J. Chuang, and C.Y. Ho, "Optimization of Photovoltaic Penetration with DSTATCOM in Distribution Systems", in *2012 IEEE Power Engineering Society General Meeting, Toronto, Canada*, July 2012.
- [24] Rajiv K. Varma, V. Khadkikar, Ravi Seethapathy, "Nighttime Application of PV Solar Farm as STATCOM to Regulate Grid Voltage", *IEEE Transactions on Energy Conversion*, Vol. 24, Issue: 4, pp. 983 – 985, 2009.
- [25] Rajiv K. Varma, Shah Arifur Rahman, A. C. Mahendra, Ravi Seethapathy, Tim Vanderheide, " Novel nighttime application of PV solar farms as STATCOM (PV- STATCOM)", *IEEE Power and Energy Society General Meeting, IEEE Conference Publications*, pp. 1-8, 22-26 July 2012.
- [26] Vivek Nandan Lal, S. N. Singh, " Control and Performance Analysis of a Single-Stage Utility-Scale Grid-Connected PV System", *IEEE Systems Journal* Vol. PP, Issue: 99, pp. 1-11, 2015.
- [27] Rajiv Varma, Shah Arifur Rahman, Tim Vanderheide, "New control of PV solar farm as STATCOM (PV-STATCOM) for increasing grid power transmission limits during night and day", *IEEE PES T&D Conference and Exposition 2014, IEEE Conference Publications*, pp. 1-1, 2014.
- [28] Rajiv. K. Varma; Byomakesh Das, Iurie Axente, Tim Vanderheide, "Optimal 24-hr utilization of a PV solar system as STATCOM (PV-STATCOM) in a

distribution network", IEEE Power and Energy Society General Meeting 2011, IEEE Conference Publications, pp.1-8, 2011.

- [29] Bhim Singh, Ambrish Chandra, and Kamal Al-Haddad, "Power Quality: Problems and Mitigation Techniques", Wiley & Sons, February 2015.
- [30] M. P. Bahrman, J. G. Johansson, and B. A. Nilsson, "Voltage Source Converter Transmission Technologies – The right fit for the application", IEEE Power Engineering society General Meeting, Vol. 3, pp.1840–1847, 2003.
- [31] CIGRE, "Static Synchronous Compensator", Working Group 14.19, September 1998.
- [32] D. R. Trainer, S. B. Tennakoon, R. E. Morrison, "Analysis of GTO-based static VAR compensators", IEE Proc.-Elect. Power Appl., Vol. 141, No. 6, pp. 293-302, November 1994.
- [33] M. P. Bahrman, J. G. Johansson, and B. A. Nilsson, "Voltage Source Converter Transmission Technologies – The right fit for the application", *IEEE Power Engineering society General Meeting*, Vol. 3, pp.1840–1847, 2003.
- [34] Parag Nijhawan, Ravinder Singh Bhatia, and Dinesh Kumar jain, "Application of PI Controller Based DSTATCOM for Improving the Power Quality in a Power System Network with Induction Furnace Load", *Songklanakar Journal of Science and technology*, Vol. 2, Issue No. 34, pp. 195-201, March-April 2012.
- [35] P. Bapaiah, "Power Quality Improvement by Using DSTATCOM", *International Journal of Emerging Trends In Electrical And Electronics*, Vol. 2, Issue No. 4, pp. 1-12, April 2013.
- [36] P. Venkata Kishore, S. Rama Reddy and P.V. Kishore, "Modeling and Simulation of Thirty Bus System with DSTATCOM for Power Quality Improvement", *International Journal of Scientific and Technology Research*, Vol. 2, Issue No. 9, pp. 4560-4569, 2010.
- [37] H. Akagi, E. H. Watanabe, and M. Aredes, "*Instantaneous Power Theory and Applications to Power Conditioning*", Hoboken, NJ: Wiley, 2007.
- [38] R. S. Herrera, P. Salmeron, and H. Kim, "Instantaneous reactive power theory applied to active power filter compensation: Different approaches, assessment, and experimental results", *IEEE Trans. Ind. Electron.*, Vol. 55, No. 1, pp. 184–196, Jan. 2008.

- [39] D. M. Divan, S. Bhattacharya, and B. Banerjee, "Synchronous frame harmonic isolator using active series filter", in *Proc. Eur. Power Electron. Conf.*, 1991, pp. 3030–3035.
- [40] B. Singh and V. Verma, "Selective compensation of power-quality problems through active power filter by current decomposition", *IEEE Trans. Power Del.*, Vol. 23, No. 2, pp. 792–799, Apr. 2008.
- [41] G.-C. Hsieh and J. C. Hung, "Phase-locked loop techniques. A survey", *IEEE Trans. Ind. Electron.*, Vol. 43, No. 6, pp. 609–615, Dec. 1996.
- [42] B. Singh, V. Verma, and J. Solanki, "Neural network-based selective compensation current quality problems in distribution system", *IEEE Trans. Ind. Electron.*, Vol. 54, No. 1, pp. 53–60, Feb. 2007.
- [43] B. Widrow, J. M. McCool, and M. Ball, "The complex LMS algorithm", *Proc. IEEE*, Vol. 63, No. 4, pp. 719–720, Apr. 1975.
- [44] Sen, Kalyan K., "STATCOM - STATic synchronous COMPensator: Theory, modeling, and applications", IEEE Power Engineering Society, Winter Meeting, USA, 1999.
- [45] Chin-Yuan Hsu, Horng-Yuan Wu., "A New Single-Phase Active Filter with Reduced Energy Storage Capacitor", Power Electronics Specialists Conference, 1995, PESC '95 Record, 26th Annual IEEE, Vol.1, pp. 202 – 208, 18-22 June 1995.

## **CURRICULUM VITAE**

### **PERSONAL INFORMATION**

Name, Surname : Raad Salih Jawad  
Date and Place of Birth : 20.11.1969/Iraq - Baghdad  
Marital Status : Married  
Phone : 00905382521668  
E-mail : raad.saleh@gmail.com



### **EDUCATION**

High School : Al-Jumhouria Secondary School, 1987.  
Undergraduate : University of Technology / Electrical Engineering Department,  
1992.

### **PUBLISHED PAPERS**

Raad S. Jawad, Israa I. Hussein, I. Mahariq , "Design and Simulation of Three Phase and Single Phase Z-Source Inverters", ICEEP IV, researchgate.net, pp. 58-64, 6-7 April 2016.  
Raad S. Jawad, Israa I. Hussein, I. Mahariq , "FACTS Technology: Current Challenges and Future Trends", ICEEP IV, researchgate.net, pp. 45-50, 6-7 April 2016.